


Project no: 99-018  
Date: 2001-12-17  
Version: Rev. A

# Multi-storey Structures, Behaviour in Case of Fire Initial Theoretical Analyses

		Document Information
<b>FSD Project no:</b>	99-018	
<b>Document Title:</b>	Initial Theoretical Analyses	
<b>Project Title:</b>	Multi-storey Structures, Behaviour in Case of Fire	
<b>Document number:</b>	99-018-0	
<b>Client:</b>		
<b>Clients Ref:</b>		

<b>Issued by:</b>	MSc Sebastian Jeansson / PhD Yngve Anderberg
<b>Checked by:</b>	PhD Yngve Anderberg

<b>Key words:</b>	
<b>Report Status:</b>	Confidential <input type="checkbox"/> Internal <input type="checkbox"/> Open <input type="checkbox"/>

Version	Date	Issue	Issued by	Checked by
Rev. A	2001-12-17	Final version	SJ/YA	YA
0	2001-11-13	Final version	SJ/YA	YA
Draft	2001-03-05	Draft		
Draft	2001-02-16	Draft		
Draft 0	1999-10-05	Preliminary Draft		

## Contents

1	Introduction .....	4
1.1	Background.....	4
1.2	Aim and Scope of Work .....	4
1.3	Accomplishment and Planning .....	4
1.3.1	Sub-Project A .....	5
1.3.2	Sub-Project B.....	5
2	Initial Analyses .....	5
2.1	Parameter Study for Columns.....	5
2.1.1	Standard Fire Exposure on ~1/4, 1/2, ~3/4 and 1/1 of the Steel Profile Circumference... 6	6
2.1.2	Slenderness .....	6
2.1.3	Axial Loading Degree with Different Eccentricities.....	6
2.1.4	Partially Restrained Elongation.....	6
2.1.5	Insulation .....	6
2.2	Parameter Study for Beams .....	6
2.2.1	Standard Fire Exposure on ~1/4, 1/2, ~3/4 and 1/1 of the Steel Profile Circumference... 6	6
2.3	Verification Tests .....	6
2.4	Parameter Study of Frames.....	7
3	Properties of Steel .....	7
3.1	Thermal Properties .....	7
3.2	Mechanical Properties .....	8
3.2.1	Stress - Strain Relationship .....	8
3.2.2	Compression/Tension Strength .....	9
3.2.3	Modulus of Elasticity (Young's Modulus).....	10
4	Fire Exposure .....	10
4.1	Definition of ~1/4, 1/2, ~3/4 and 1/1 fire exposure.....	10
4.2	ISO 834 standard fire exposure .....	11
4.3	Boundary Conditions.....	11
5	Modelling Steel Columns.....	12
5.1	Definition of Slenderness .....	13
5.2	Eccentricities .....	14
5.3	Degree of Loading.....	15
6	Thermal Analysis.....	17
6.1	Super-Tempcalc.....	17
6.2	Results from Thermal Analyses .....	18
7	Structural Analysis .....	21
7.1	Global Collapse Analysis (GCA) .....	21
7.2	TCD - FIRE DESIGN.....	28
7.2.1	SBEAM .....	28
7.2.2	COMPRES.....	29
8	Structural Analyses of Columns.....	32
8.1	Simulations .....	32

8.1.1	Structural Behaviour for Partially Exposed Columns .....	32
8.1.2	Structural Behaviour of Columns with Eccentric Loads .....	35
8.1.3	Columns with Partially Restrained Axial Elongation .....	36
8.1.4	Verification of Steel Quality, Profile Type and Slenderness as Design Parameters for Columns .....	40
8.1.5	Verification of Applied Degree of Loading .....	41
8.1.6	Verification of Applied Design Load and Initial Out-of-straightness .....	41
8.2	Test .....	42
8.2.1	Temperature Simulation of Steel Column Fire Test Conducted in UK .....	42
9	Structural Analyses of Beams.....	45
9.1	Simulations .....	45
9.1.1	Structural Behaviour for Partially Exposed Beams .....	45
9.1.2	Verification of Applied Design Load .....	46
9.2	Test (Beam with Concrete Slab).....	49
9.2.1	Temperature Simulation of Steel Beam Fire Test Conducted in UK.....	49
9.3	Continuous beams.....	52
10	Analyses of Frame .....	57
10.1	Frame Model.....	57
10.1.1	Geometry .....	57
10.1.2	Boundary Conditions .....	59
10.1.3	Loading .....	59
10.1.4	Fire Exposure.....	60
10.2	Fully Fire-Exposed Frame .....	61
10.3	Single-Compartmentation Fire Exposure .....	65
11	Conclusions .....	72
11.1	Columns.....	72
11.2	Beams .....	73
11.3	Frames .....	73
12	Condensed Literature Review .....	75
12.1	A: Experience of structural behaviour and extent of damages in real building fires .....	75
12.2	B: Fire tests on structures .....	76
12.3	C: Basic research on mechanical properties and on behaviour of structural elements ..	77
12.4	D: FEM-modelling and computer simulation of fire tests.....	78
12.5	E: Structural fire design methods .....	79
12.6	References to Condensed Literature Review .....	80
A	Experience of structural behaviour and extent of damages in real building fires .....	80
B	Fire tests of structures.....	80
C	Basic research on mechanical properties and on behaviour of structural elements .....	81
D	FEM-modelling and computer simulation of fire tests.....	81
E	Structural fire design methods.....	82
13	References .....	85

## 1 Introduction

This report is part of the project Multi-storey Structures, Behaviour in Case of Fire which is a project held in co-operation between Fire Safety Design AB and the Swedish Institute of Steel Construction and covers the initial computer simulations of single columns.

The goal of the project is to improve the understanding of the behaviour of fire exposed steel structures and to prepare a design basis for a future design handbook for fire exposed steel constructions.

### 1.1 Background

During the last years important changes have occurred in the steel construction field. There are signs that imply that more optimised constructional fire state solutions could be developed. This has been confirmed by a number of occurred fires in multi-storey buildings /15, 16/, where the fire resistance time has turned out to be better than can be calculated using standard methods that are based on standard tests of single members such as beams and columns. Further understanding can be gained from documented full-scale tests /17, 18, 19/.

The design rules that are applied today are based on simplifications, for instance that the cross-sectional temperature over the steel profile is constant and that each single member is designed at fire state. This is rarely the case in reality. Usually just one part is subjected to fire exposure and large temperature deviations are present. This gives rise to a different behaviour of a partially exposed construction. The following issues are of main interest:

- The behaviour of single columns of frameworks at different types of exposure
- The effect of beams, columns and systems of joists that are partially constrained
- The behaviour of multi-storey constructions in fire
- To identify redundant members
- What kind of members should be given priority with respect to loadbearing function
- The magnitude of load redistribution in structures at large deformations
- How the support conditions change at intersections

### 1.2 Aim and Scope of Work

The goal of this initial study is to delineate and improve the understanding of the behaviour of fire exposed steel structures and to prepare a design basis for a future design handbook for fire exposed steel constructions. The outcome of the final work includes:

- To increase the understanding of the collapse behaviour of steel columns in fire
- To analyse the influence of partially restrained thermal elongation of beams, columns and frames
- To develop analysis models for multi-storey steel frames in fire, considering the different behaviour at large deformations
- To give practical recommendations of the combination of measurements that gives a building sufficient safety in the fire state

### 1.3 Accomplishment and Planning

A thorough literature study and a knowledge specification of documented theoretical and experimental studies are important for theoretical part of the work. The initial literature study is

conducted by Fire Safety Design AB, FSD, with literature support from the Swedish Institute of Steel Construction, SBI. FSD and SBI are to carry out the project, which is divided into two clearly defined and separate sub-projects A and B, in co-operation.

The analytical part with computer simulations including documentation is divided in the following parts:

- Fire tests
- Behaviour of columns
- Behaviour of beams
- Behaviour of frames

### 1.3.1 Sub-Project A

Fire Safety Design AB will perform initial verification analyses, computer simulations of individual members. Results from some chosen fire tests on loaded columns, such as measured fire resistance times and deformations will be done to verify the models. This will initially be done for profiles that are exposed on all surfaces, but comparisons of tests for cases with partial exposure is desired too. Computer simulations of the collapse behaviour will be done for steel columns that are free to expand.

A parameter study is to be performed to analyse how different factors such as fire exposure, slenderness, eccentricity and initial out of straightness influence the load-bearing capacity of steel columns of different geometrical properties in fire. Computer simulations of the behaviour of columns and frames with columns being subjected to partial axial restraint are to be done as well as a couple of simulations of locally exposed frames. Specially developed computer tools, Super-Tempcalc and Global Collapse Analysis will be used for studies of temperature development and structural response. New findings will be used to develop improved and new methods for fire design.

### 1.3.2 Sub-Project B

The Swedish Institute of Steel Construction will study and develop analysis models for multi-storey steel frames in fire, considering the changes in behaviour due to large deformations with the help of ECSC's experiences and give practical recommendations about the combinations of measurements that gives a building sufficient safety in the case of fire.

## 2 Initial Analyses

### 2.1 Parameter Study for Columns

A parameter study was carried out to analyse how different factors effect the load-bearing capacity for geometrical differences of fire:

- Fire exposure (ISO 834)
- Slenderness
- Axial load levels with different eccentricities
- Partially restrained elongation
- Insulation (intumescent paint)

The initial analyses can be found in sections 8 - 10.

### 2.1.1 Standard Fire Exposure on ~1/4, 1/2, ~3/4 and 1/1 of the Steel Profile Circumference

Standard fire according to ISO 834 is to be focused on exposure of 1/1 (100%) of the circumference. Partially exposed columns will be analysed separately.

### 2.1.2 Slenderness

Five different values of slenderness will be studied for columns: 0, 0.5, 0.75, 1.0 and 1.5.

### 2.1.3 Axial Loading Degree with Different Eccentricities

The degree of axial loading is chosen to 60%, 50%, 40% and 25% of the characteristic buckling compression resistance load at room temperature, 20 °C. The *characteristic resistance load* corresponds to design in the fire state, as opposed to the *normal design resistance load*.

The eccentricity is chosen to 0,  $\pm 3$  cm and  $\pm 5$  cm. An initial out of straightness, defined by the first eigenmode with a maximum amplitude of 1/400 of the column length, is added for all columns. The direction of the out of straightness is chosen to that of the fire-related deflections.

### 2.1.4 Partially Restrained Elongation

The influence of partially restrained axial elongation is studied for 100% fire exposure, an eccentricity of 0 and with slenderness values of 0.5 and 1.0. The calculations are performed with initial axial degrees of freedom of 0.8, 0.9 and 1.0. A value of 1.0 means free elongation and 0 means totally restrained. Further analyses include a frame under influence of local fire exposure.

### 2.1.5 Insulation

Steel columns to be simulated are insulated in order to control the development of temperatures. An intumescent paint is chosen to achieve about 60 minutes of fire resistance time for 100% exposure and a slenderness of 1.0. The frames are modelled without insulation.

## 2.2 Parameter Study for Beams

- Fire exposure (ISO 834 and natural fires)
- Insulation (intumescent paint)

### 2.2.1 Standard Fire Exposure on ~1/4, 1/2, ~3/4 and 1/1 of the Steel Profile Circumference

Standard fire according to ISO 834 is to be focused on exposure of ~1/4 - ~3/4 of the circumference.

## 2.3 Verification Tests

Simulations of fire tests were done for verification of the non-linear GCA approach and corresponding, applicable design approach. Measured results from fire tests of unloaded and loaded steel columns in terms of stress, strain and deformations are compared to the results from computer simulations of identical conditions. This concerns profiles that are exposed on all surfaces and cases where the degree of fire exposure vary.

Considered relevant fire tests were:

- Tests performed in England with standard fire exposure and natural fires.
- Some loaded steel columns that have been tested in fire by Nils Forsén and Björn Aasen at the Norwegian Fire Research Laboratory
- Experimental results found in the literature study.

Full scale fire tests of a beam and a fully exposed column conducted at Firtio Borehamwood, U.K. 1984, were finally chosen for simulations. Tests of partially exposed columns conducted at Firtio Borehamwood involved a wall which was impossible to simulate since the columns reached the wall within a few minutes after which the direction of horizontal deformations was reversed.

The results from the simulations can be found in sections 8.2 and 9.2.

## 2.4 Parameter Study of Frames

One 3-storey steel frame was modelled. The different scenarios were

- Fully fire exposed
- Exposure in a single compartment

The results can be found in section 10.2.

## 3 Properties of Steel

The knowledge of thermal and mechanical properties are necessary in the thermal and structural analysis of fire-exposed steel columns. The temperature-dependence of the material properties are described in this section.

### 3.1 Thermal Properties

Thermal properties are essential to heat transfer calculations. These are, essentially, heat conductivity, heat capacitvity and thermal expansion, all of which vary with increasing temperature.

Thermal capacitvity is defined as the product between specific heat and density. It expresses the magnitude of energy storage potential of the material. Typical insulation products feature low thermal conductivity, whilst metals like steel are excellent conductors. The density of steel is 7850 kg/m<sup>3</sup>.

The thermal properties of steel used in the analyses are illustrated in figure 3-1.



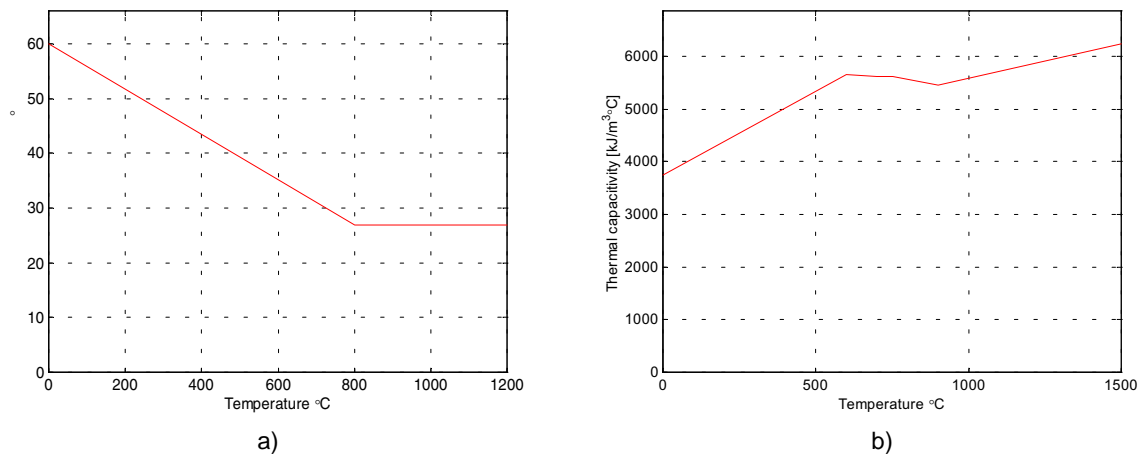


Figure 3-1 a) *Thermal conductivity of steel /10/.*  
 b) *Thermal capacity of steel /10/.*

Steel, being an isotropic material, has equal properties in all directions. One of these is the ability to expand when subjected to a temperature elevation. This expansion will cause a strain in the material. The thermal expansion can be described by:

$$\varepsilon_{th} = \alpha \Delta T \quad (\text{eq. 3-1})$$

The variable  $\alpha$  can be expressed in many ways, for instance as a constant or as a linear variation of the temperature or as a polynomial function of the temperature.

The polynomial expression of the thermal elongation is described by

$$\varepsilon_{th} = -2.416 \cdot 10^{-4} + 1.2 \cdot 10^{-5} T + 0.4 \cdot 10^{-8} T^2 \quad (\text{eq. 3-2})$$

The property of expanding is of particular interest when considering complex structures with fixed end connections. The rigidity of connections and external attachment restricts desired expansion, thus generating constraint stresses.

## 3.2 Mechanical Properties

Stress-strain relationships ( $\sigma$ - $\varepsilon$  curves) at elevated temperatures are must be known to be able to calculate stress and deformations of fire exposed shell structures. Tension and compression strength and modulus of elasticity as function of temperature can be derived from  $\sigma$ - $\varepsilon$  curves.

### 3.2.1 Stress - Strain Relationship

The adopted stress-strain relationship for steel follows the idealised analytical expression proposed in Eurocode /1/. Each steel core temperature has its own stress-strain curve. Figure 3-2 displays the stress-strain curves for steel at different temperatures.

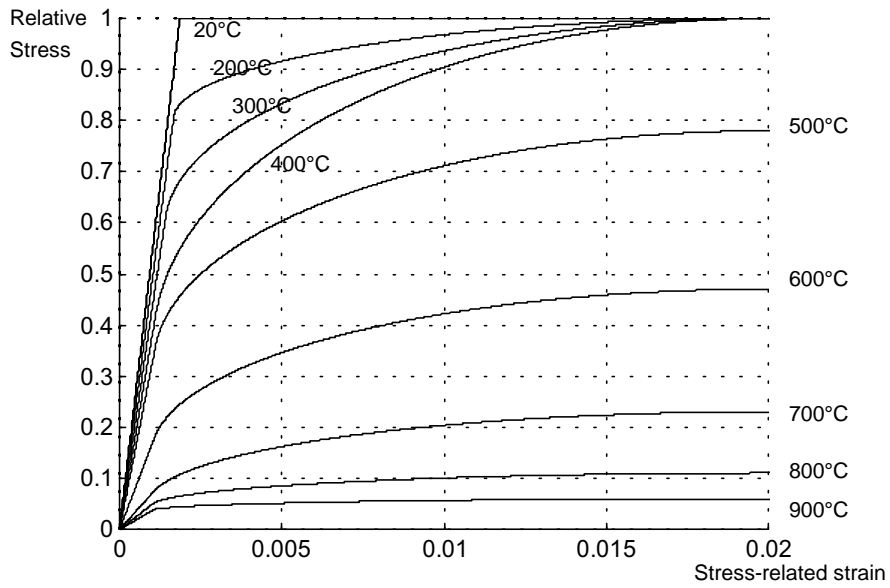


Figure 3-2 Relative stress-strain curves at 20-900°C. /1/

It is emphasised that the stress-strain relation changes in form at temperatures above 100 °C, such that plastic deformation occurs at lower stress levels, thus rendering the stress-strain relation more like a polynomial in shape rather than the characteristic yield "plateau", evident at room temperature.

### 3.2.2 Compression/Tension Strength

The steel strength is decreasing with temperature. For steel with a critical strain of 2 % the strength reduction starts at 400 °C as indicated in figure 3-3. If the critical strain is 0.2% the strength reduction starts already at 100 °C.

For analyses the characteristic yield strength  $f_{yk}$  is chosen to 390 MPa.

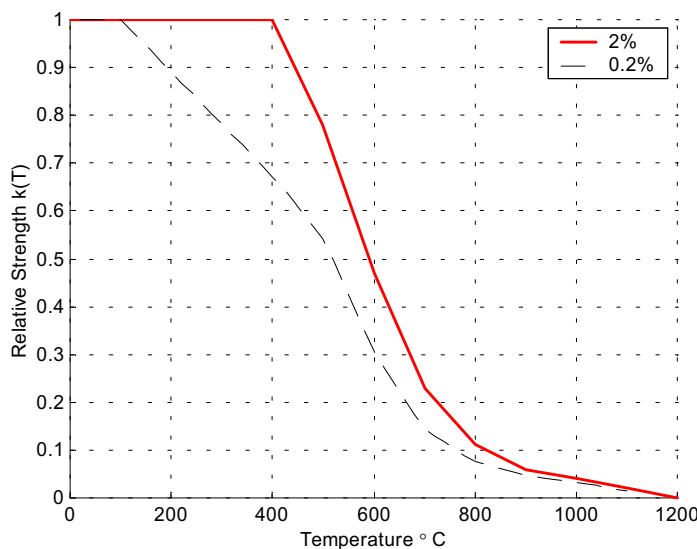


Figure 3-3 Relative steel strength as function of temperature /1/.

### 3.2.3 Modulus of Elasticity (Young's Modulus)

The modulus of elasticity, much like the strength, shows a decreasing path as the temperature increases in the steel material. The decreasing branch starts at 100 °C. At 1200 °C all initial stiffness is lost. The modulus of elasticity is 210 GPa.

The relationship between modulus of elasticity and temperature is given in figure 3-4.

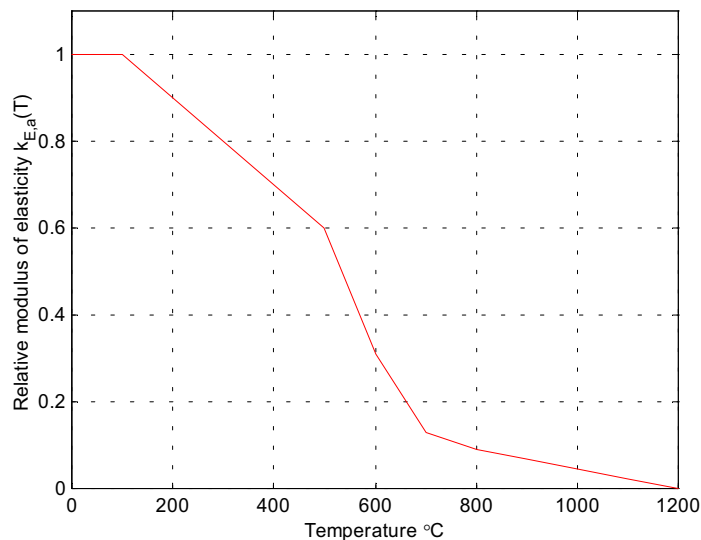


Figure 3-4 Relative modulus of elasticity as function of temperature. /1/

## 4 Fire Exposure

### 4.1 Definition of ~1/4, 1/2, ~3/4 and 1/1 fire exposure

“~1/4” refers to 1-sided fire exposure, “1/2” refers to exposure on half of the steel profile circumference, “~3/4” refers to 3-sided fire exposure and “1/1” refers to 4-sided fire exposure. The symbol “~” (tilde character) should read “approximately”. The actual percentage of fire exposed circumference for 1-sided and 3-sided exposure depends on profile type.

In order to protect the exposed surfaces of the steel profiles, HEB300 and HEB200, a layer of intumescent paint (Hensotherm 4 Ks) is applied. This means that the temperature increase of the steel will be delayed and a fire resistance of about 50-60 minutes for 100% exposure and 40 % load is obtained. Four cases of partial fire exposure are studied viz. ~1/4 (19 %), 1/2 (50 %), ~3/4 (83%) and 1/1 (100%), all defined as percentages of exposed surface for the profile HEB300. 19% exposure means that only the lower part of the bottom flange is exposed and the rest is not in contact with fire. This is arranged by surrounding the unexposed part with a material of concrete-type, which is illustrated in figure 4-1. 50% means that half of the profile is exposed and ~3/4 (83 %) means that only the upper part of the upper flange is not exposed to fire. The thermal properties of concrete were taken according to /10/.

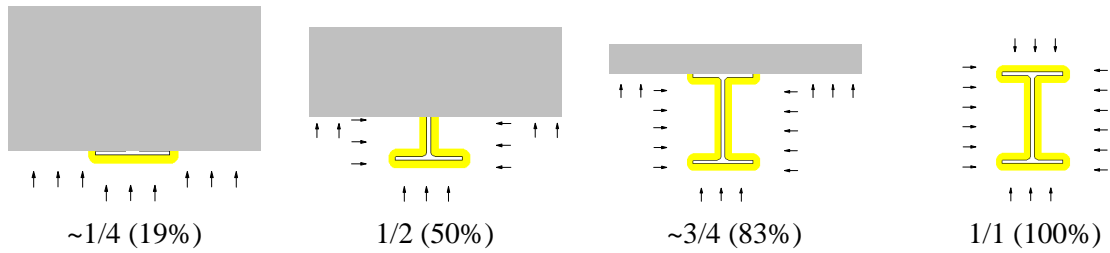


Figure 4-1 Four cases of fire exposure studied.

## 4.2 ISO 834 standard fire exposure

The standard ISO 834 time temperature development is described by

$$T(t) = 345 \cdot \log(480t + 1) + T_0 \quad t > 0 \quad (\text{eq. 4-1})$$

where

- $t$  = time (h)
- $T(t)$  = gas temperature at time  $t$  (°C)
- $T_0$  = initial temperature (°C)

The time temperature development is presented in a chart in figure 4-2.

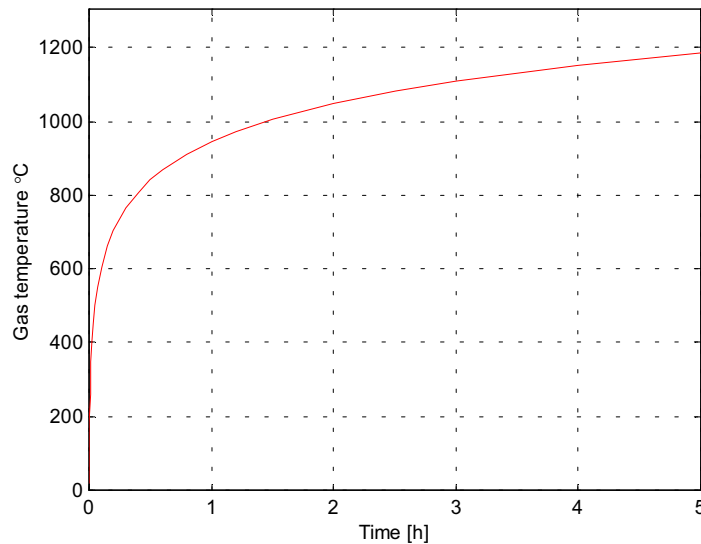


Figure 4-2 Time-temperature development of ISO 834 fire exposure /2/.

## 4.3 Boundary Conditions

The heat is transferred from the fire gases to the exposed structure through radiation and convection (see equation 4-2). The radiation, which dominates at high temperatures, is expressed by the resultant emissivity factor (second term of equation 4-2). The convection is calculated from the

temperature difference between the structure and ambient gases, depending on the gas velocity (first term of equation 4-2). Resulting emissivity and convection factors used, are shown in table 4-1. These are in accordance with recommendations by ISO and Eurocode /2/.

Emissivity/Convection	$\epsilon_r$ [-]	$H_c$ [W/m <sup>2</sup> K]
Exposed surface	0.56	25

Table 4-1 Resulting emissivity and convection factor for ISO 834 fire exposure /2/.

$$q_n = h_c(T_g - T_b) + \epsilon_r \sigma (T_g^4 - T_b^4) \quad (\text{eq. 4-2})$$

where

- $\sigma$  = Stefan-Boltzmann constant [5.67x10<sup>-8</sup> W/m<sup>2</sup> K<sup>4</sup>]
- $T_g$  = absolute temperature of radiation source [K]
- $T_b$  = boundary temperature [K]
- $\epsilon_r$  = emissivity factor of radiation source
- $q_n$  = heat flow at the boundary [W/m<sup>2</sup>]
- $h_c$  = convection heat transfer coefficient [W/m<sup>2</sup>K]

Surfaces of a structure that are not exposed to fire will imply a certain potential for cooling of the steel. Heat entering the structure along an exposed boundary may, to a certain extent, leave the profile in unexposed areas. Thus the parameters of emissivity and convection defined in the previous section will under these circumstances take other values; see table 4-2.

Emissivity/Convection	$\epsilon_r$ [-]	$h_c$ [W/m <sup>2</sup> K]
Unexposed surface	0.8	9

Table 4-2 Resulting emissivity and convection factor for unexposed surfaces /2/.

Including the changes in the parameters above and switching the gas temperature for the ambient temperature, equation 4-1 defined previously will be applicable.

A boundary where no heat is said to pass ( $q_n = 0$ ) is often referred to as an adiabatic boundary. These are for example symmetry lines. Structures with extreme extension in two of the three directions are often considered to have a one-dimensional heat flow and consequently adiabatic boundaries will be adopted in the calculation. A steel plate is an example of such a structure.

## 5 Modelling Steel Columns

Four magnitudes of slenderness have been studied, viz.  $\lambda=1.5, 1.0, 0.75$  and  $0.5$ . Since the cross-section profile has been selected (HEB300) and the material parameters are determined, the corresponding lengths are 8.7 m, 5.8 m and 2.9 m respectively for a column restrained at the bottom and free at the top.

Steel cross-sections are generally divided into four classes depending on their ability to form a plastic hinge. The method is practically the same in all design codes; here the Eurocode version is represented.

## 5.1 Definition of Slenderness

Slenderness expresses the degree of sensitivity to the buckling phenomenon (flexural buckling), and links the strength, the length, the stiffness and the cross-section dimensions together. The slenderness ratio,  $\lambda$ , is defined in equation 5-1. The ratio relates the characteristic compression resistance,  $N_{c,R}$ , to the critical axial buckling force,  $N_{cr}$ , according to the Euler buckling theory.

$$\lambda = \sqrt{\frac{A \cdot f_y}{N_{cr}}} = \frac{l_c}{\pi i} \sqrt{\frac{f_y}{E}} \quad (\text{eq. 5-1})$$

$$N_{c,R} = A \cdot f_y \quad (\text{eq. 5-2})$$

$$N_{cr} = \frac{\pi^2 EI}{l_c^2} \quad (\text{eq. 5-3})$$

where

$l_c$  = buckling length of column

Equation 5-1 indicates the turning point between two different modes of failure. Values of  $\lambda$  exceeding 1.0 applies to a buckling failure mainly in accordance with equation 5-3 (flexural buckling). For lower values of  $\lambda$  the failure will be governed by the cross-sectional stress reaching the yield strength. The following parameters are all affecting steel columns in one way or the other:

- initial out of straightness
- unintentional eccentricity
- secondary geometrical effects
- initial stresses
- plasticizing during the buckling process

Taking these effects into account, the curve found in figure 5-1 is obtained.

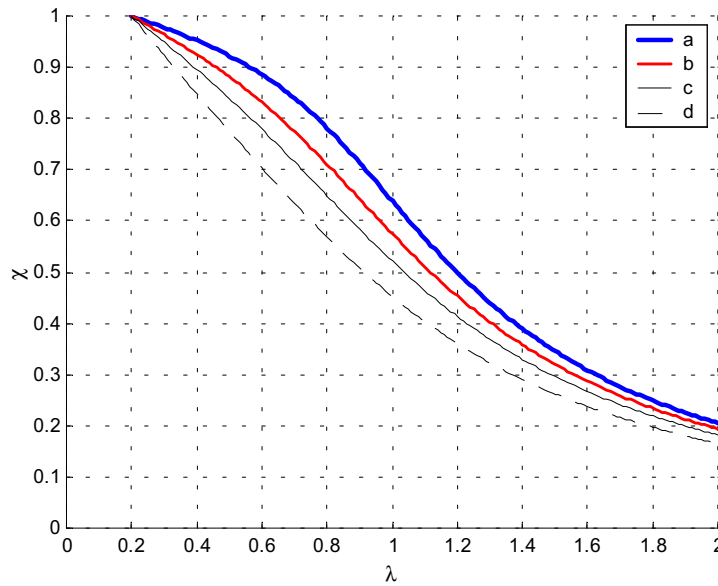


Figure 5-1 Reduction factor as function of slenderness for cross-section types a-d /12/.

The reduction factor in figure 5-1 is denoted  $\chi$  and is a function of the slenderness ratio and depends on the type of cross-section (a-d). It can be obtained in ENV 1993-1-1 or in BSK 94 (named  $\omega$  in BSK 94).

The characteristic buckling resistance of a compression member can be defined as:

$$N_{b,R} = \chi \cdot N_{c,R} \quad (\text{eq. 5-4})$$

Slenderness and stiffness, defined as the product  $EI$ , are two essential parameters concerning columns. A decrease in stiffness will cause an increase in slenderness, and vice versa.

## 5.2 Eccentricities

Eccentricities as initial out of straightness and thermal bending will vary along the length of the column. These eccentricities influence the behaviour of fire exposed columns because it will implicate a moment due to the axial load in accordance with equation 5-5.

$$M = N \cdot e \quad (\text{eq. 5-5})$$

The columns were modelled structurally with a geometrical eccentricity in the nodes to compensate for initial out of straightness, as indicated in figure 5-3. The initial out of straightness is modelled according to the first eigenmode with the maximum deflection taken as the system length divided by 400.

The difference in temperature over the cross-section implies a varying desire to expand thermally. The Bernoulli assumption states that the cross-section plane remains perpendicular to the beam axis during the progress of deformation. It is thus concluded that the beam axis must bend and a thermal eccentricity is obtained. The stress contribution from the moment will be superposed to the compression stress generated by the axial force. During the progress of the fire scenario the temperature gradient grows larger and the "thermal eccentricity" is increasing continuously, with

escalating stresses as a result, and finally the critical design strength will be attained. This is the reason why partial fire exposure is so critical to a column's load-bearing capacity and thus needs to be investigated thoroughly in order to determine the most appropriate approach of design. Presuming a structural model as showed in figure 5-3 the total thermal eccentricity,  $e_{th}$ , is indicated.

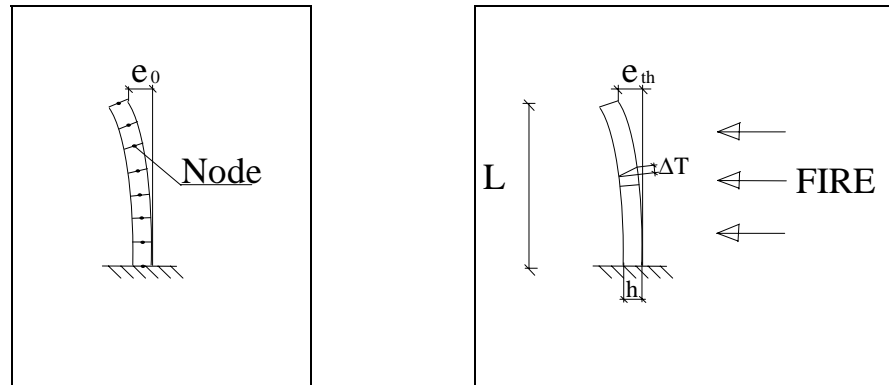


Figure 5-3 *Structural model of studied columns. Lower end fixed, upper end free. Initial eccentricity modelled in the nodes.*

*Indication of thermal eccentricity,  $e_{th}$ , descending from the temperature difference between the flanges,  $\Delta T$ , caused by partial fire exposure.*

### 5.3 Degree of Loading

The degree of loading is taken as a percentage of the characteristic buckling resistance load in the fire state, represented by the expression defined in equation 5-4. Appropriate magnitudes of relative loading were found to be 25%, 40%, 50% and 60%. Supplementary analyses were done with a relative loading between 0-80%.



Slenderness $\lambda$	~0	0.5	0.75	1.0	1.5
Column length	(0.3 m)	2.37 m	3.56 m	4.74 m	7.11 m
0 % load	-	-	-	0 MN	-
25 % load	1.39 MN	1.23 MN	1.03 MN	0.80 MN	0.45 MN
40 % load	2.23 MN	1.96 MN	1.66 MN	1.28 MN	0.71 MN
50 % load	2.78 MN	2.45 MN	2.07 MN	1.60 MN	0.89 MN
60 % load	3.34 MN	2.95 MN	2.48 MN	1.92 MN	1.06 MN
70 % load	-	-	-	2.24 MN	-
80 % load	-	-	-	2.56 MN	-

Table 5-1 *Applied degrees of loading for HEB 300 column and steel with a characteristic strength of 390 MPa.*

Slenderness $\lambda$	~0	0.5	0.75	1.0	1.5
Column length	(0.3 m)	2.90 m	4.36 m	5.81 m	8.71 m
25 % load	0.93 MN	0.82 MN	4.36 MN	0.53 MN	0.30 MN
40 % load	1.49 MN	1.31 MN	1.10 MN	0.85 MN	0.48 MN
50 % load	1.86 MN	1.63 MN	1.37 MN	1.07 MN	0.59 MN
60 % load	2.23 MN	1.96 MN	1.66 MN	1.28 MN	0.71 MN

Table 5-2 *Applied degrees of loading for HEB 300 column and steel with a characteristic strength of 260 MPa.*

Slenderness $\lambda$	~0	0.5	0.75	1.0	1.5
Column length m	(0.3 m)	-	-	3.12 m	-
25 % load	0.73 MN	-	-	0.42 MN	-
40 % load	1.17 MN	-	-	0.67 MN	-
50 % load	1.46 MN	-	-	0.84 MN	-
60 % load	1.76 MN	-	-	1.01 MN	-

Table 5-3 *Applied degrees of loading for HEB 200 column and steel with a characteristic strength of 390 MPa.*

Slenderness $\lambda$	~0	0.5	0.75	1.0	1.5
Column length m	(0.3 m)	-	-	3.82 m	-
25 % load	0.49 MN	-	-	0.28 MN	-
40 % load	0.78 MN	-	-	0.45 MN	-
50 % load	0.98 MN	-	-	0.56 MN	-
60 % load	1.17 MN	-	-	0.67 MN	-

Table 5-4 *Applied degrees of loading for HEB 200 column and steel with a characteristic strength of 260 MPa.*

## 6 Thermal Analysis

The following information is essential when calculating nodal temperatures as function of time during a specified fire scenario:

- thermal properties
- boundary conditions
- fire exposure

The key engineering tool in this analytical procedure is the finite element temperature calculation program, Super-Tempcalc, which facilitates calculations of heat transfer, temperature redistribution and temperature development in modelled materials. The features and background theory of Super-Tempcalc are described in detail in section 6.1.

The difference between the four cases is the modelling technique in the temperature simulations. figure 6-1 illustrates how ~1/4, 1/2, ~3/4 and 1/1 exposure are being modelled in the temperature calculation.

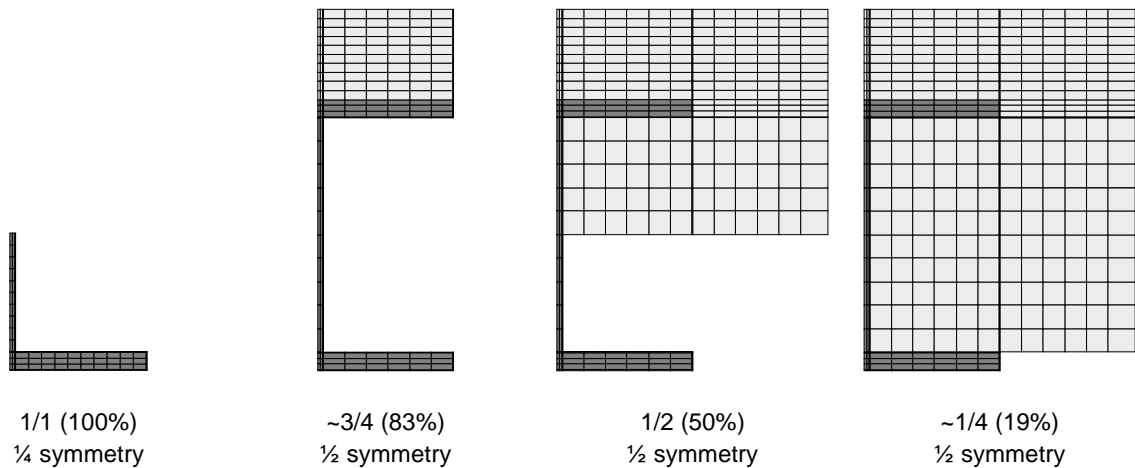


Figure 6-1 *Modelling of the four fire exposure degrees ( insulation alternatives). Exposed steel is insulated with intumescent paint.*

### 6.1 Super-Tempcalc

Super-Tempcalc /4/ is a fire-adapted two-dimensional finite element program developed by FSD for use on personal and mainframe computers. It is a further development of Tempcalc, originally developed in 1985.

The program is widely used in the field of passive fire protection, and as part of structural analysis, in buildings and on offshore platforms. It is accepted for North Sea applications by a number of countries and organisations.

The program solves the two-dimensional, transient, heat transfer differential equation 6-1 incorporating thermal properties that vary with temperature.

$$\frac{\partial}{\partial x} \left( k_x \frac{\partial T}{\partial x} \right) + \frac{\partial}{\partial y} \left( k_y \frac{\partial T}{\partial y} \right) + Q = \rho c \frac{\partial T}{\partial t} \quad (\text{eq. 6-1})$$

where

- $T$  = temperature [ $^{\circ}\text{C}$ ]
- $k_x, k_y$  = thermal conductivity [ $\text{W}/\text{m}^{\circ}\text{C}$ ]
- $c$  = specific thermal capacity [ $\text{J}/\text{kg } ^{\circ}\text{C}$ ]
- $\rho$  = density [ $\text{kg}/\text{m}^3$ ]
- $Q$  = internal heat generation [ $\text{W}/\text{m}^3$ ]

The program allows the use of rectangular or triangular finite elements, in cylindrical or rectangular co-ordinates. Heat transferred by convection and radiation at the boundaries can be modelled as a function of time. Structures comprising several materials can be analysed and the heat absorbed by any existing void in the structure is also taken into account.

A materials properties database is integrated with the main program. Also integrated with the program are pre- and post-processors which allow fast and user-friendly input/output procedures. The pre-processor generates the finite element division and retrieves the relevant information from the database for use in the calculation. Finally, the post-processor presents the results graphically on screen or on plotter in a variety of forms, including time-temperature curves, isotherms, and temperature gradients.

## 6.2 Results from Thermal Analyses

The steel profile has been subjected to a heat transfer calculation for a given fire scenario, resulting in a cross-sectional temperature gradient over time. The temperature development of the profile denotes an essential input data for the subsequent global collapse analysis. Gradients over the HEB 300 profile height can be found for the four different exposure alternatives in figures 6-2 – 6-5. The gradient for the used profile HEB 200 with 100% exposure is presented in figure 6-6.

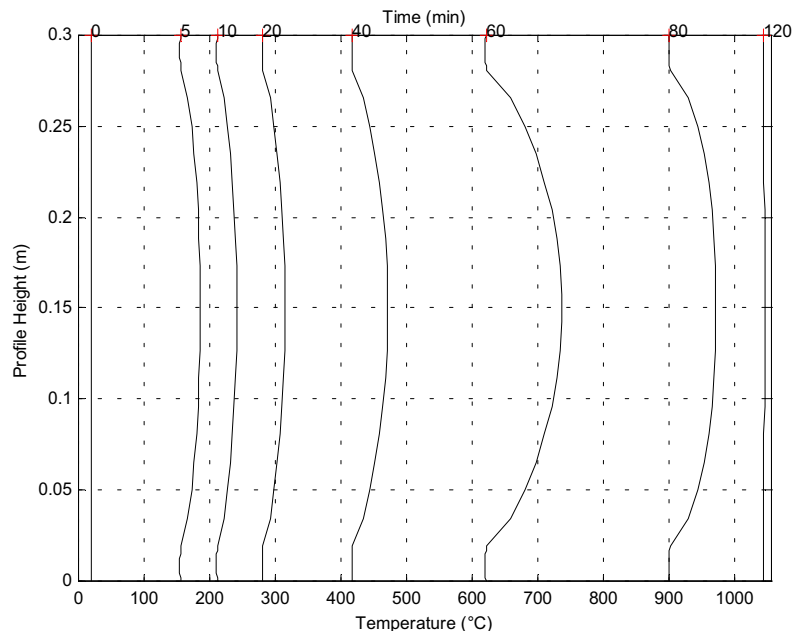


Figure 6-2 100 % fire exposure. Temperature gradient along the height of the HEB300 profile after 0, 5, 10, 20 40, 60, 80 and 120 minutes.

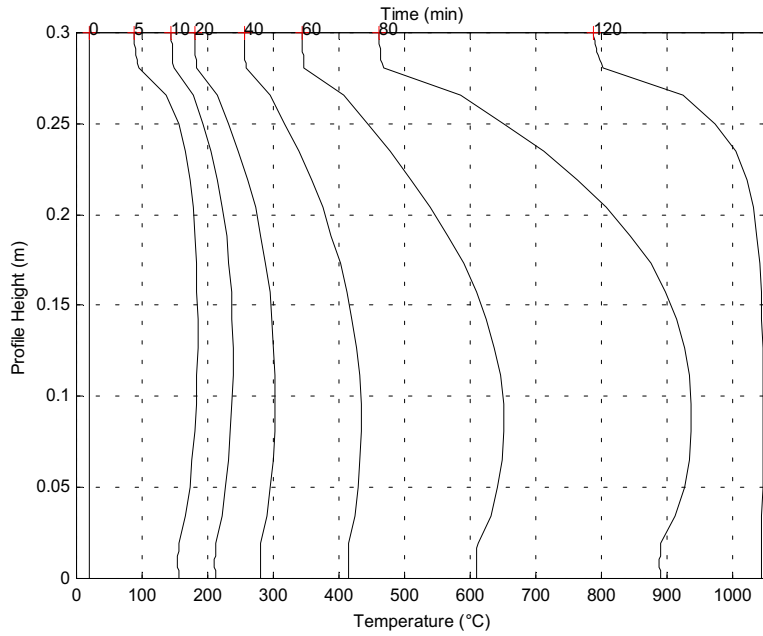


Figure 6-3 ~3/4 (83 %) fire exposure. Temperature gradient along the height of the HEB300 profile after 0, 5, 10, 20, 40, 60, 80 and 120 minutes.

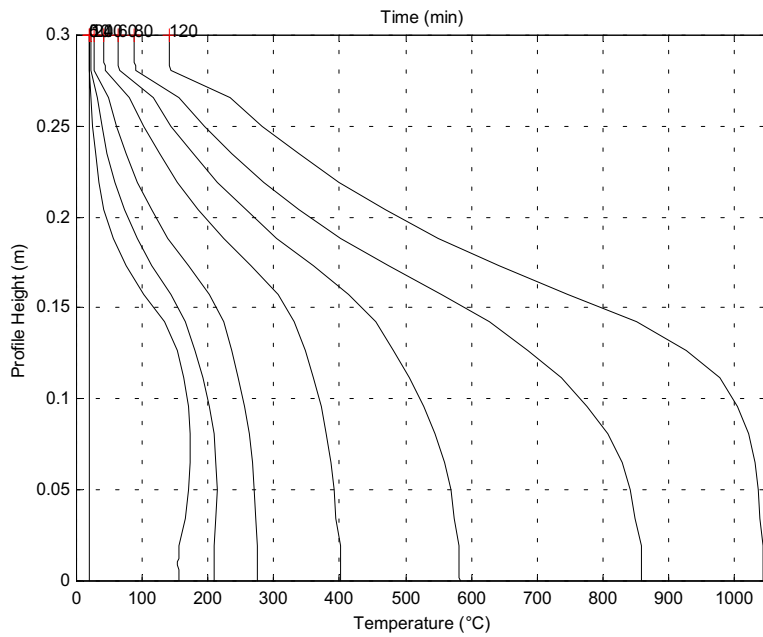


Figure 6-4 1/2 (50 %) fire exposure. Temperature gradient along the height of the HEB 300 profile after 0, 5, 10, 20, 40, 60, 80 and 120 minutes.

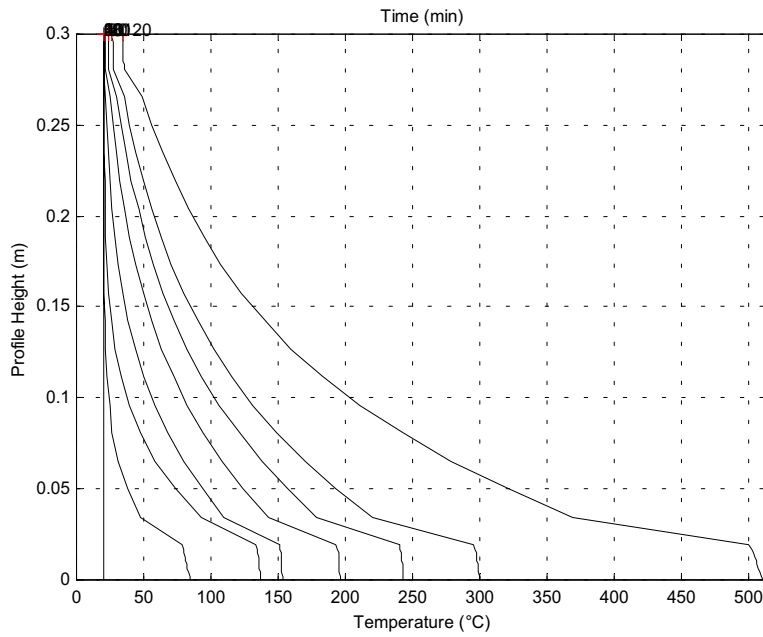


Figure 6-5 *~1/4 (19 %) fire exposure. Temperature gradient along the height of the HEB300 profile after 0, 5, 10, 20 40, 60, 80 and 120 minutes.*

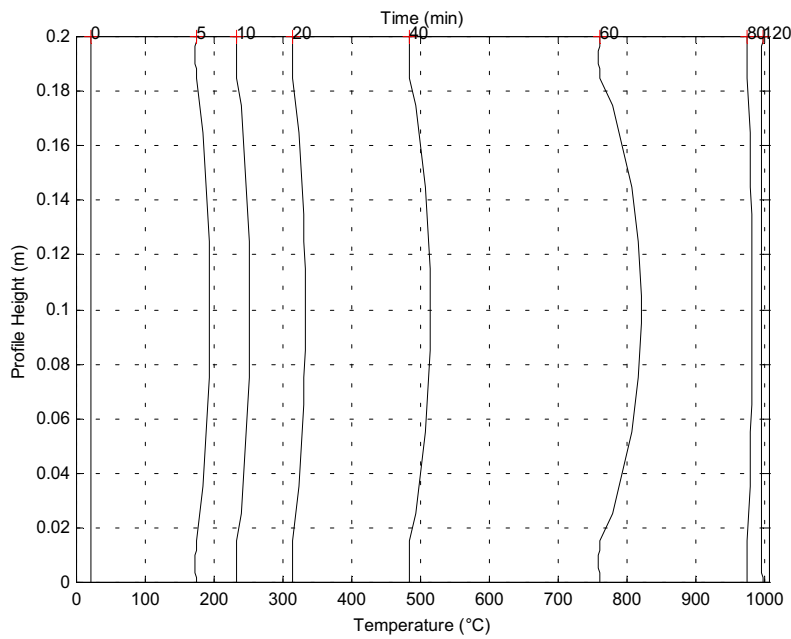


Figure 6-6 *1/1 (100 %) fire exposure. Temperature gradient along the height of the HEB200 profile after 0, 5, 10, 20 40, 60, 80 and 120 minutes.*

## 7 Structural Analysis

The results of the thermal analysis are incorporated in the structural ditto for computerised prediction of structural stability. Elevating temperatures affect the steel by reduced strength and modulus of elasticity, stress-strain relationship and the ability to expand thermally.

The main tool for current analyses has been the program Global Collapse Analysis. Comparisons of tests have been done with Fire Design, the beam and column tools integrated in TCD.

Columns differ significantly from other structures, being subjected to effects from instability. This means that failure generally occurs from the axial load reaching the critical load (equation 4-5), and not from the cross-sectional strain attaining the yield limit. The primary task of a column is generally to transfer loads vertically down to the foundation, i.e. columns in structures are carrying axial loads. This makes the column a very essential part of a structure.

### 7.1 Global Collapse Analysis (GCA)

In some elastic solid mechanics problems the governing differential equations are linear and with a linear form of stress-strain relationship. However, in fire-related structural problems the linearity of constitutive relations is not preserved. The problem is actually a combination of material non-linearity together with geometrical non-linearity.

Global Collapse Analysis (GCA) is a finite element program providing computer prediction of the structural behaviour of load-bearing systems.

Essential input to the program comprise:

- cross-sectional geometry
- cross-sectional time-temperature fields from thermal analysis
- geometry (column and beam geometry)
- boundary conditions (rigidity, external attachments)
- material data (steel strength, variation of stress-strain relationship)
- external loads

GCA is integrated with the temperature calculation program Super-Tempcalc, thus incorporating steel temperature field data versus time of the adopted fire scenario.

The overall stability of a structure, due to a local fire, can be analysed and global progressive and local collapse respectively, can be predicted. Upgrading of identified separate critical members provides possible extension of initially calculated fire resistance time. Under certain conditions local collapses can be accepted.

Generation of restraint stresses and strains, due to rigid external connections combined with the thermal expansion in the steel, makes the model reasonably accurate.

Results in terms of stresses, strains, cross-sectional stiffness, deflections, displacements, forces and moments may be presented at selected times through out the fire scenario.

The 2-dimensional Bernoulli beam element with 6 degrees of freedom is used in the finite element model. The kinematic assumption of this element is that plane sections normal to the beam axis remain plane and normal to the beam axis during the deformation.

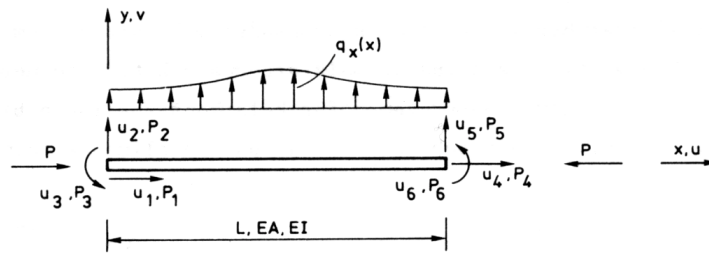


Figure 7-1 The Bernoulli beam element with 6 degrees of freedom.

The two differential equations that describe the beam element are:

$$\frac{d}{dx} \left( EA \frac{du}{dx} \right) + q_x = 0 \quad (\text{eq. 7-1})$$

and

$$\frac{d^2}{dx^2} \left( EI \frac{d^2v}{dx^2} \right) + P \frac{d^2v}{dx^2} - q_y = 0 \quad (\text{eq. 7-2})$$

The symbols used are described in Table 7-1.

Symbol	Quantity
$EA$	Stiffness in beam axis direction
$EI$	Bending stiffness
$u$	Displacement in beam axis direction
$v$	Displacement in direction perpendicular to beam axis
$q_x$	Distributed load in beam axis direction
$q_y$	Distributed load perpendicular to beam axis
$P$	Axial load

Table 7-1 Description of symbols.

With known value of the displacement in the direction perpendicular to beam axis equation the equilibrium when taking into account the non-linear geometrical second-order effect is given by equation 7-3 with symbols according figure 7-2.

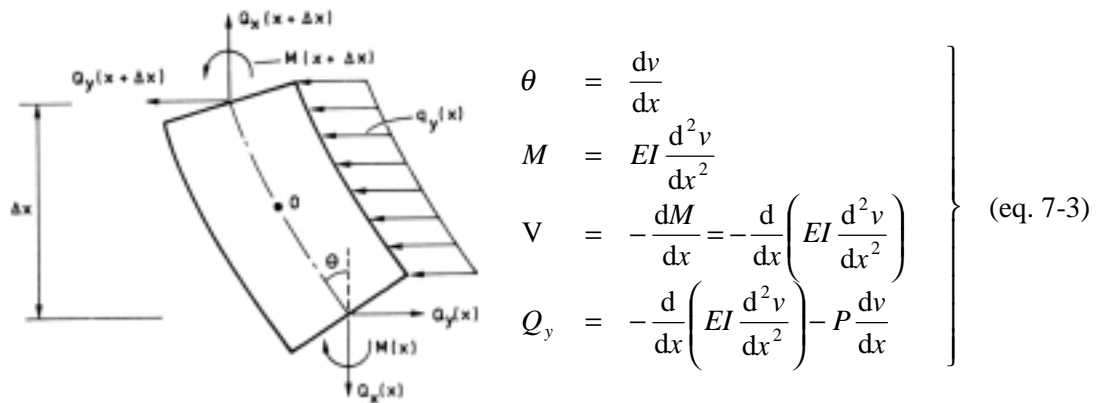


Figure 7-2 Properties derived from equilibrium of beam segment  $\Delta x$ .

With  $k$  defined as:

$$k = \sqrt{\frac{P}{EI}}$$

equation 7-2 becomes:

$$v^{IV} + k^2 v'' = 0 \quad \text{for compression} \quad \text{(eq. 7-4 a)}$$

$$v^{IV} - k^2 v'' = 0 \quad \text{for tension} \quad \text{(eq. 7-4 b)}$$

The solutions to equations 7-4 a and b are obtained by integrating twice. With the introduction of stability functions  $\phi_1$ - $\phi_5$  according to equations 7-6 a and 7-6 b, the second-order beam element matrix can be written as:

$$K^e = \begin{bmatrix}
 \frac{EA}{L} & 0 & 0 & -\frac{EA}{L} & 0 & 0 \\
 0 & \frac{12EI}{L^3} \phi_5 & \frac{6EI}{L^2} \phi_2 & 0 & -\frac{12EI}{L^3} \phi_5 & \frac{6EI}{L^2} \phi_2 \\
 0 & \frac{6EI}{L^2} \phi_2 & \frac{4EI}{L} \phi_3 & 0 & -\frac{6EI}{L^2} \phi_2 & \frac{2EI}{L} \phi_4 \\
 -\frac{EA}{L} & 0 & 0 & \frac{EA}{L} & 0 & 0 \\
 0 & -\frac{12EI}{L^3} \phi_5 & -\frac{6EI}{L^2} \phi_2 & 0 & \frac{12EI}{L^3} \phi_5 & -\frac{6EI}{L^2} \phi_2 \\
 0 & \frac{6EI}{L^2} \phi_2 & \frac{2EI}{L} \phi_4 & 0 & -\frac{6EI}{L^2} \phi_2 & \frac{4EI}{L} \phi_4
 \end{bmatrix} \quad \text{(eq. 7-5)}$$



$$\left. \begin{aligned}
 \phi_1 &= \frac{kL}{2} \cot \frac{kL}{2} \\
 \phi_2 &= \frac{1}{12} \frac{k^2 L^2}{(1 - \phi_1)} \\
 \phi_3 &= \frac{1}{4} \phi_1 + \frac{3}{4} \phi_2 \\
 \phi_4 &= -\frac{1}{2} \phi_1 + \frac{3}{2} \phi_2 \\
 \phi_5 &= \phi_1 \phi_2
 \end{aligned} \right\} \begin{array}{l} \text{(eq. 7-6 a)} \\ \text{compression} \\ \text{/14/} \end{array}$$

$$\left. \begin{aligned}
 \phi_1 &= \frac{kL}{2} \coth \frac{kL}{2} \\
 \phi_2 &= -\frac{1}{12} \frac{k^2 L^2}{(1 - \phi_1)} \\
 \phi_3 &= \frac{1}{4} \phi_1 + \frac{3}{4} \phi_2 \\
 \phi_4 &= -\frac{1}{2} \phi_1 + \frac{3}{2} \phi_2 \\
 \phi_5 &= \phi_1 \phi_2
 \end{aligned} \right\} \begin{array}{l} \text{(eq. 7-6 b)} \\ \text{tension} \\ \text{/14/} \end{array}$$

With the introduction of the parameter

$$\rho = \frac{PL^2}{\pi^2 EI}$$

the stability functions of eq. 7-6 can be represented graphically as shown in figure 7-3 /14/.

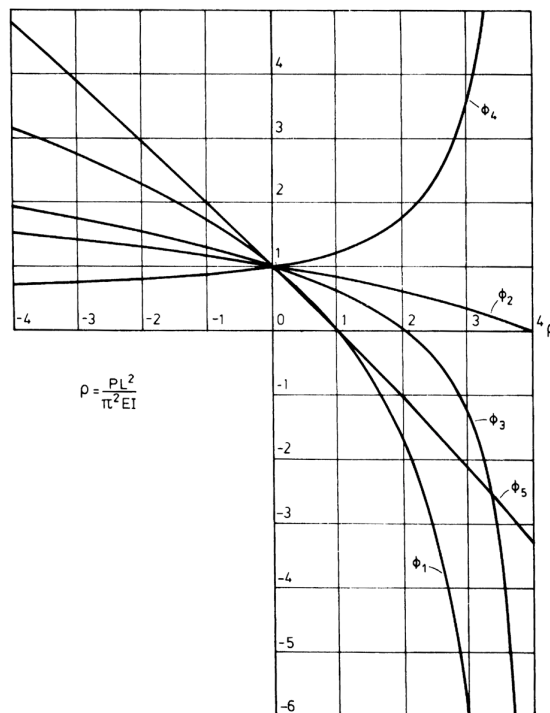


Figure 7-3 Graphical representation of the stability functions /14/.  
 Compression:  $\rho > 0$ ; Tension:  $\rho < 0$

The described formulation of the geometrical non-linearity implemented in GCA is complex, with the normal force being implicitly included in the stability functions. A more common, approximate form can be achieved using a third degree polynomial. The main benefit of the approximate form is explicit inclusion of the normal force in a geometrical stiffness matrix, which would be more convenient to implement. However, such an approximation will result in a need of smaller beam

elements, especially in the situation of increasing temperatures. So the main benefit of the formulation described, is that more accurate results can be obtained using large elements. For assessment and storage of temperature gradients, strains, stresses and modulus of elasticity, a cross-sectional division of beams is done at each beam node.

The total strain can be written as:

$$\varepsilon_{total} = \varepsilon_{\sigma} + \varepsilon_{thermal} + \varepsilon_{creep} \quad (\text{eq. 7-7})$$

The temperature-dependent thermal strain is determined according to Eurocode 3:

$$\begin{aligned} \varepsilon_{thermal} &= 1.2 \cdot 10^{-5} T + 0.4 \cdot 10^{-8} T^2 - 2.416 \cdot 10^{-4}; & 20^{\circ}\text{C} \leq T < 750^{\circ}\text{C} \\ \varepsilon_{thermal} &= 1.1 \cdot 10^{-2}; & 750^{\circ}\text{C} \leq T \leq 860^{\circ}\text{C} \\ \varepsilon_{thermal} &= 2 \cdot 10^{-5} T - 6.2 \cdot 10^{-3}; & 860^{\circ}\text{C} < T \leq 1200^{\circ}\text{C} \end{aligned} \quad (\text{eq. 7-8})$$

The total cross-sectional strains are given by the calculated deformations from the system analyses in each iteration as:

$$\varepsilon_{total} = \frac{du}{dx} - y \frac{d^2v}{dx^2} \quad (\text{eq. 7-9})$$

Modelling the creep strain has been excluded from the current GCA analyses, since effects of creep are included in the Eurocode 3 definition of the stress-related strain. Creep strain models in general often generates a large discrepancy between measured and predicted results.

The stress-related strain is determined from:

$$\varepsilon_{\sigma} = \varepsilon_{total} - \varepsilon_{thermal} \quad (\text{eq. 7-10})$$

The stress-related strain can be divided into elastic and plastic components.

For each cross-sectional point of all members in the system the stress-related strains are inserted in the temperature-dependent expression describing the stress and modulus of elasticity as given by Eurocode 3 (see figure 7-4). The number of points in the vertical direction of a beam cross-section is typically between 30-40. A member has two nodes, resulting in a need for 60-80 vertical cross-sectional points per member for storage of *temperature*, *total strain*, *stress-related strain*, *thermal strain*, *stress* and *modulus of elasticity*. So for one member about 360-480 values are stored. With each structural member node having its own neutral layer at any given time, the neutral layer-related contribution from a member to the system matrix must be transposed to a mutual reference point in order for the solved system deformations to be equally related to nodes belonging to more than one member. The reference point is chosen as the centroid of profiles. This means that two beams of different height are connected so that the centroid of both members are located in the same global node.

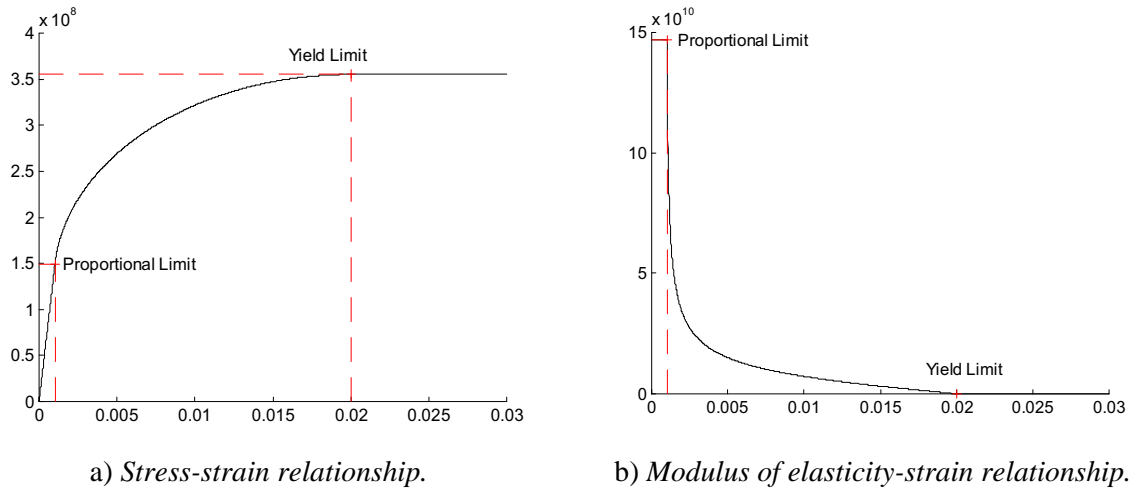


Figure 7-4 Description of proportional and yield limits for stress-strain and modulus of elasticity-strain curves at 20 °C. /1/

The influences of the temperature and the escalating deformations are obvious when following the decrease of the cross-sectional modulus of elasticity in figure 7-4 b. Load-bearing capacity is continuously lost as the time of the fire scenario proceeds. Eventually the stiffness of the member will be insufficient for provision of structural integrity under the applied loads.

The stiffness contribution etc. from each member is then defined according to eq. 7-5, transposed from the neutral layer of each adjacent member to a fixed point and then assembled to the global system matrix. It should be emphasised that it is the modulus of elasticity and not the stress component that is explicitly used to define the system matrix, although there is a relationship between stress and modulus of elasticity as given by the Eurocode relationship.

For each time step, each constitutive iteration and each geometrical second-order iteration the finite element system is solved.

$$\mathbf{K}(\mathbf{a})_{n+1}^{i,j} \mathbf{a}_{n+1}^{i+1,j+1} = \mathbf{f}(\mathbf{a}, \mathbf{K})_{n+1}^i \quad (\text{eq. 7-11})$$

where

- K** = global system matrix
- a** = global displacement vector
- f** = global load vector
- n* = time step number
- i* = constitutive iteration number
- j* = geometrical stability iteration number

While in linear problems the solution is unique this is not the case in many non-linear situations. A solution achieved may not necessarily be the solution sought. Different procedures with repeated solution of linear equations may have to be considered for different problems.

There are no convergence problems involved in the geometrical, second-order iteration procedure. However, the constitutive non-linearity is of very complex nature. One important reason is that stress-related strains in certain cross-sectional points can be either increasing or decreasing, even if temperature is constantly increasing and the loading is constant.

Another problem is that the temperature-dependent reduction of modulus of elasticity is different than the yield stress reduction.

The iteration process in GCA is a modification of direct(Picard) iteration that has proven more successful than the traditional Newton-Raphson method with stress-related strains possibly changing from decreasing to increasing during heating. The properties verified against convergence criteria can be set to any combination of allowed stress and displacement deviation to allow for different conditions. A compressed column with a free end would typically converge with displacements chosen as main criterion whereas the stress criterion would be better suited for a freely supported beam with large displacements near the time of collapse.

In the case of pure direct iteration  $\mathbf{a}_n = \mathbf{0}$  would be taken and the iteration process would proceed without increments as

$$\mathbf{a}_{n+1}^{i+1} = [\mathbf{K}(\mathbf{a})_{n+1}^i]^{-1} \mathbf{f}(\mathbf{a})_{n+1}^i \quad (\text{eq. 7-12})$$

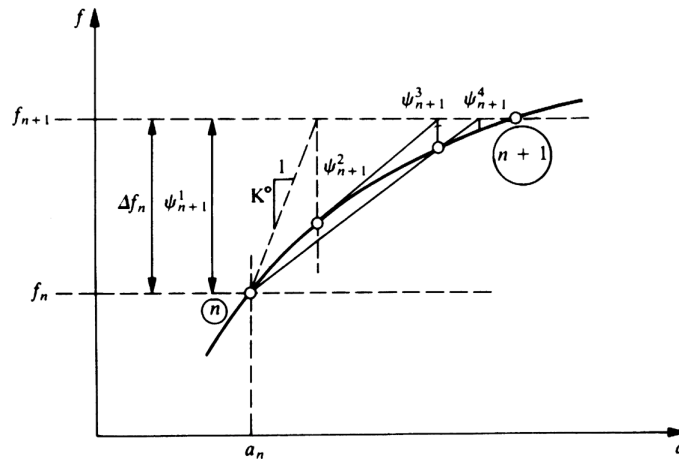


Figure 7-5 Generic description of direct iteration for external forces. /5/

In the GCA iteration procedure, the path-dependency is stored in the system matrix, the displacement vector and corresponding total strains derived from previous time step. When entering a new time step, the system matrix of the first constitutive iteration is derived from the total strains of the last time step and the thermal strains of the updated temperature field. The system is then solved as described in eq. 7-12, but considering boundary conditions.

Global and local collapse analysis is governed by the determinant and the eigenvalue problem according to eq. 7-13, considering boundary conditions. Both are performed in each constitutive iteration of each time step.

$$(\mathbf{K} - \lambda \mathbf{I}) \mathbf{a} = \mathbf{0} \quad (\text{eq. 7-13})$$

where

- $\mathbf{I}$  = unity matrix
- $\lambda$  = eigenvalue

## 7.2 TCD - FIRE DESIGN

FIRE DESIGN is a set of structural fire design tools that are interfaced with SUPER-TEMPCALC in the application TCD (Temperature Calculation and Design) /13/. The tools are SBEAM, CBEAM and COMPRES. The governing equations and the background theory for the calculations undertaken in FIRE DESIGN are outlined in this section. Output from SUPER TEMPCALC provides the essential heat transfer data upon which the FIRE DESIGN calculations are based. The design principals follow the intentions in the Eurocode documents ENV 1991-1-2, ENV 1992-1-2, ENV 1993-1-2 and ENV 1994-1-2.

For beams and slabs no second order geometry effects apply and thus the load bearing capacity (moment capacity) of a member can be calculated solely by studying the cross-section and its temperatures and strength relations.

### 7.2.1 SBEAM

SBEAM calculates the moment capacity of fire exposed structural steel beams in the ultimate limit state. Steel is an isotropic material with equal tensile and compressive properties. Hence the plastic sagging bending moment capacity of a beam is calculated based on the tensile capacity at elevated temperatures in the lower part of the beam cross-section and similarly the compressive capacity in the upper part. For some calculations documented in this report, SBEAM has been used to calculate the moment capacity of cast iron structures with different compressive and tensile properties. In such cases, the lower tensile capacity of cast iron has been used for the complete sections.

The neutral axis is determined so that cross-sectional equilibrium of forces

$$\sum F = 0 \quad (\text{eq. 7-14})$$

is maintained throughout. The neutral axis deviates from the geometrical centre of gravity when an unsymmetrical temperature gradient develops in the cross-section.

$$\rightarrow \sum_{i=1}^n f_{ay} k_{a,f}(T_i) A_i = 0 \quad (\text{eq. 7-15})$$

/ENV1993-1-2  
section 4.2.3.3/

When the neutral axis is determined the moment capacity is calculated using:

$$M_{cap} = \sum_{i=1}^n f_{ay} k_{a,f}(T_i) A_i y_i \quad (\text{eq. 7-16})$$

/ENV1993-1-2  
section 4.2.3.3/

where

- $M_{cap}$  = moment capacity in fire
- $f_{ay}$  = structural steel design yield strength
- $k_{a,f}(T_i)$  = structural steel strength reduction factor with respect to temperature  $T_i$
- $T_i$  = temperature of finite element  $i$
- $A_i$  = area of finite element  $i$
- $y_i$  = lever arm between neutral axis and centroid of finite element  $i$

Based on the characteristic yield strength values, the design strength in fire design can be calculated using equation 7-17. The material design strength values for fire design should be employed in equations 7-15 and 7-16.

$$f_{d,fi} = \frac{f_{c,fi}}{\gamma_{n,fi} \gamma_{m,fi}} \quad (\text{eq. 7-17})$$

where

- $f_{d,fi}$  = design material strength in fire design
- $f_{c,fi}$  = characteristic material strength in fire design
- $\gamma_{m,fi}$  = material partial safety coefficient in fire design
- $\gamma_{n,fi}$  = partial safety coefficient with respect to safety class in fire design

## 7.2.2 COMPRES

COMPRES calculates the:

- plastic yield compression resistance
- critical Euler buckling load
- design load

of fire exposed structural steel compression members in the fire limit state in accordance with the guidelines in Eurocode 3.

Each individual material is accounted for by considering its contribution to the overall strength and stiffness of the composite structure.

The plastic yield compression resistance (no consideration of flexural buckling) is calculated in accordance with equation 7-18.

$$N_{fi,pl.Rd} = \sum_j (A_{a,j} f_{ay,d} k_{a,f}(T_j)) \quad (\text{eq. 7-18})$$

/ENV1994-1-2  
Section 4.3.6.1/

where

- $A_{a,j}$  = area of structural steel finite element  $j$
- $f_{ay,d}$  = structural steel design yield strength
- $k_{a,f}(T_j)$  = structural steel strength reduction factor with respect to temperature  $T_j$

Based on the characteristic strength values, the design strength in fire design (fire limit state) can be calculated using equation 7-19. The material design strength values should be employed in equation 7-18.

$$f_d = \frac{f_c}{(\gamma_{m,fi})_f} \quad (\text{eq. 7-19})$$

where

- $f_d$  = design material strength  
 $f_c$  = characteristic material strength  
 $(\gamma_{m,fi})_f$  = material partial safety coefficient with respect to strength (=1.0)

The partial safety coefficient with respect to safety class is always equal to 1.0 in the fire limit state.

The total stiffness of the compression member is calculated by employing the expression in equation 7-20.

$$(EI)_{fi,eff} = \sum_j (\varphi_a E_{a,d} k_{a,E}(T_j) I_a) \quad (\text{eq. 7-20})$$

/ENV1994-1-2  
section 4.3.6.1/

where

- $\varphi_a$  = reduction coefficient depending on the effect of thermal stresses for structural steel.  
 $E_{a,d}$  = design modulus of elasticity for structural steel  
 $k_{a,E}(T_j)$  = steel modulus of elasticity reduction factor with respect to temperature  $T_j$   
 $T_j$  = temperature of structural steel finite element  $j$   
 $I_a$  = moment of inertia around neutral layer of structural steel finite element  $j$

Based on the characteristic modulus of elasticity values, the design strength in fire design (fire limit state) can be calculated using equation 7-21. The material design modulus of elasticity values should be employed in equation 7-20.

$$E_d = \frac{E_c}{(\gamma_{m,fi})_E} \quad (\text{eq. 7-21})$$

where

- $E_d$  = design modulus of elasticity  
 $E_c$  = characteristic modulus of elasticity  
 $(\gamma_{m,fi})_E$  = material partial safety coefficient with respect to modulus of elasticity (=1.0)

Based on the stiffness and the critical buckling length in the fire limit state,  $l_{\theta}$ , the critical Euler buckling load can be calculated in accordance with equation 7-22. The critical buckling length in the fire limit state can be determined from ENV 1994-1-2 section 4.3.6.1.

$$N_{fi,cr} = \frac{\pi^2 (EI)_{fi,eff}}{l_{\Theta}^2} \quad \text{(eq. 7-22)}$$

/ENV1994-1-2  
section 4.3.6.1/

The plastic yield compression resistance (eq. 7-18) is the theoretical failure load for structures with a slenderness ratio below 1.0, whilst the Euler buckling load (eq. 7-22) applies for slenderness ratios above 1.0.

For design purposes, however, a design equation has been assessed which consistently keeps the design load below the yield compression resistance as well as the Euler buckling load. The design load is determined by applying a reduction factor,  $\chi$ , on the yield compression resistance.

$$N_d = (\chi/1.2)N_{fi,pl.Rd} \quad \text{(eq. 7-23)}$$

/ENV1994-1-2  
section 4.3.6.1/

The factor  $\chi$  is a function of the slenderness ratio. It can be obtained in ENV 1993-1-1 or in BSK 94 (named  $\omega$  in BSK 94). The constant 1.2 is a correction factor that allows for a number of effects, including the difference in the strain at failure compared to yield strain. The value is empirical.

$$N_d = (\chi/1.2)N_{fi,pl.Rd} \quad \text{(eq. 7-24)}$$

/ENV1993-1-1  
section 5.5.1.2/

The reduction factor for the relevant buckling mode is defined as

$$\chi = \frac{1}{\Phi + \sqrt{\Phi^2 - \bar{\lambda}_{\Theta}^2}} \quad \text{(eq. 7-25)}$$

with

$$\Phi = 0.5(1 + \alpha(\bar{\lambda}_{\Theta} - 0.2) + \bar{\lambda}_{\Theta}^2) \quad \text{(eq. 7-26)}$$

/ENV1993-1-1  
Section 5.5.1.2/

The imperfection factor  $\alpha$  is taken from buckling curve c in fire

$$\alpha = 0.49 \quad \text{(eq. 7-27)}$$

ENV1993-1-1  
section 5.5.1.2

The slenderness ratio in the fire limit state is calculated according to equation (7-28).

$$\bar{\lambda}_{\Theta} = \sqrt{\frac{N_{fi,pl.Rd}}{N_{fi,cr}}} \quad \text{(eq. 7-28)}$$

ENV1994-1-2  
Section 4.3.6.1



## 8 Structural Analyses of Columns

### 8.1 Simulations

#### 8.1.1 Structural Behaviour for Partially Exposed Columns

The behaviour and collapse mode of partially exposed columns have been studied in 80 computer simulations with centric loading. In the simulations of no eccentricity, the combinations of percent exposed area, slenderness and axial load are presented in tables 8-1 – 8-5. In these tables the times at collapse obtained from the GCA-analysis are presented.

The fire exposure was 120 minutes ISO 834. Modelled steel profile was HEB 300 that was insulated with 0.93 mm of intumescent paint in order to extend the overall time to collapse for the purpose. Structural steel with a yield strength of 390 MPa was chosen. The degree of loading in the fire limit state is expressed as a percentage of the characteristic buckling compression resistance load at room temperature.

Exposure	Slenderness = 0 (L=0.3 m)			
	25% load	40% load	50% load	60% load
	1.39 MN	2.23 MN	2.78 MN	3.34 MN
100 %	54	36	26	17
83 %	59	50	34	20
50 %	65	59	53	34
19 %	>120	>120	106	84

Table 8-1 Calculated fire resistance times for a slenderness  $\lambda \approx 0$ .

Exposure	Slenderness = 0.5 (L=2.37 m)			
	25% load	40% load	50% load	60% load
	1.23 MN	1.96 MN	2.45 MN	2.95
100 %	54	38	22	17
83 %	58	45	33	20
50 %	59	53	39	23
19 %	>120	114	95	71

Table 8-2 Calculated fire resistance times for a slenderness  $\lambda = 0.5$ .

Exposure	Slenderness = 0.75 (L=3.56 m)			
	25% load	40% load	50% load	60% load
	1.03 MN	1.66 MN	2.07 MN	2.48 MN
100 %	55	44	27	21
83 %	58	42	31	20
50 %	55	44	29	13
19 %	>120	100	77	48

Table 8-3 Calculated fire resistance times for a slenderness  $\lambda = 0.75$ .

Exposure	Slenderness = 1.0 (L=4.74 m)			
	25% load 0.80 MN	40% load 1.28 MN	50% load 1.60 MN	60% load 1.92 MN
100 %	57	51	41	29
83 %	56	42	31	20
50 %	47	35	30	8
19 %	118	92	65	38

Table 8-4 Calculated fire resistance times for a slenderness  $\lambda = 1.0$ .

Exposure	Slenderness = 1.5 (L=7.11 m)			
	25% load 0.45 MN	40% load 0.71 MN	50% load 0.89 MN	60% load 1.06 MN
100 %	60	54	51	45
83 %	53	41	32	22
50 %	39	25	18	8
19 %	107	88	62	36

Table 8-5 Calculated fire resistance times for a slenderness  $\lambda = 1.5$ .

From the tables it can be observed that minimum time for collapse occurs at about 50% of partial exposure with a slenderness exceeding 0.5. The reason for this exception is that virtually no buckling occurs but only axial compressive stresses arise. However, the thermal gradient causes thermal bending and an extra eccentricity for the axial load. Due to that the horizontal deformation and the eccentricity increases when exposed area decreases from 100 % to 50 %. This means that partial exposure may cause earlier collapse of the column compared with full exposure.

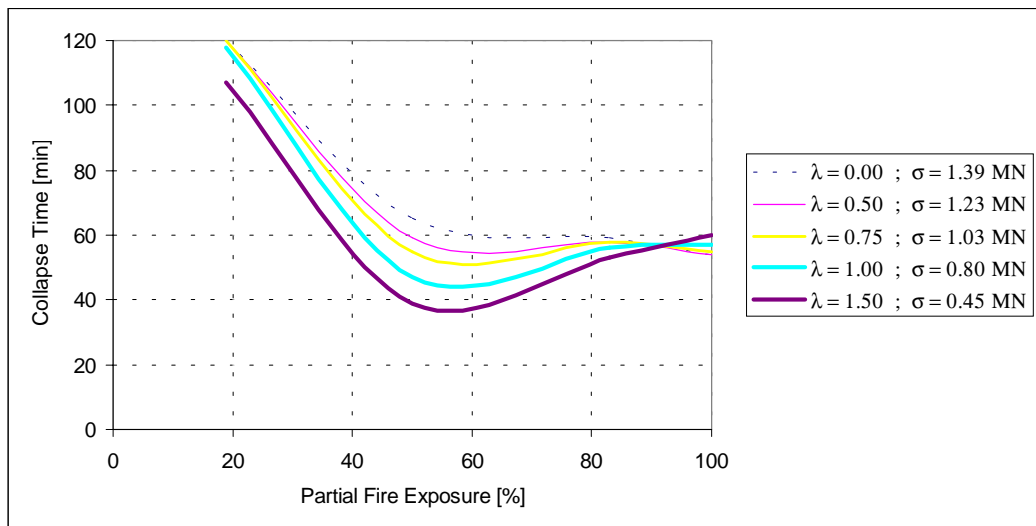


Figure 8-1 Calculated column fire resistance times with a degree of loading of 25%.

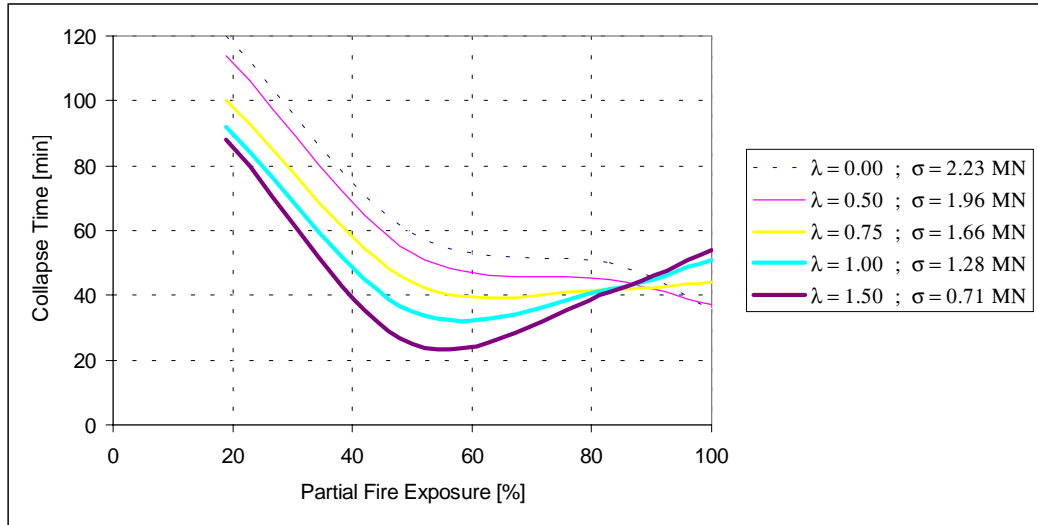


Figure 8-2 *Calculated column fire resistance times with a degree of loading of 40%.*

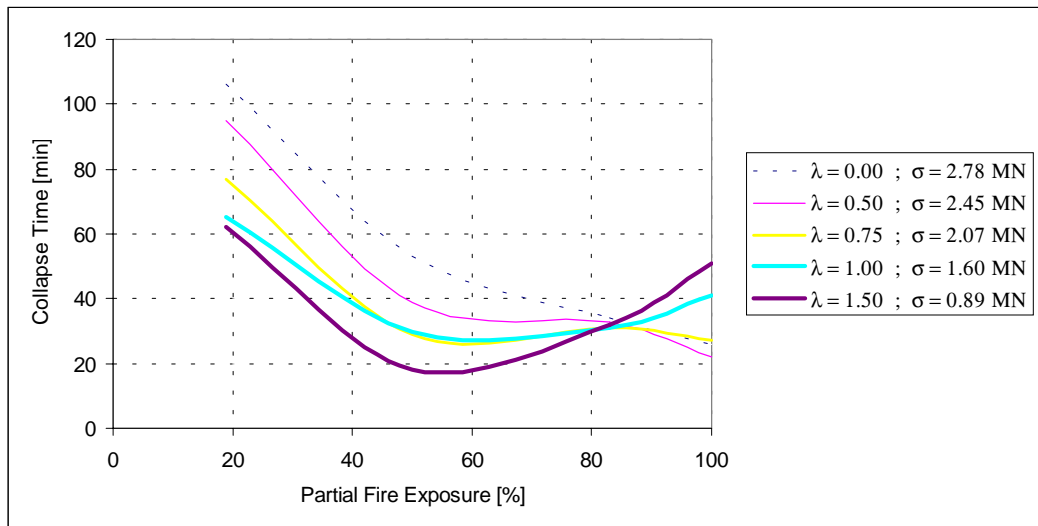


Figure 8-3 *Calculated column fire resistance times with a degree of loading of 50%.*

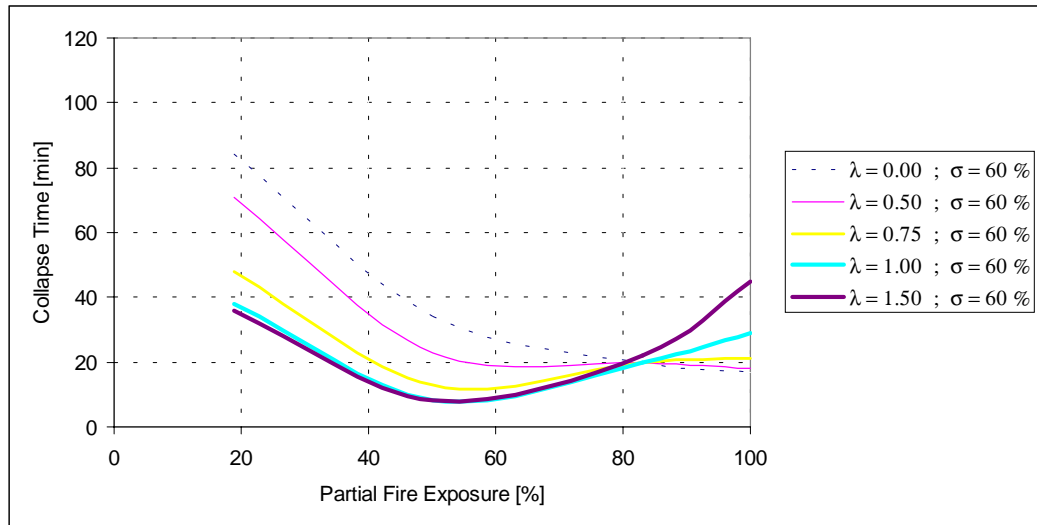


Figure 8-4 Calculated column fire resistance times with a degree of loading of 60%.

### 8.1.2 Structural Behaviour of Columns with Eccentric Loads

The behaviour and collapse mode of eccentrically loaded columns have been studied in 8 computer simulations. The results in terms of collapse time are presented in table 8-6.

The fire exposure was 120 minutes ISO 834. Modelled steel profile was HEB 300 that was insulated with 0.93 mm of intumescent paint. Structural steel with a yield strength of 390 MPa was chosen. The degree of loading, expressed as a percentage of the design load, was set to 40%. Eccentricities studied were +/- 3 cm and +/- 5 cm.

Slenderness	100% exposure, 40% load				
	e = +5 cm	e = +3 cm	e = 0	e = -3 cm	e = -5 cm
1.0 (1.28 MN)	37	42	51	52	49
1.5 (0.71 MN)	51	52	54	57	56

Table 8-6 Calculated fire resistance times for the different combinations of eccentricity and slenderness.

As expected, eccentricities adding moment in the same direction as the thermal bending, governed by the initial out-of straightness for the 100 % exposure case, resulted in shorter resistance times. With load eccentricities oriented so that a moment, acting opposite the thermal movement, is added, the resulting resistance times were longer. The -3 cm eccentricity even resulted in a minute more before collapse compared to the case with completely centric load.

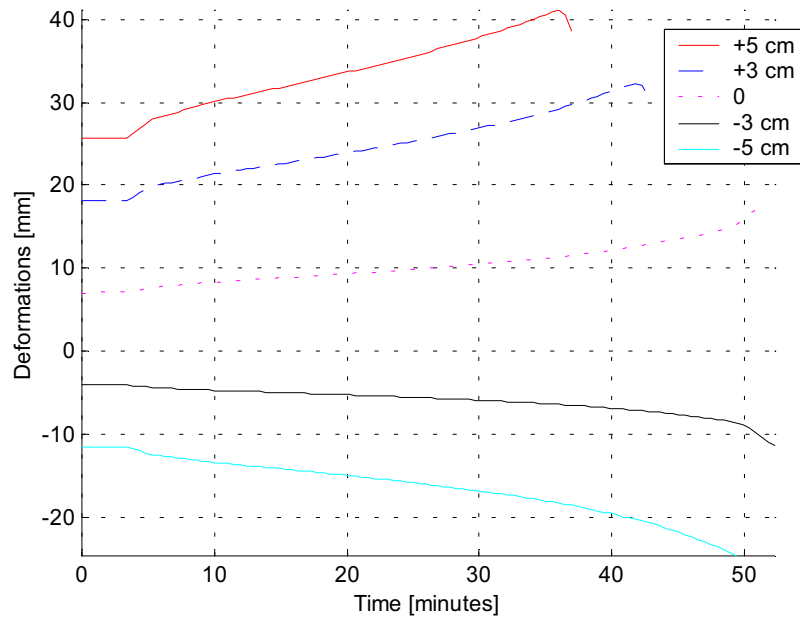


Figure 8-5 Calculated lateral displacements for different cases of load eccentricities and slenderness  $\lambda = 1.0$ .

### 8.1.3 Columns with Partially Restrained Axial Elongation

Four complementary analyses were done to evaluate the theoretical performance of partially restrained columns. The results are presented in table 8-7 and figures 8-7 – 8-8. The fire exposure was 120 minutes of ISO 834. Modelled steel profile was HEB 300 that was insulated with 0.93 mm of intumescent paint. Structural steel with a strength of 390 MPa was chosen. The degree of loading, expressed as a percentage of the characteristic buckling compression resistance load at room temperature, was chosen to 40% of the of column's capacity. The initial degree of axial freedom of movement was set to 80%, 90% and 100%.

The modelling of partially restrained elongation was done by connecting a beam to the top of the column according to *Fire Engineering Design of Steel Structures* /3/ (see figure 8-6). The modelled beam can be either exposed or unexposed. The beam was modelled as exposed in order to better preserve the initial conditions.

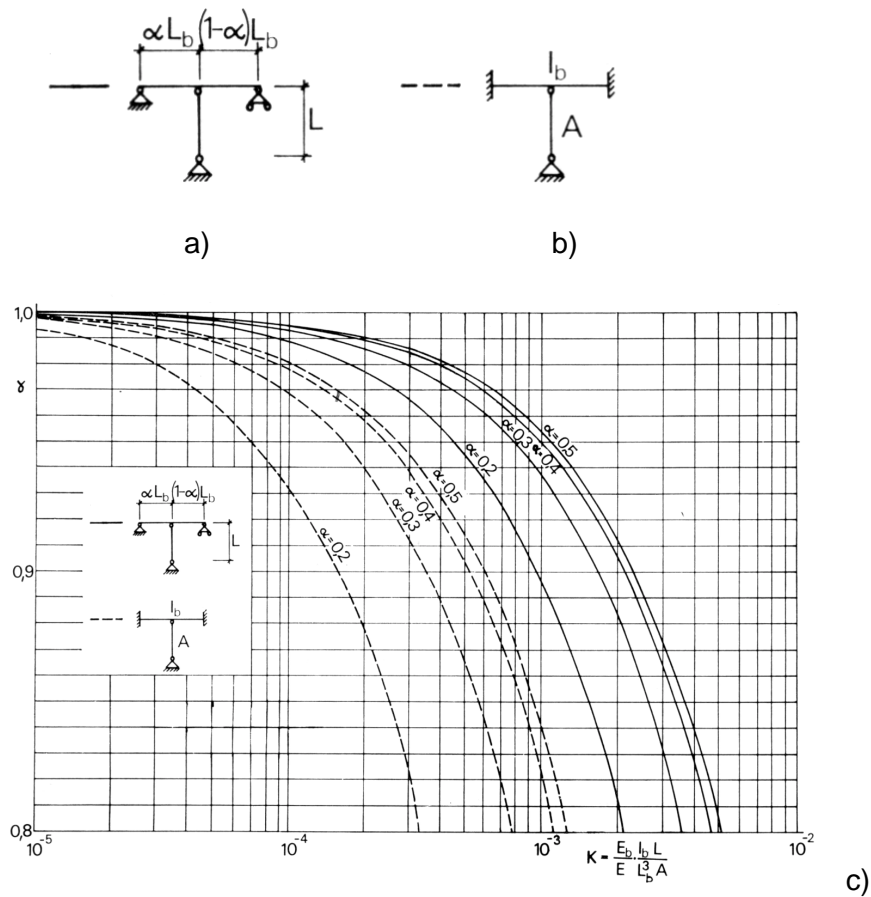


Figure 8-6 A method of modelling a partially restrained column as defined in *Fire Engineering Design of Steel Structures* /3/. With defined column, axial restraint, restraining beam cross-section and stiffness, the appropriate beam length can be determined (with the parameters  $\alpha$  and  $K$  taken from curve c) as

$$L_b = \left( \frac{E_b I_b L}{KEA} \right)^{1/3}$$

The axial deformations of the simulations of partially restrained elongation that can be found in table 8-7, resulted in apparent shorter fire resistance times. It should be pointed out that since the restraint was modelled using a beam rigidly restrained at both ends small lateral displacements were achieved. The given degree of axial freedom is valid at the start of the fire scenario after which it decreases due to more loss of resistance in the column than in the modelled beam during the scenario.

One verification analysis was done with the modelled beam unexposed. The fire resistance time was only 2 minutes shorter in general. As expected, the stiffness ratio between the column and the beam was the same at the time of collapse as for the examples with the beam exposed. Moreover, the path was very similar, implying that this ratio changes mainly at the time shortly before collapse of the column.

Column	Axial freedom of movement at start time		
	$\gamma = 0.8$	$\gamma = 0.9$	$\gamma = 1.0$
Slenderness=0.5 (L=4.74) (1.28 MN)	20*	25*	38
Slenderness=1.0 (L=2.37) (1.96 MN)	28*	38*	51

Table 8-7 Calculated fire resistance times for the different combinations of axial freedom of movement and slenderness.

\*True collapse not reported until later, but this time refers to the time of lost capacity.

The used restraint model involving a beam may be suited to determine the axial degree of freedom at any given time. However, the model is limited for theoretical studies of fixed partial restraint of columns and it is obvious that fixed partial restraint situations would not occur in any real fire scenario.

The resulting axial deformation plots for a slenderness of 1.0 and 0.5, presented in figures 8-7 – 8-8 respectively, indicate what appears to be sudden structural failure of restrained columns.

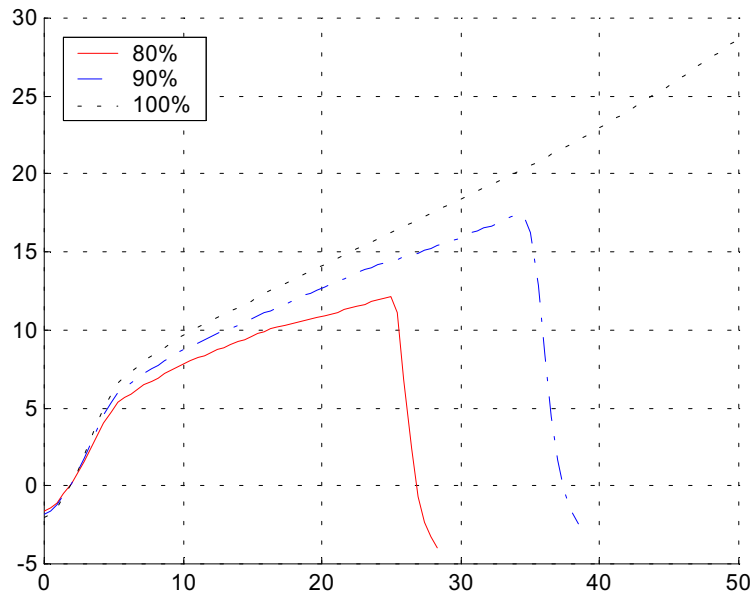


Figure 8-7 Calculated axial deformations over time for initial axial degrees of freedom between 80% and 100% and a slenderness  $\lambda = 1.0$ . [minutes, mm]

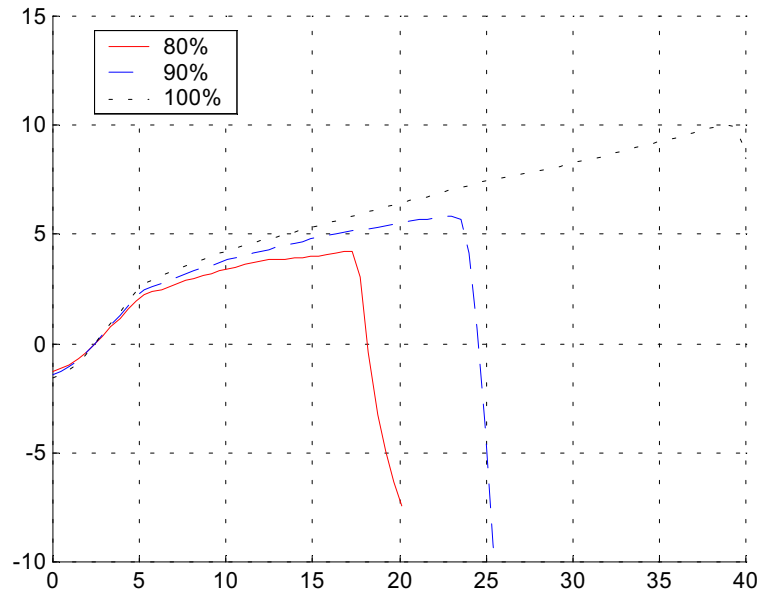


Figure 8-8 *Calculated axial deformations over time for initial axial degrees of freedom between 80% and 100% and a slenderness  $\lambda = 0.5$ . [minutes, mm]*

It was concluded that the true degree of axial freedom decreases with increasing steel temperatures. Observations related to the decrease in axial freedom involve two effects in opposition to each other in terms of performance of partly restrained columns during fire and one effect that was found to be advantageous to the overall performance of the loadbearing system.

In one of the analyses with slenderness 0.5 the axial degree of freedom was kept at the initially set 80% for 16.8 minutes exposure after which it suddenly dropped towards zero. In reality this would mean that the initial boundary condition at the column-beam connection changes from being almost rigid to nearly fixed before the time of column collapse. In a design situation this in turn would mean that an exaggerated buckling length was being used in fire design, that does not correspond to the actual collapse state. The initial degree of axial freedom can not necessarily be separated into a relevant criteria for a fire-exposed member, since its progress is determined by the structure providing the restraint as well as the interaction between the two. Possible design criterias should focus on the final degree of freedom near the fire-related collapse.

The decreasing degree of axial freedom and the resulting, near-fixed connection, at the time of collapse will on the other hand help generating large thermal stresses in fire that can be critical and that are not always considered in fire design.

The third effect observed was load redistribution. During and after the sudden drop of stability of the column, loads are redistributed to the modelled beam. The column almost reaches collapse state before all of the applied load is redistributed to the modelled beam. In order to reach true column collapse near the time of sudden loss of loadbearing capacity it may be necessary to raise the load a little above the capacity of the beam alone, but the resulting state of the column has to be regarded as collapse.

The results from the analyses indicate that the disadvantageous effect of increased thermal stress may surpass the advantageous effect of the reduced buckling length. On the other hand, the increased restraint does increase the degree of load redistribution to the rest of the structural system. In order



to take advantage of load redistributions for design purposes the degree of redistribution needs to be quantified. The results from these analyses of initially restrained columns were considered for modelling strategies of the following frame analyses.

### 8.1.4 Verification of Steel Quality, Profile Type and Slenderness as Design Parameters for Columns

The different behaviour with equal slenderness and degree of loading were studied for two different profiles and two steel qualities in 32 computer simulations with no eccentric loads.

The steel quality and profile verification simulations were done to find possible deviations between the design approach and the physical model used for all analyses. The actual behaviour of two different steel structures with equal slenderness and loading degree, but with different values of strength can never be the same, mainly because the decrease in modulus of elasticity does not follow that of yield strength. The purpose of the verification is to determine if the proportions of the fire resistance times due to this deviation may be significant.

The fire exposure was 120 minutes of ISO 834. Modelled steel profiles were HEB 200 and HEB 300, insulated with 0.93 mm of intumescent paint. Structural steel with yield strength values of 260 MPa and 390 MPa were chosen. Applied degree of loading is expressed as a percentage of the characteristic buckling compression resistance load at room temperature.

The results, presented in tables 8-8 – 8-11, indicate that the choice of material quality has little effect for the resistance time in the studied interval with steel strength values between 260-390 MPa. The profile dimensions, on the other hand, did show slightly different behaviour for low load levels that could be investigated further. The higher temperatures developed in the HEB 200 profile ought to result in overall shorter fire resistance.

Steel	Profile: HEB 200, Slenderness = 0			
	25% load	40% load	50% load	60% load
fy =260 MPa	46 minutes (0.49 MN)	34 minutes (0.78 MN)	25 minutes (0.98 MN)	18 minutes (1.17 MN)
fy=390 MPa	47 minutes (0.73 MN)	37 minutes (1.17 MN)	28 minutes (1.46 MN)	20 minutes (1.76 MN)

Table 8-8 Calculated fire resistance times for HEB 200 profile of two different steel qualities and with a slenderness  $\lambda \approx 0$ . [Minutes]

Steel	Profile: HEB 200, Slenderness = 1.0			
	25% load	40% load	50% load	60% load
fy=260 MPa (L=3.82 m)	49 minutes (0.28 MN)	44 minutes (0.45 MN)	39 minutes (0.56 MN)	30 minutes (0.67 MN)
fy=390 MPa (L=3.12 m)	50 minutes (0.42 MN)	46 minutes (0.67 MN)	42 minutes (0.84 MN)	35 minutes (1.01 MN)

Table 8-9 Calculated fire resistance times for HEB 200 profile of two different steel qualities and with a slenderness  $\lambda = 1.0$ .

Steel	Profile: HEB 300, Slenderness = 0			
	25% load	40% load	50% load	60% load
$f_y=260$ MPa	53 minutes (0.93 MN)	34 minutes (1.49 MN)	25 minutes (1.86 MN)	14 minutes (2.23 MN)
$f_y=390$ MPa	53 minutes (1.39 MN)	36 minutes (2.23 MN)	27 minutes (2.78 MN)	16 minutes (3.34 MN)

Table 8-10 Calculated fire resistance times for HEB 300 profile of two different steel qualities and with a slenderness  $\lambda \approx 0$ .

Steel	Profile: HEB 300, Slenderness = 1.0			
	25% load	40% load	50% load	60% load
$f_y=260$ MPa (L=5.81 m)	56 minutes (0.53 MN)	49 minutes (0.85 MN)	37 minutes (1.07 MN)	29 minutes (1.28 MN)
$f_y=390$ MPa (L=4.74 m)	57 minutes (0.80 MN)	51 minutes (1.28 MN)	41 minutes (1.60 MN)	32 minutes (1.92 MN)

Table 8-11 Calculated fire resistance times for HEB 300 profile of two different steel qualities and with a slenderness  $\lambda = 1.0$ .

### 8.1.5 Verification of Applied Degree of Loading

A supplementing analysis of a previously studied column (HEB 300,  $f_y=390$  MPa, 100% exposure, slenderness=1.0) was done with loading degree increased to up to 80%. The results are compared in table 8-12.

0% load	25% load	40% load	50% load	60% load	70% load	80% load
-	0.80 MN	1.28 MN	1.60 MN	1.92 MN	2.24 MN	2.56 MN
-	57	51	41	29	24	19

Table 8-12 Calculated fire resistance times for a slenderness  $\lambda = 1.0$ .

### 8.1.6 Verification of Applied Design Load and Initial Out-of-straightness

Comparisons between applied degrees of loading as a percentage of the axial design load and corresponding maximum loads at room temperature, 20 °C, as calculated by GCA have been done for profile HEB 300 and steel with a yield strength of 390 MPa.

The maximum load as determined by GCA, compared to the characteristic buckling compression resistance, increases with increasing slenderness. This indicates that the slenderness dependence of the characteristic buckling compression resistance may be conservative at room temperature as well as for 100% exposure as was indicated by the results in section 8.1.1, even when a non-linear second-order model and a non-linear material model is applied.

For studied profile and steel quality a slenderness of 0.5 the GCA and design load approach resulted in almost equal maximum loads.

Slenderness $\lambda$ Column length	~0 (0.3 m)	0.5 2.37 m	0.75 3.56 m	1.0 4.74 m	1.5 7.11 m
Degree of loading according to GCA	Corresponding percentage of design load [Degree of Loading according to GCA*(Design Load/Max GCA load)]				
25 % load	26%	25%	24%	23%	22%
40 % load	41%	40%	38%	36%	35%
50 % load	52%	50%	48%	45%	44%
60 % load	62%	60%	57%	54%	53%

Table 8-13 *Degree of loading as determined by GCA compared to applied design loads for HEB 300 profile and steel with a yield strength of 390 MPa.*

The design value of the maximum load has been compared to the maximum load as determined by GCA using different models of the initial out-of-straightness and COMPRES (see section 7.2.2) with implemented and actual buckling curve.

In all column simulations in this report, the initial out-of-straightness has been set to L/400. In comparison to two different Eurocode-methods this has resulted in higher values of maximum load for studied column of profile HEB 300, yield strength 390 MPa and slenderness 1.0. With the maximum deflection set to L/400 a fair accordance can be achieved when simulating tests. The proposed Eurocode models may be well suited in a design situation, but would result in extremely short fire resistance times if used in non-linear analysis. One possible reason could be that some of the physical effects may be taken into account twice although the complete origin of the different out-of-straightness models must be evaluated in order to make any such conclusions.

In COMPRES, buckling curve c is used in fire design ( $\alpha=0.49$  see eq. 7-27). For the compared column, applicable buckling curve b in normal design has been compared as well ( $\alpha=0.34$ ).

Method	Design value 20°C	GCA L/400	GCA L/154*	GCA L/107**	COMPRES $\alpha=0.49$	COMPRES $\alpha=0.34$
<b>Max. load</b>	3.20 MN	3.54 MN	2.71 MN	2.36 MN	2.75 MN	3.03 MN
<b>%</b>	100%	111%	85%	74%	86%	95%

Table 8-14 *Maximum load as determined using different methods and initial-out-of-straightness models for a column of profile HEB 300, steel with yield strength 390 MPa and slenderness 1.0.*  
\*ENV 1993:2:1997 (5.2.4.3)  
\*\*ENV 1993-1-1:1992 (5.5.1.5)

## 8.2 Test

### 8.2.1 Temperature Simulation of Steel Column Fire Test Conducted in UK

A full scale fire test on a steel column exposed to fire on 100 % of the profile circumference that was tested at Firtro Borehamwood, U.K. in 1984 /9/ has been simulated. The test will be referred to as fire test 41. The column has an exposed length of 3 m. The temperature as function of time over the cross-section has been calculated by Super-Tempcalc. The fire exposure curve has been taken from documented readings during the tests and has been used in the calculations. The temperature for the

100 % exposure is presented in figure 7-8 where measured and computed temperatures are compared for the exposed web and unexposed flange respectively. The agreement between calculated and measured temperatures is considered adequate.

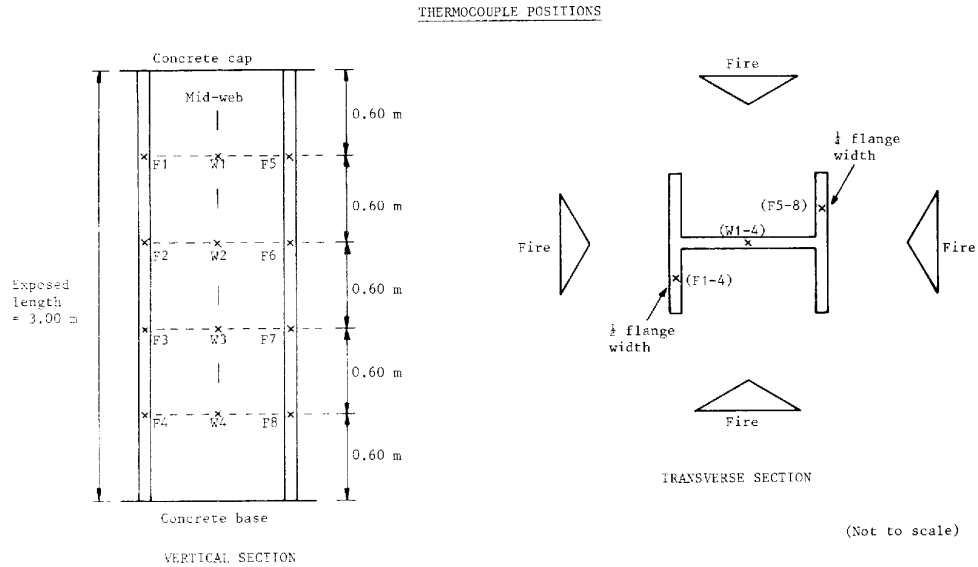


Figure 8-9 Description of fire test 41 on steel column ( $h*w*t_w*t_f = 206x204x8x12.5$  mm) fully fire exposed /3/

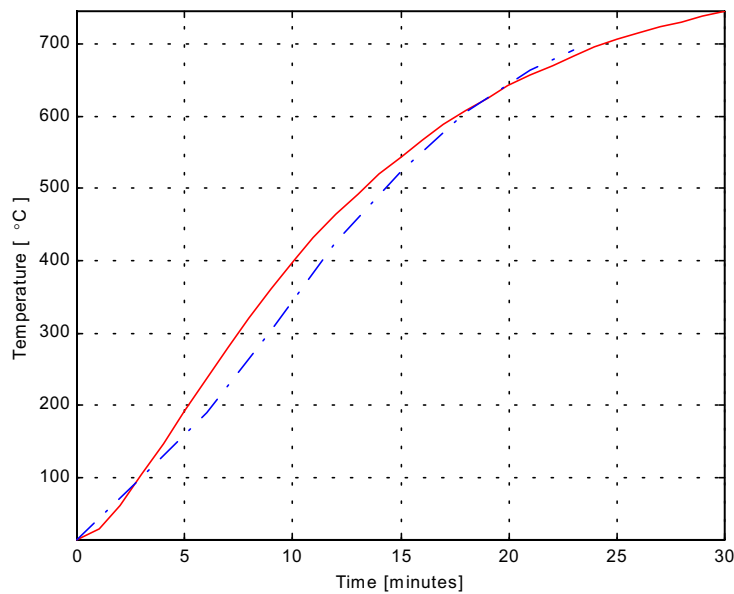


Figure 8-10 Comparison of predicted and measured temperature of fire exposed steel column ( $w*h*t_w*t_f = 204x206x12.5x8$  mm) web for fire test 41 under 100 % fire exposure. (Dashed line = measured, solid line = predicted)

The tested steel column has an effective length of 2.1 m (fully exposed). The slenderness ratio is 0.45 (weak axis) and 0.24 (strong axis) respectively i.e. a short column with almost no buckling influence. The deformation behaviour and the collapse time for the fire tested column (100% fire

exposure and 60% of allowed maximum load according to test standard) has been predicted by Global Collapse Analysis and compared with measured results.

The measured value of steel strength was 349 MPa, to be compared with the design value of 255 MPa. The actual degree of loading is therefore less than the allowed 60%. The actual, measured value of strength was used in the simulations. The modulus of elasticity modulus was set to 210 GPa since it was not measured during the test.

In figure 8-11 the predicted and measured axial deformation as function of time is compared. The concordance in deformation process is good and the collapse time is predicted to 19 minutes compared to the measured 23 minutes. Due to all testing uncertainties and the normal variation of results (sometimes up to 50% for columns) from fire testing on identical specimens this difference is quite acceptable.

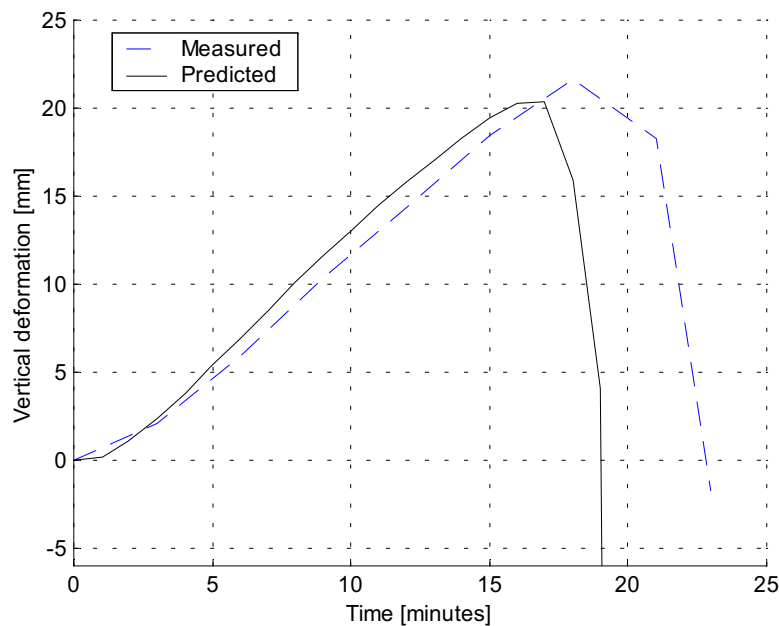


Figure 8-11 Measured axial deformations of column (fire test 41) compared to predicted.  
(Dotted line = measured, solid line = predicted)

A comparison was done with the column analysed using the tool COMPRES. With a measured initial value of steel strength the resistance time was determined to 22 minutes. For further comparisons the design value of steel strength resulted in a resistance time of 19 minutes. The design value is of little importance here since given another sample, the measured strength could be close to the design value.

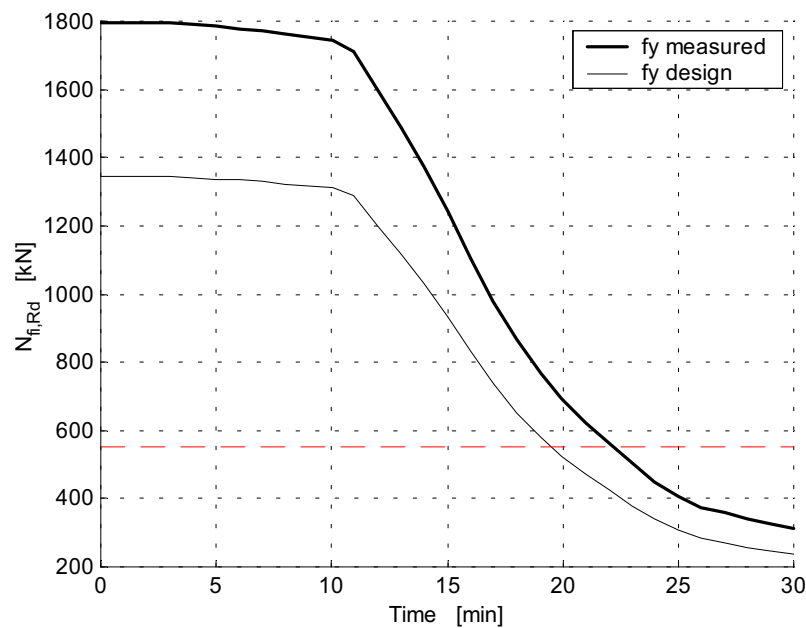


Figure 8-12 Loadbearing capacity as calculated by the design tool COMPRES. Only the measured strength value is valid when comparing with test.

## 9 Structural Analyses of Beams

### 9.1 Simulations

#### 9.1.1 Structural Behaviour for Partially Exposed Beams

The behaviour and collapse mode of simply supported and partially exposed beams of length 4 m have been studied in computer simulations using GCA.

Modelled steel profile was HEB 300 that was insulated with 0.93 mm of intumescent paint in order to extend the overall time to collapse for the purpose. The exposure was 120 minutes of standard ISO 834 fire. Structural steel with a yield strength of 390 MPa was chosen. The degree of loading, expressed as a percentage of the *characteristic* bending moment capacity at room temperature, was chosen to 60% (fire limit state).

The resulting fire resistance times are presented in table 9-1 in section 9.1.2.

The vertical displacements for the different scenarios can be found in figure 9-1. During the first 45 minutes the beam with 50% exposure deflects more due to the increased thermal moment. After 45 minutes the effect of loss in strength outweighs the effect of the thermal moment and the 75% and 100% exposed beams deflect more. As expected the beam subjected to fire on all sides reaches the chosen collapse criteria( $L/30$ ) first.

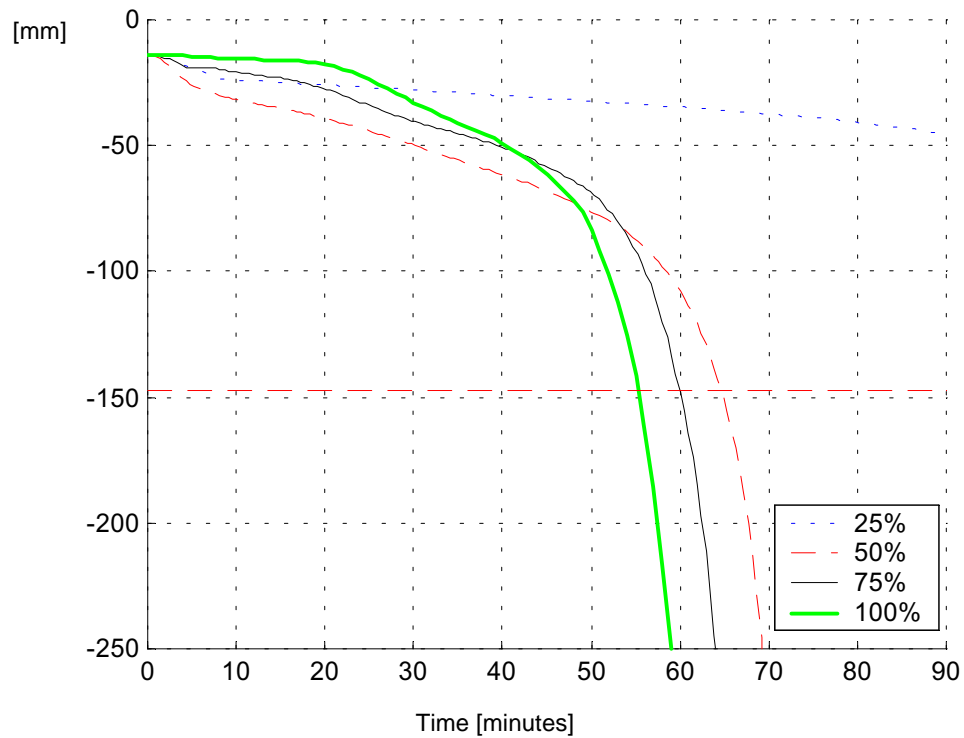


Figure 9-1 Vertical displacements at centre of span of beam HEB 300 subjected to exposure between 25-100% of the circumference.

### 9.1.2 Verification of Applied Design Load

Applied degrees of loading as percentage of the *characteristic* bending moment capacity at room temperature 20 °C have been verified according to Eurocode 3 /1/, using the tool SBEAM (see section 7.2.1). The fire resistance time comparisons are presented in table 9-1.

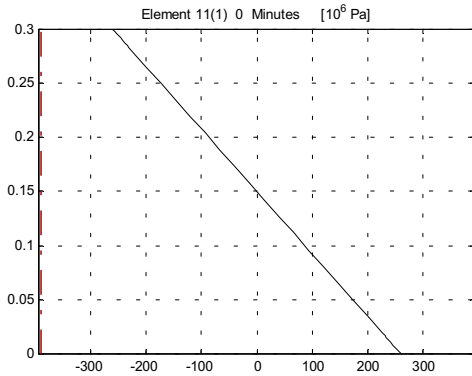
Since SBEAM considers the bending moment capacity only and not deflections and since the entire cross-section is allowed to reach yield, the small difference is not easy to explain. The fire resistance time for the fully exposed circumference was even 1 minute shorter with SBEAM. The thermal moment is what prevents similar deviations for the simulations with the beam partially exposed.

Exposure	Beam HEB 300, $f_y=390$ MPa, Load =60%, L=4 m			
	100%	83%	50%	19%
GCA	55 minutes	59 minutes	64 minutes	>>120 minutes
SBEAM	54 minutes	60 minutes	64 minutes	>>120 minutes

Table 9-1 Calculated fire resistance times for partially exposed beams. [minutes]

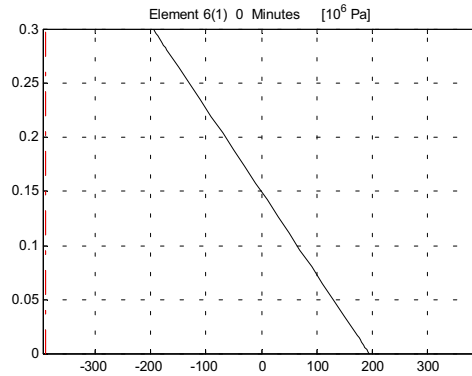
In order to verify a possible reason for the similar results using the different methods, the GCA-calculated cross-sectional stress distribution at mid-span and L/4-span is presented in figure 9-2 for 100% fire exposure at 3 different times. By studying the cross-sectional stress development in figure 9-2 it turns out that while beyond the proportional limit, no point has reached yield stress within the time set by the collapse criteria (L/30). This may be important since the cross-sectional design simplification assumes full yield in the entire cross-section at displacements that are only beyond the proportional limit (see figure 9-3).

**Cross-sectional stress distribution  
 at  $x=L/2$  (2 m)**

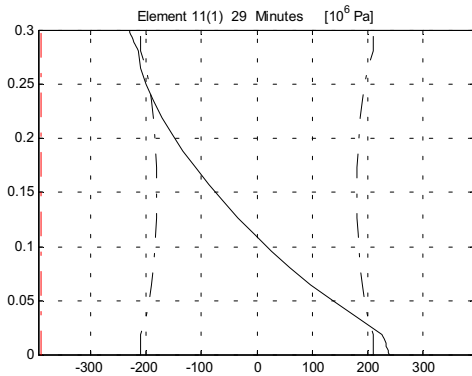


0 minutes

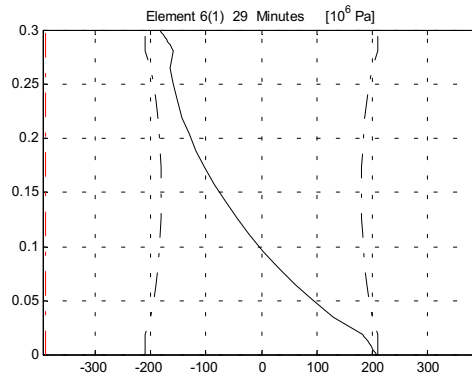
**Cross-sectional stress distribution  
 at  $x=L/4$  (1 m)**



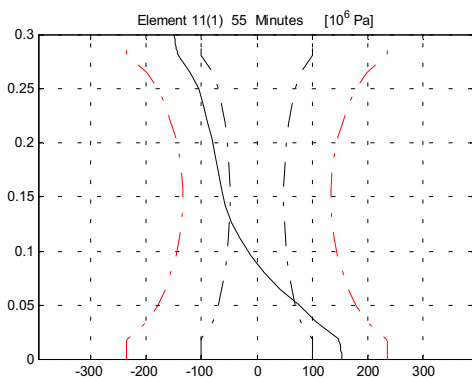
0 minutes



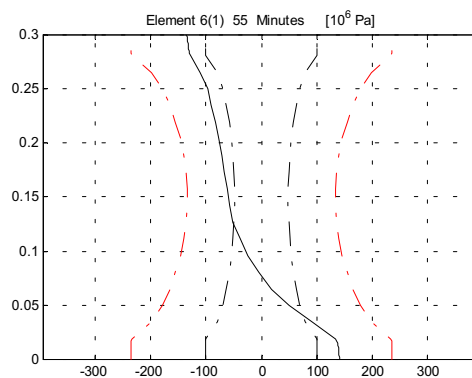
29 minutes



29 minutes



55 minutes



55 minutes

Figure 9-2 Cross-sectional stress-distribution(solid line) at  $x=L/2$  and  $x=L/4$  as calculated by GCA for the simulation with 100% exposure. Proportional limit: dash-dotted. Yield limit:dashed.



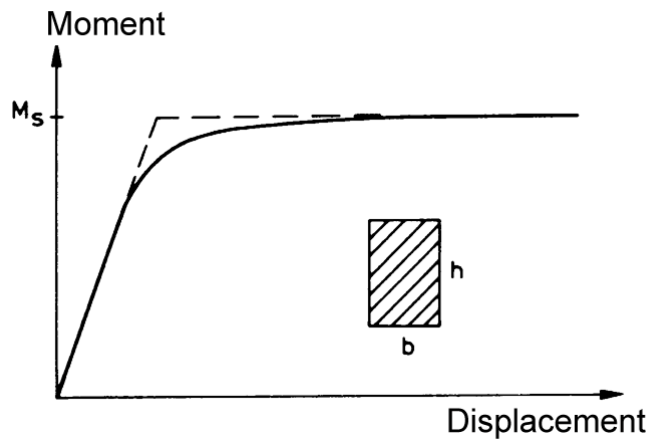
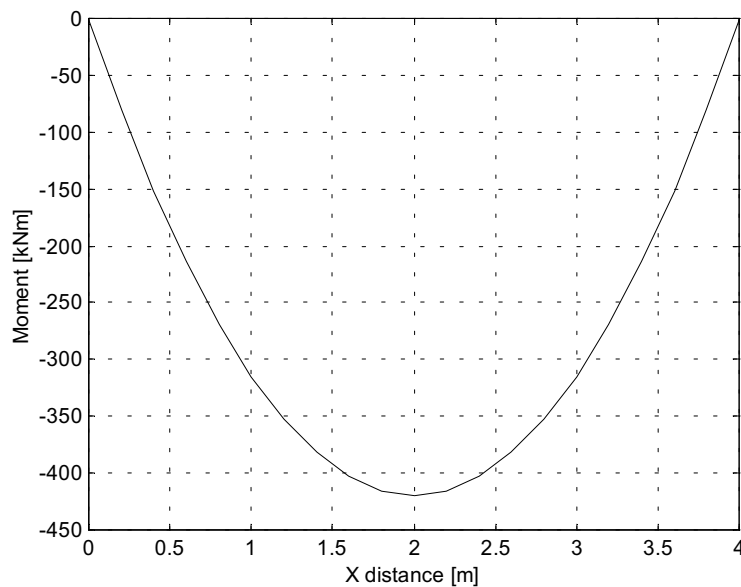


Figure 9-3 *The moment as function of displacement. The dashed line represents the usual simplification in design. Displacements beyond the proportional limit, but prior to the yield limit will be treated as fully yielded in a design situation at cross-sectional level.*

Finally the moment distribution over the beam length is shown in figure 9-5. At the time of the displacement-governed collapse, the moment capacity criteria is fulfilled.



55 minutes

Figure 9-4 *The moment in the beam length direction as calculated by GCA for the simulation with 100% exposure. Applied load  $q=209.4$  kN/m resulted in a maximum moment 418.8 kNm that is constant throughout the scenario. The moment calculated as  $qL^2/8$  is 419.5 kNm. The GCA error is +1.67%, which is not much considering the complex iteration procedure and the number of iterations.*

## 9.2 Test (Beam with Concrete Slab)

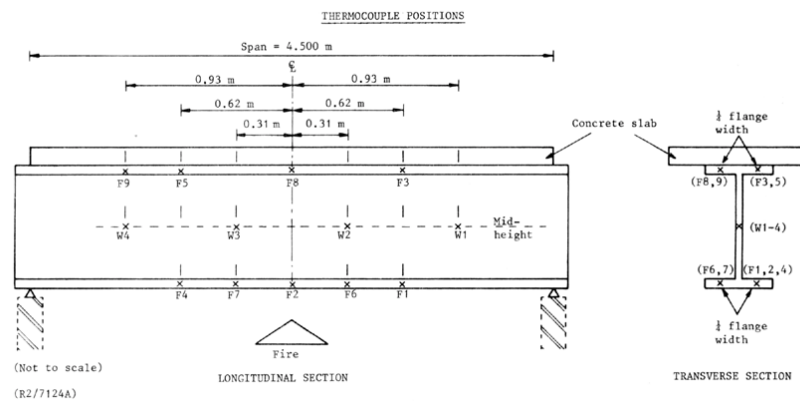


Figure 9-5 Description of fire test 11 on steel beam  $h*w*t_w*t_f = 256x145x7.47x12.79$  mm. /9/

### 9.2.1 Temperature Simulation of Steel Beam Fire Test Conducted in UK

A full scale fire test on a simply supported steel beam exposed to ISO fire on three sides and with a concrete slab cast onto the upper flange that was tested at Firtio Borehamwood, U.K. in 1984 /9/ has been simulated. This test will be referred to as fire test 11. The length of the beam was 4.5 m.

The standard ISO 834 gas temperature curve was used to simulate the fire test, but with modified values of radiation and convection in order to achieve relevant temperature gradient needed to evaluate the structural models.

With design values of emissivity and convection (see table 4-1), measured steel temperatures were lower than calculated. The temperature as function of time over the cross-section has been calculated by Super-Tempcalc. The temperatures at top flange, web and exposed bottom flange are presented in figure 9-6 where measured and calculated temperatures, that were applied to the structural analysis, are compared.

The structural resistance has been calculated using both the non-linear approach of GCA and the Eurocode 3 design method implemented in SBEAM. This was done in order to get an indication of whether the Eurocode 3 method, which does not include the effect of added thermal moment due to temperature gradient, can be considered relevant.

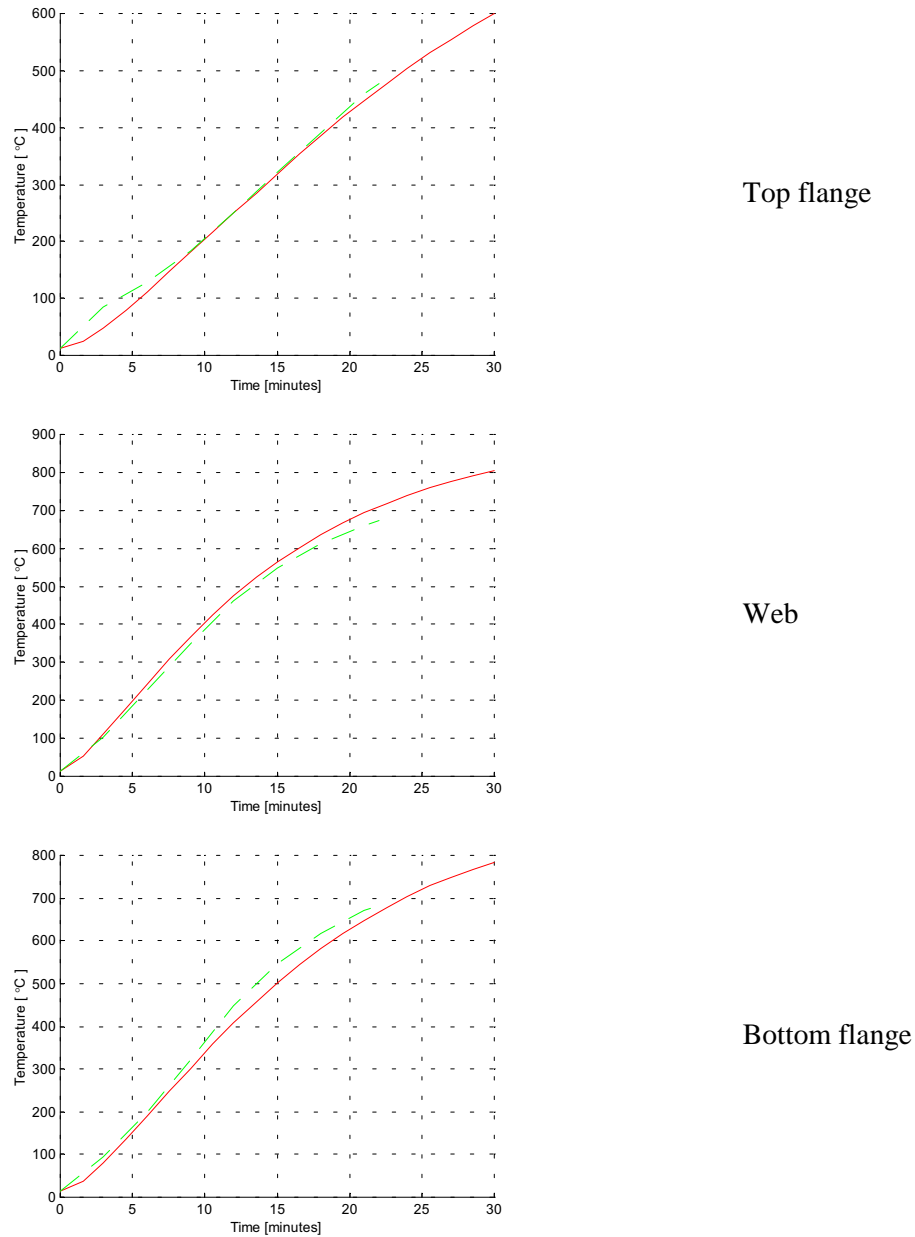


Figure 9-6 Comparison of measured and calculated temperature of fire exposed steel beam ( $h*w*t_{web}*t_{flange} = 256x145x7.47x12.79$  mm) for fire test 11 with the exposure according to figure 9-2. (Dashed line = measured, solid line = predicted/applied)

A maximum allowed deflection of  $L/30$  was used as stability criteria. With a span of 4.5 m this means a maximum deflection of 150 mm. A comparison of measured deflections and deflections as calculated with GCA is presented in figure 9-7. The fire resistance of the tested beam was 22 minutes and corresponding GCA calculation resulted in 19.6 minutes of fire resistance.

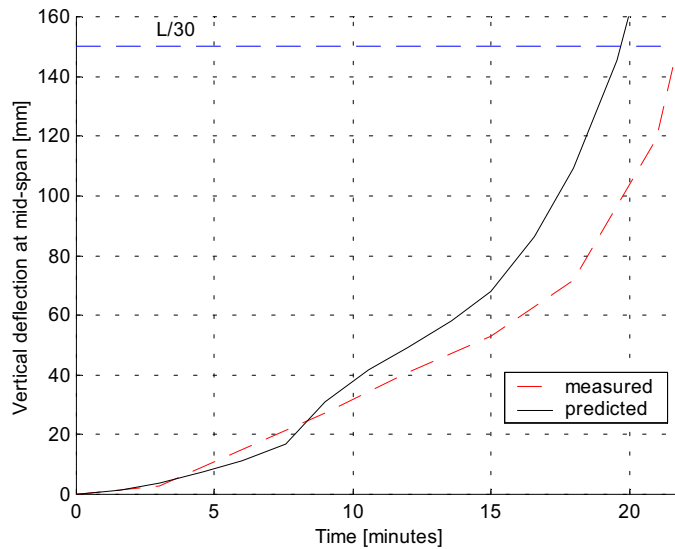


Figure 9-7 *Deflections at centre of beam. The collapse time of the GCA simulation was 19.6 minutes. The resistance time of the test was 21.7 minutes.*

A comparison to design with the tool SBEAM is shown in figure 9-8. The SBEAM calculation, that does not consider deflections, resulted in 20.8 minutes of structural stability during fire. This corresponds to the time when the load bearing capacity reached the value of the load effect of 80 kNm.

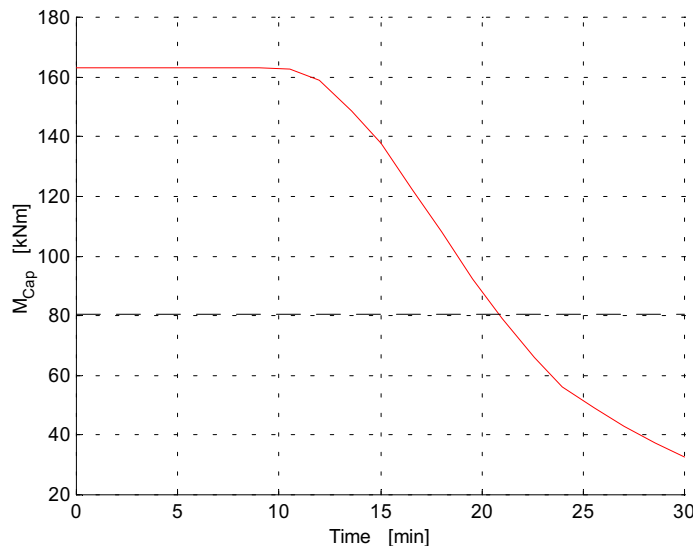


Figure 9-8 *Moment capacity as calculated using SBEAM. The fire resistance time was 20.8 minutes, to be compared with 21.7 minutes of the test.*

The deviation between measured results, simulations and the Eurocode 3 design method is too small to conclude that the effect of the thermal moment would be significant for beams in general.

### 9.3 Continuous beams

A statically indeterminate beam (continuous beam) has a greater load bearing capacity compared to a freely supported beam. The reason for this is transfer of bending moment between support and span when the continuous beam is approaching its ultimate strength capacity. Calculations according to the theory of elasticity does not consider this and will therefore not give the optimal result as regards the load bearing capacity. Another method is the theory of plasticity where yield points are introduced in critical sections of the continuous beam. The number of yield points depends on the degree of statically indeterminacy. See figure 9-9.

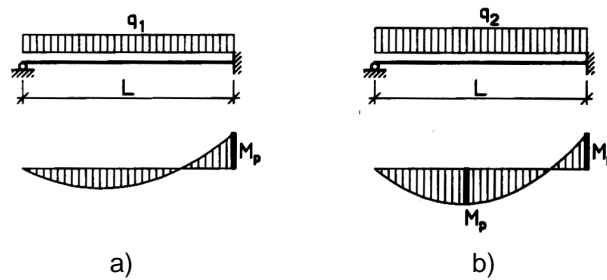


Figure 9-9 *Moment distribution for a statically indeterminate beam according to*  
 a) *theory of elasticity*  
 b) *theory of plasticity*  
 $M_p$  *is the yield point moment. /11/.*

Figure 9-10 shows an example of a continuous beam with different load combinations. Depending on the location of the free loads, different load bearing ratios considering support and span are being derived.

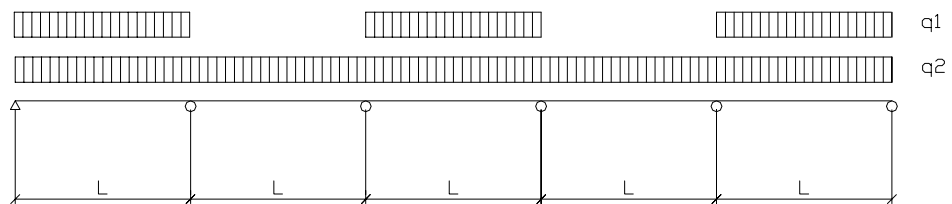


Figure 9-10 *Example of a continuous beam with different load combinations. Depending on the location of the free loads, different load bearing ratios considering support and span will be derived. Each span has a length of L.*

In order to determine the ultimate moment (yielding moment) of the beam before collapse the continuous beam in figure 9-10 is divided into two load cases. See figure 9-11.

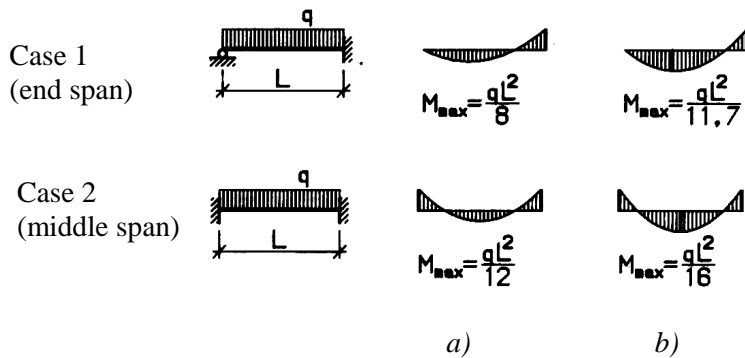


Figure 9-11 *Moment distribution for a statically indeterminate beam, according to*  
 a) *theory of elasticity*  
 b) *theory of plasticity /11/*

In order to maintain equilibrium of moments, the moment in the yield points are the same. The relationship between the theory of elasticity and the theory of plasticity gives the modified load bearing capacity in the fire limit state according to figure 9-12.

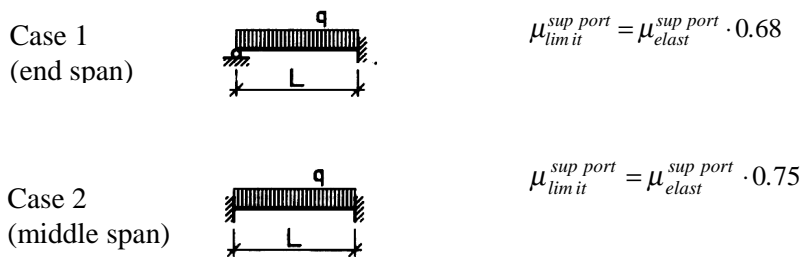


Figure 9-12 *Modifying factors of the load bearing capacity in the fire limit state for a continuous beam with distributed load. Explanation:*

$\mu_{limit}^{sup port}$  = modified load bearing capacity according to the theory of plasticity  
 at support.

$\mu_{elast}^{sup port}$  = modified load bearing capacity according to the theory of elasticity  
 at support.

The theory of plasticity considers transfer of bending moment between support and span at room temperature. At 20 °C yield points appear suddenly as the stress-related strain reaches the proportional limit, which is equal to the yield limit. At higher temperatures, the yield limit is reached after the proportional limit and the corresponding loss of strength is progressive. This might indicate that a moment redistribution as given by the theory of plasticity at room temperature would be valid in fire, provided loads start to take other paths as soon as one section becomes weaker than others.

A statically indeterminate beam was analysed using GCA in order to verify the theory of plasticity in fire. The beam is shown figure 9-13.

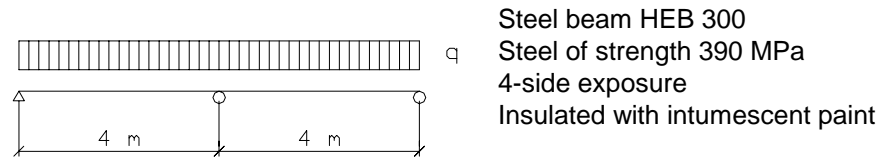


Figure 9-13 Continuous steel beam modelled for non-linear analysis.

The maximum cross-sectional bending moment capacity is 698.2 kNm.

The allowed moment according to the theory of elasticity becomes:

$$349,1 \text{ kN/m} \quad (698.2 = q_d \cdot 4^2 / 8).$$

The allowed moment according to the theory of plasticity becomes:

$$510,6 \text{ kN/m} \quad (698.2 = q_d \cdot 4^2 / 11.7).$$

In the analysis a uniformly distributed load of  $q=320 \text{ kN/m}$  was applied as shown in figure 9-13.

Corresponding maximum moment of applied load is:

$$M = 320 \cdot 4^2 / 8 = 640 \text{ kNm} \text{ according to the theory of elasticity (92\% load utilisation)}$$

$$M = 320 \cdot 4^2 / 11.7 = 438 \text{ kNm} \text{ according to the theory of plasticity (63\% load utilisation)}$$

A simple cross-sectional analysis as performed with SBEAM gives a fire resistance time of:

42 minutes according with loading degree determined according to the theory of elasticity

53 minutes according with loading degree determined according to the theory of plasticity

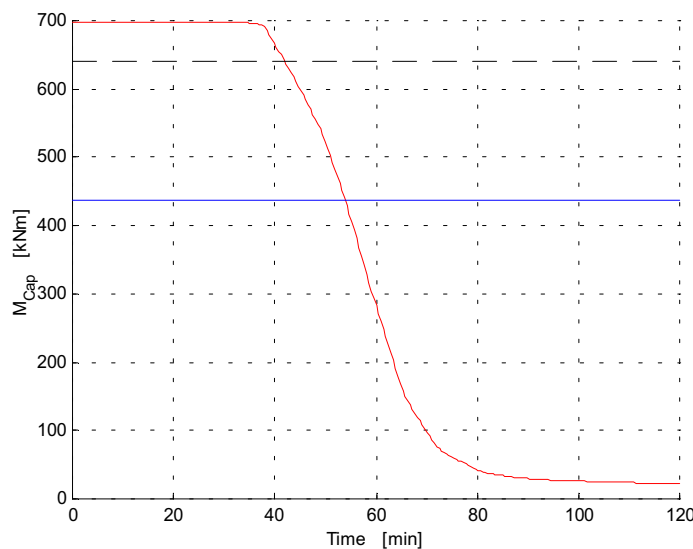


Figure 9-14 Moment capacity over time as determined by SBEAM calculation.  
 Solid line: moment according to theory of elasticity  
 Dashed line: moment according to theory of plasticity

The resistance time as given by the non-linear analysis was 58 minutes. The deflection at center of one span is shown in figure 9-15.

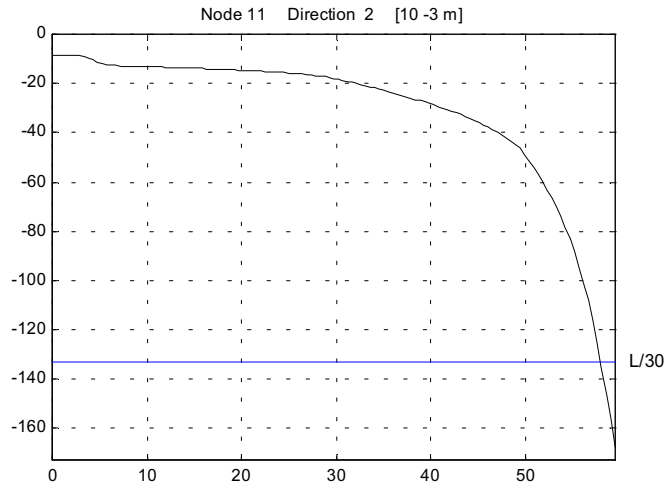


Figure 9-15 Deflection at center of one span of analysed continuous beam.

The moment distribution after 0 and 27.4 minutes are shown in figure 9-16.

At the start, after loads have been applied, the moment at the center support was determined to 628 kNm which should be compared to 640 kNm according to the theory of elasticity. At any of the center spans the moment was 365 kNm, compared to 358 kNm according to theory of elasticity.

After 27 minutes moment redistribution results in equal moment at support and in center span, 439 kNm, which can be compared to 438 kNm as given by the theory of plasticity.

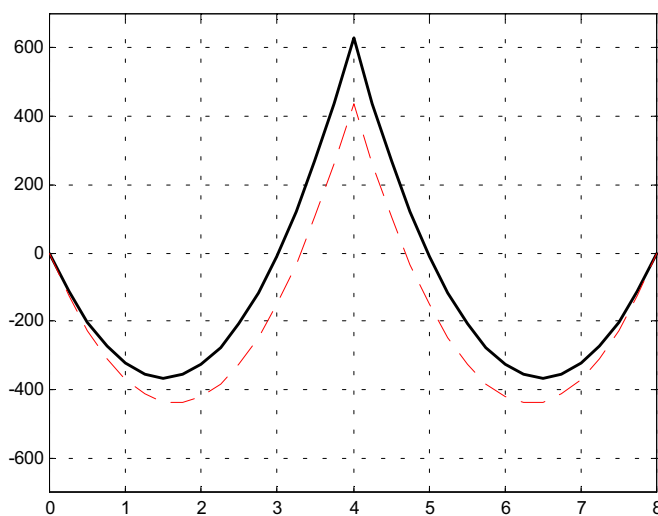


Figure 9-16 The moment distribution after 0 minutes (solid) and 27.4 minutes (dashed).



The cross-sectional distribution of stress and E-modulus (solid line curves) at time of failure are shown in figures 9-17 – 9-19 for sections at end support, center span and center support. The loss of stiffness is greatest at the center support, which may explain why load redistributions from that section started early. There is an indication, although it can not be fully concluded, that load redistributions begin as soon as loss of strength and stiffness starts to develop in any section.

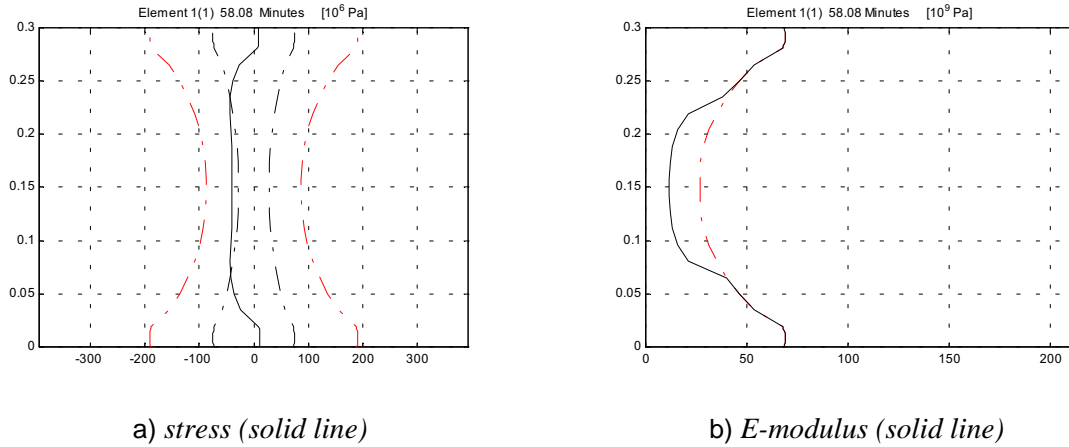


Figure 9-17 The cross-sectional stress and E-modulus at end support at time of failure, after 58 minutes of fire exposure.

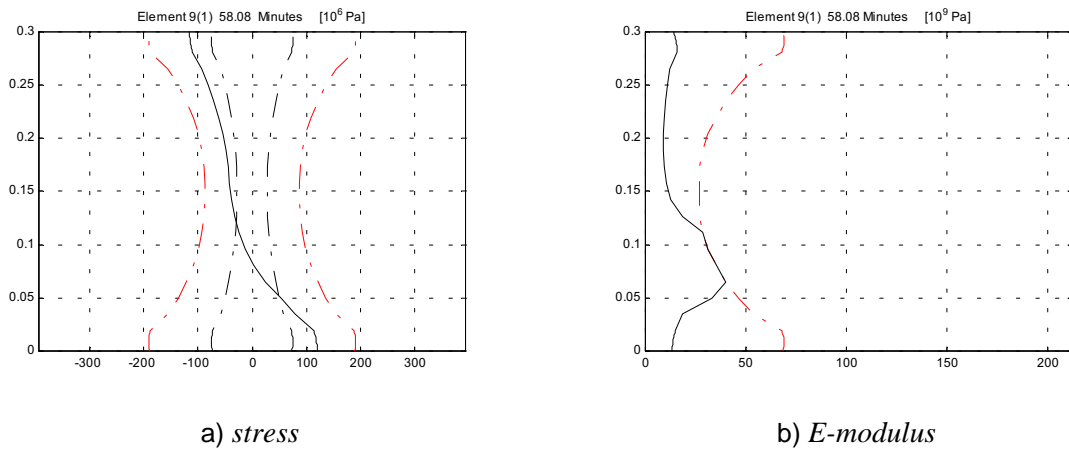


Figure 9-18 The cross-sectional stress and E-modulus at center span at time of failure, after 58 minutes of fire exposure.

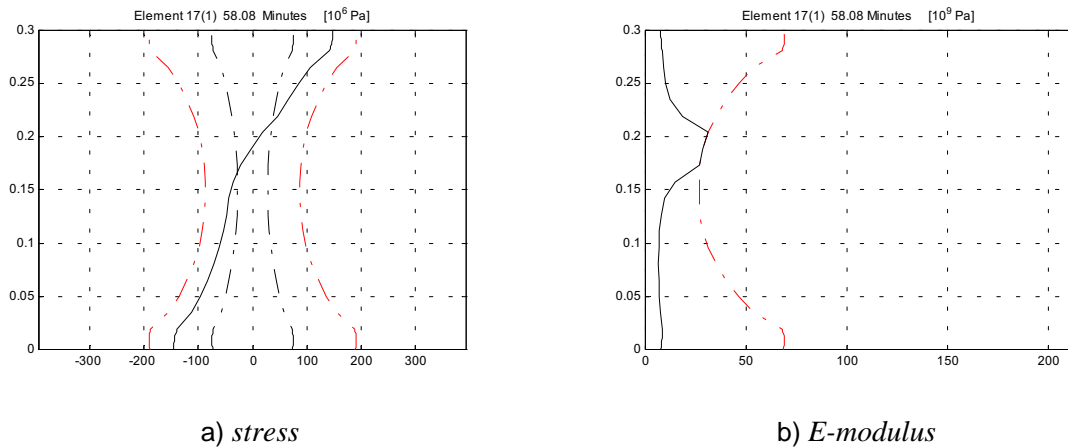


Figure 9-19 *The cross-sectional stress and E-modulus at center support at time of failure, after 58 minutes of fire exposure.*

## 10 Analyses of Frame

An unprotected steel frame with width 12 m and height 12 m was defined for non-linear global collapse analysis with two different fire scenarios. One scenario was with the frame fully exposed, the other involved fire in just one section. Design loads were applied according to BKR /21/.

More than 30 full frame simulations had to be performed in order to obtain relevant case and reliable results.

### 10.1 Frame Model

#### 10.1.1 Geometry

A 3-storey steel frame with bay width 4 m and column height 4 m was chosen for global collapse analyses. Profile HEB 300 of steel grade S355 was chosen for all beam and column members.

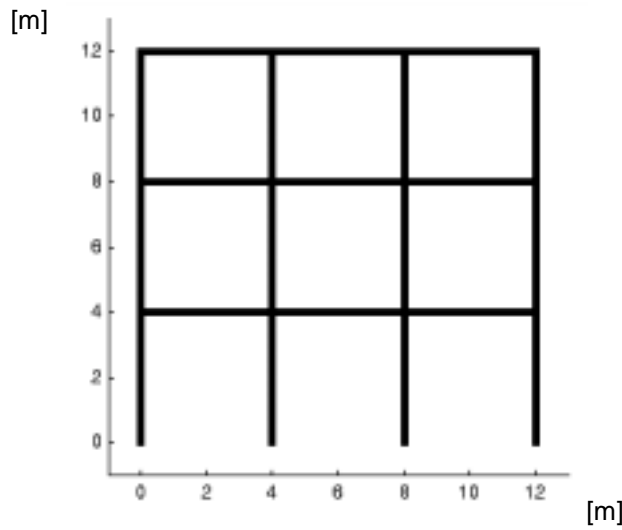


Figure 10-1 *Geometry of studied frame.*

The frames were initially deformed according to the first eigenmode with maximum deflection due to initial out of straightness fixed to 10 mm ( $L_{Max}/400$ ). A magnification of the initially deformed structure is shown in figure 10-2. With symmetrical structural properties and loading situation, this orientation of the mode will force the collapse to the left.

The initial out-of-straightness is modelled as a modification of the global co-ordinates and not treated as deformations.

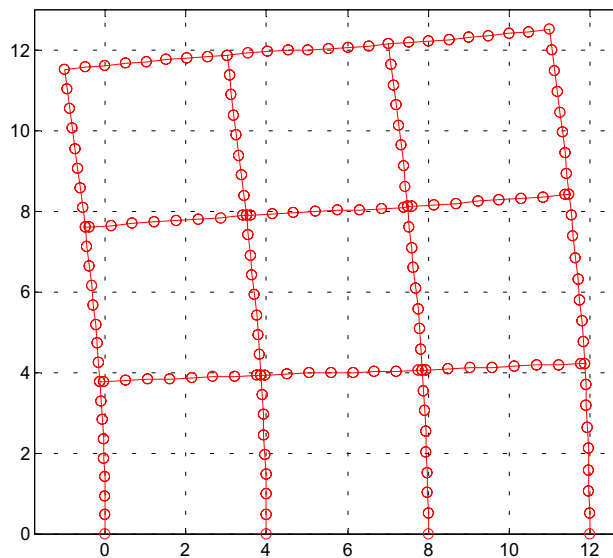


Figure 10-2 *100 x magnification of initial out-of straightness as determined by a maximum deflection of 10 mm and the first eigenmode. With symmetrically applied vertical loads the collapse of the frame will be forced to left.*

### 10.1.2 Boundary Conditions

Connections between columns and girders were stiffened, except on the top of the frame, but not modelled as completely rigid. The stiffeners were modelled by short beam elements with high strength and modulus of elasticity. The stiffener temperature was kept 20 °C throughout the scenario, thus preserving the near-infinity rigidity.

The bottom nodes of the frame were locked in all nodal directions.

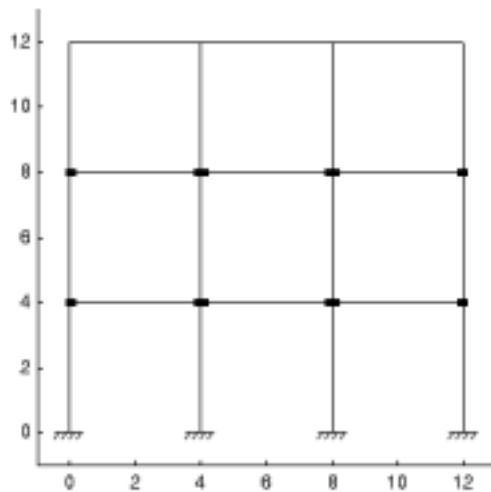


Figure 10-3 *Boundary conditions and location of modelled stiffeners.*

### 10.1.3 Loading

Design loads were determined according to BKR (2:321) are presented in table 10-1.

#### Variable Load

Shopping centres and stores:  $q=4 \text{ kN/m}^2$   $\psi=0.5$  (“Lastgrupp 3” according to BKR)

#### Snow Load

Building in Stockholm:  $s_k=2 \text{ kN/m}^2$   $\psi=0.7$

#### Wind Load

$q_k = 0.69 \text{ kN/m}^2$   $\psi = 0.25$

#### Weight Load

Roof:  $q = 1.0 \text{ kN/m}^2$

System of joists:  $q = 2.0 \text{ kN/m}^2$

	Normal state limit (LK 1)	Fire state limit (LK 7)
Roof	$q_{snow}^{HL} = 10.4 \text{ kN/m}^2$ $q_{snow}^{VL} = 5.6 \text{ kN/m}^2$ $q_{roof} = 4.0 \text{ kN/m}^2$	$q_{snow} = 5.6 \text{ kN/m}^2$ $q_{roof} = 4.0 \text{ kN/m}^2$
System of joists	$q_{NL}^{HL} = 20.8 \text{ kN/m}^2$ $q_{slab} = 8.0 \text{ kN/m}^2$	$q_{NL} = 8.0 \text{ kN/m}^2$ $q_{slab} = 8.0 \text{ kN/m}^2$
Wind	$q_{wind}^{HL} = 3.6 \text{ kN/m}^2$ $q_{wind}^{VL} = 0.69 \text{ kN/m}^2$	$q_{wind} = 0$

Table 10-1 Design load according to BKR..

Distributed load on top level was set to 9.6 kN/m. For all other beams the modelled load was 16 kN/m. Loads applied in the model are illustrated in figure 10-4.

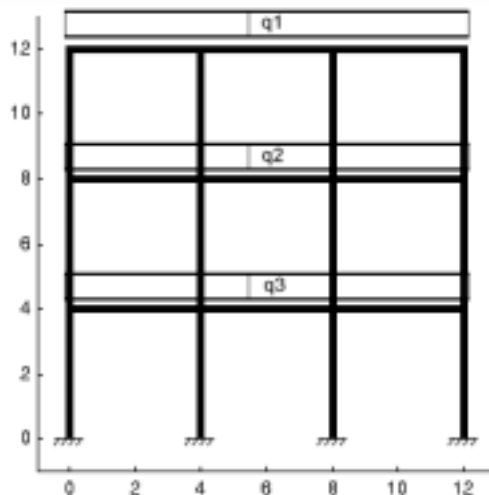


Figure 10-4 Applied loads in the frame model.  $q_1 = 9.6 \text{ kN/m}$ .  $q_2 = q_3 = 16 \text{ kN/m}$ .

### 10.1.4 Fire Exposure

Two exposure conditions were studied. In the first case, the unprotected frame was completely exposed to standard ISO 834 fire. The scenario of fully exposed frame was chosen to obtain an estimation of the overall performance of the frame.

In the second chosen scenario, only the centre section of the unexposed frame was exposed. This scenario was chosen to simulate local fire in a single fire compartmentation and to study the development of load redistribution, even without steel-concrete interaction, as exposed structural members or unexposed members subjected to high thermal stresses lose strength.

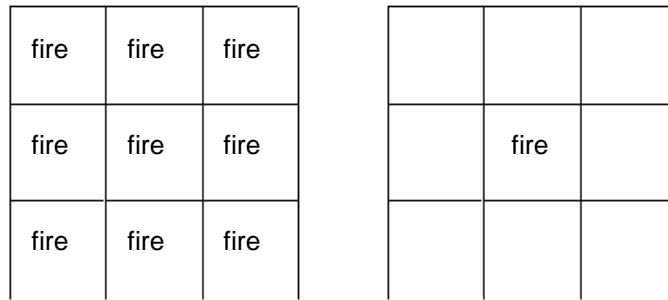


Figure 10-5 *The studied fire scenarios for full frame analyses.*

## 10.2 Fully Fire-Exposed Frame

For the fully exposed frame analysis the structure was divided into 159 Bernoulli beam elements. Each member in turn was divided into 29 cross-sectional elements for each beam element node. Thus 9.540 cross-sectional points per timestep and iteration were used for the incremental calculation of each of the properties stress, strain, etc. With a time domain division of 121 steps the number of stored points becomes 1.154.340 per physical property or 5.771.700 totally. It is obvious that the necessary cross-sectional division is the single most important issue for the limit of performance. The double non-linearity with geometrical second order iterations performed within the stress iteration loop is the second most important issue, since a full matrix eigenvalue analysis is performed within each such iteration. The main system equation is solved with sparse matrices and is not a performance issue as such.

The finite element model of the analyzed frame is shown in figure 10-5. Individually studied elements are denoted E#. Individually studied nodes are denoted N#.

Loads and boundary conditions were applied according to section 10.1. Distributed loads on top level were set to 9.6 kN/m and for all other beams the modelled distributed load was 16 kN/m.

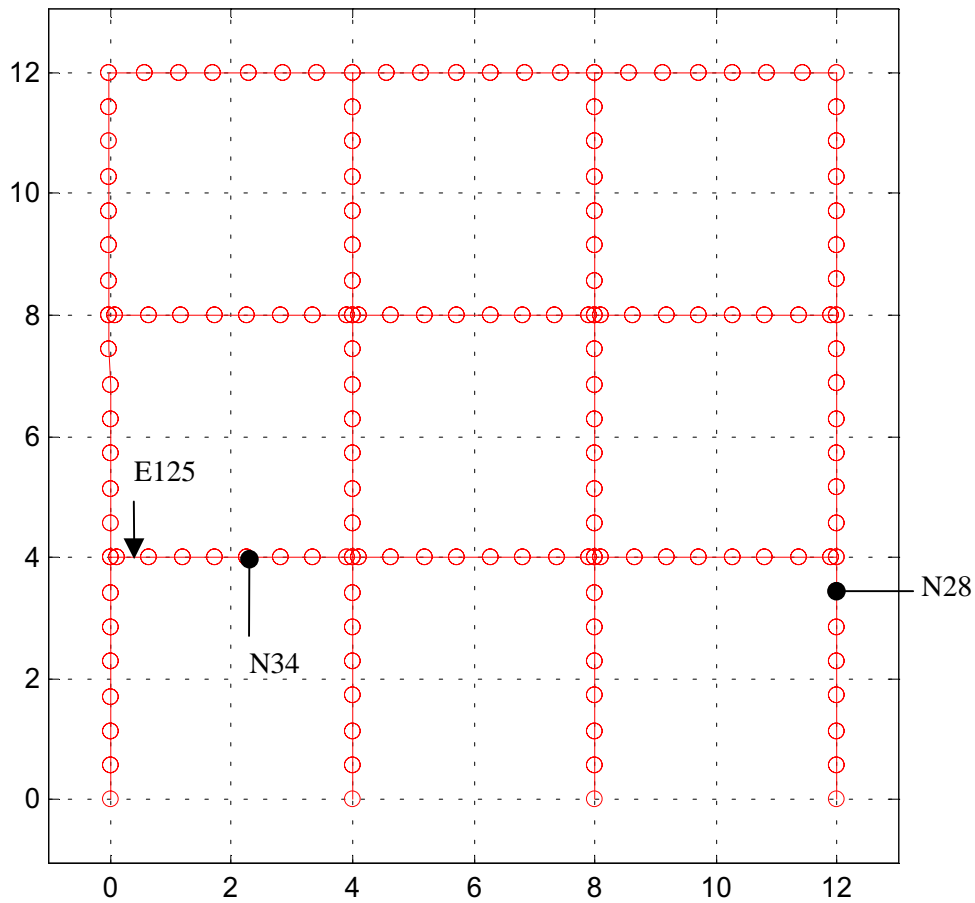


Figure 10-6 *Finite Element model of frame with identification of studied nodes and elements.*

The initial out-of-straightness is modelled as a modification of the global co-ordinates as described in section 10.1 and not treated as deformations. This means that the initial out-of-straightness will not be magnified in the deformation plots. With symmetrical structural properties and loading situation, this orientation of the mode will force the collapse to the left.

The initial structural deformations after loads are applied are shown in figure 10-7.

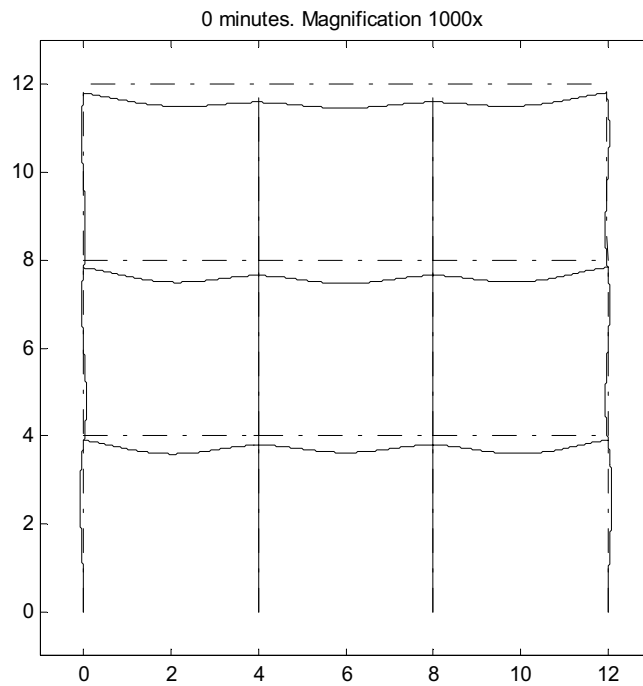


Figure 10-7 Deformations with loads applied at start of fire scenario. (Magnification 1000 x).

The thermal strains forces the fire-exposed frame to expand until sudden loss of strength occurs shortly before the time of collapse. After 28 minutes global collapse occurs with failure of the leftmost beam (Element #125) above the first floor and the carrying column below it which has been displaced by the thermal expansion of the beam.

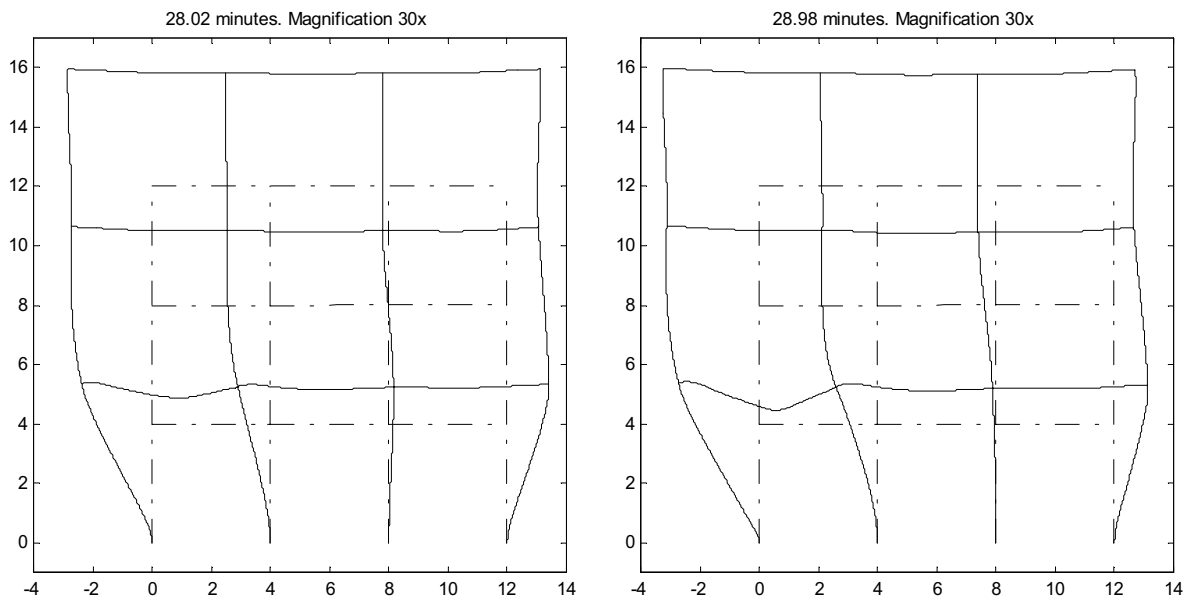


Figure 10-8 Deformed frame during collapse after 28-29 minutes of fire exposure. Global collapse starts with failure of Element #125. (Magnification 30 x)



Vertical deformations over time are shown in figure 10-9 for Node #34, which is the node nearest the centre of the critical beam. It should be pointed out that actual, absolute deformations in one point are affected by the complete behaviour of the global structure.

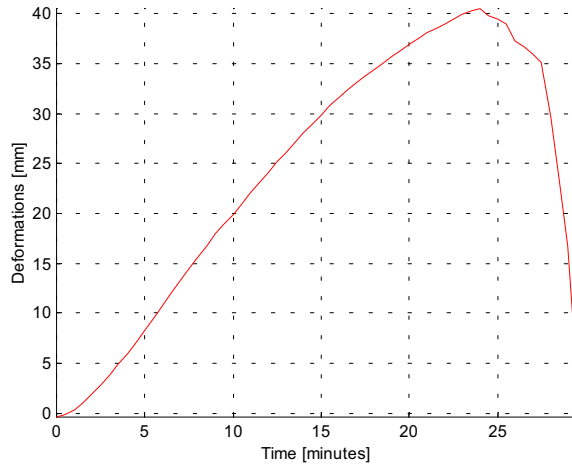


Figure 10-9 Vertical deformations for Node #34.

The displacements of Node #28, in the rightmost lower span column, confirms a uniform collapse behaviour of the fully exposed frame.

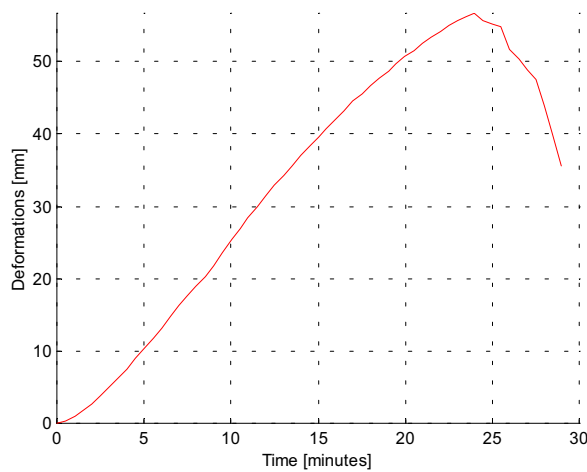


Figure 10-10 Horizontal displacements over time for Node #28.

Cross-sectional stress distribution in Element #125 is presented in figure 10-11. As expected, the beam section has not reached fully yield condition at the time of collapse.

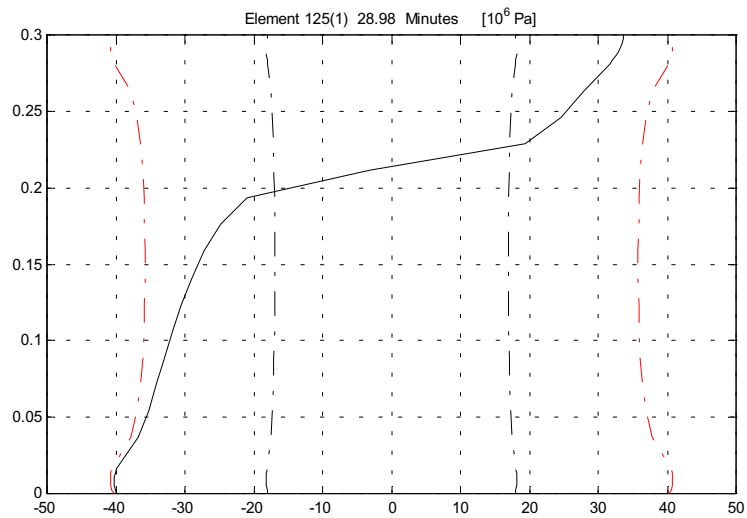


Figure 10-11 *Cross-sectional stress distribution in Element #125. The temperature-dependent proportional and yield limits are marked as dashed.*

### 10.3 Single-Compartmentation Fire Exposure

The modelled frame fire exposure in a single fire compartmentation was divided into 138 Bernoulli beam elements. The finite element mesh of the structure is shown in figure 10-12.

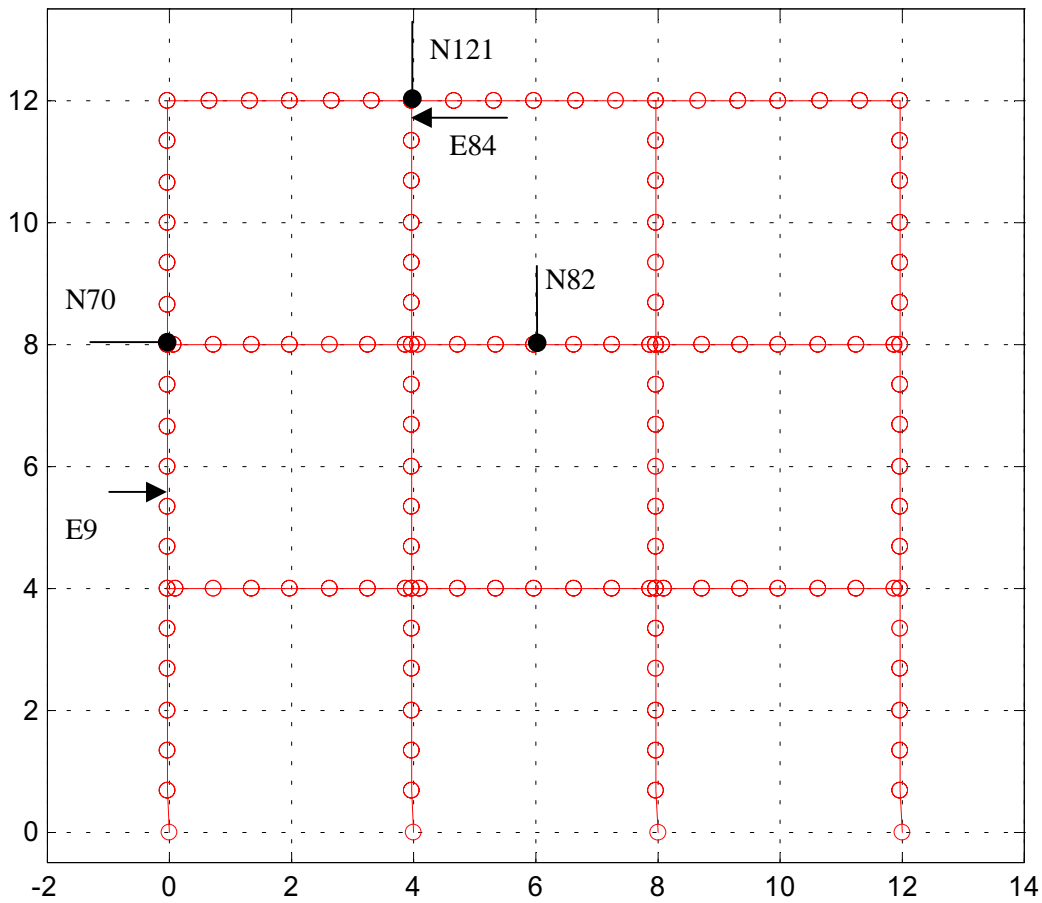
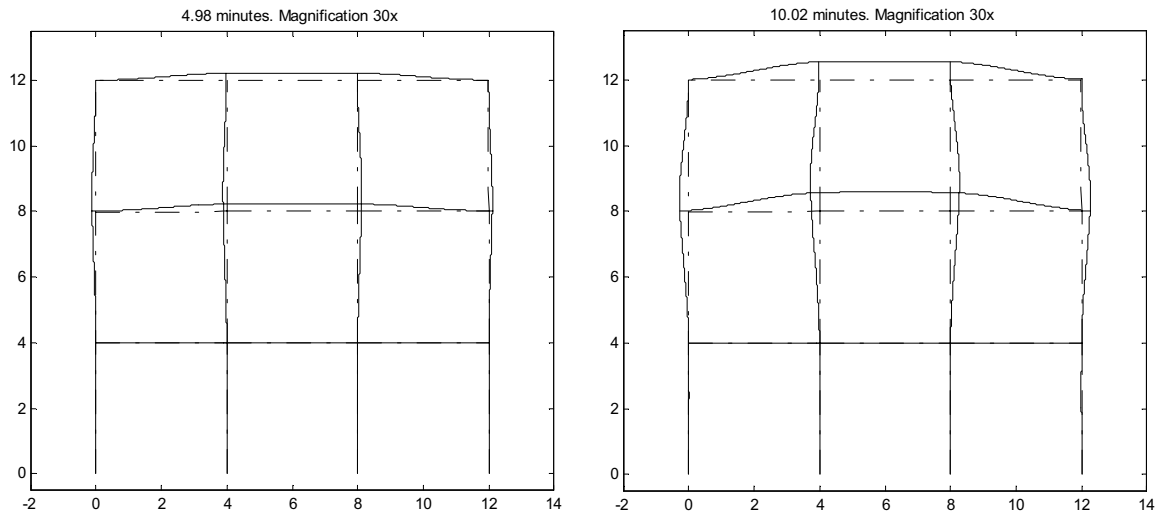


Figure 10-12 *Finite Element model of frame with exposure in a single section.*

The deformations prior to the start of fire scenario is identical to that of the fully exposed frame analysis (see figure 10-7). With fire exposure on the centre beam and two columns on the second floor adjacent unexposed members are displaced by the thermal expansion.

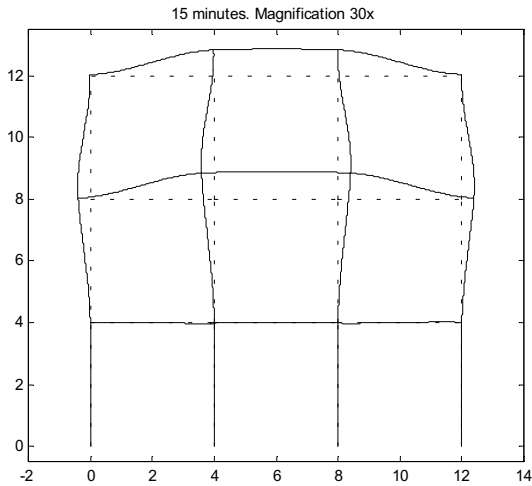
In figures 10-13 the frame deformations are presented at 12 different times during the fire. Comments are given at each sub-figure a)- l).

After 19 minutes (see figure 10-13 g) the thermal load reaches its maximum after which a decrease follows until local collapse as the stiffness reduction is larger than the increase in thermal strains. At the time of the peak thermal force, a small part of section area of the outer unexposed column just reaches yield state, but this area never increases as the thermal loads from the exposed beams diminishes.

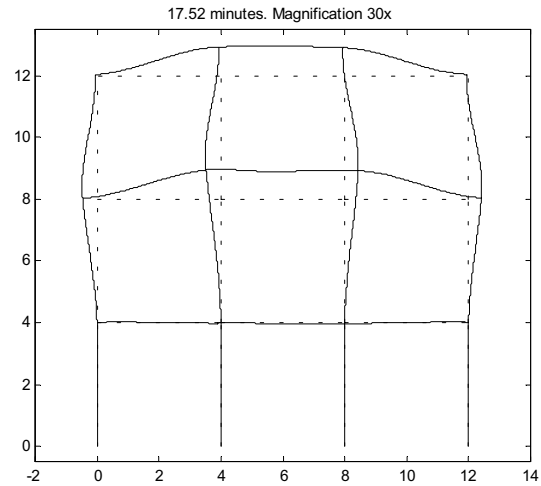


a) 4.98 minutes. The thermal expansion exceeds the effect of the applied load.

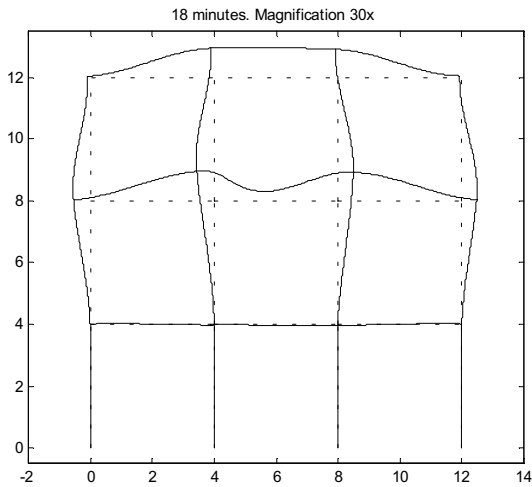
b) 10.02 minutes. Deformation of outer unexposed members from thermal loads of exposed members.



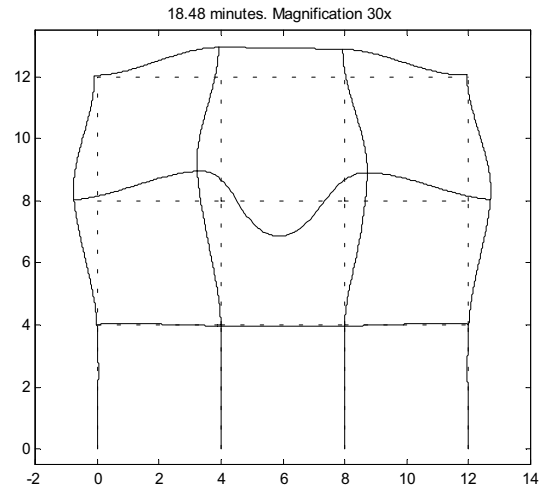
c) 15 minutes.



d) 17.52 minutes. Exposed beam has lost enough stiffness for the applied load to balance the vertical, thermal movement of the beam.

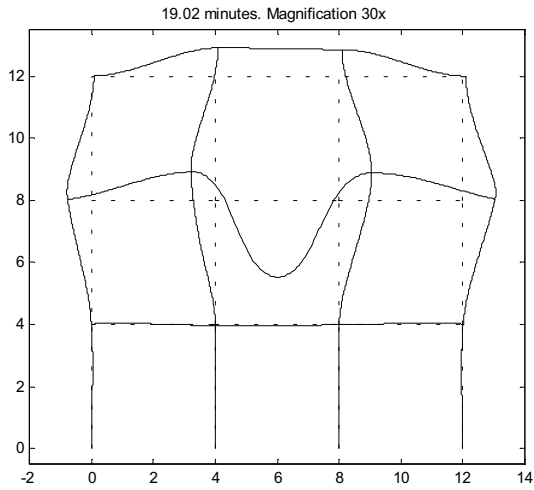


e) 18 minutes. The deformation of exposed beam is taking the shape of the collapse mode.

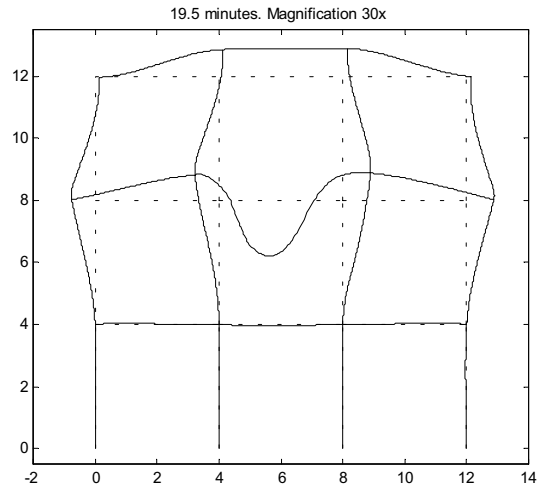


f) 18.48 minutes. All exposed members near collapse. Large thermal forces on unexposed members.

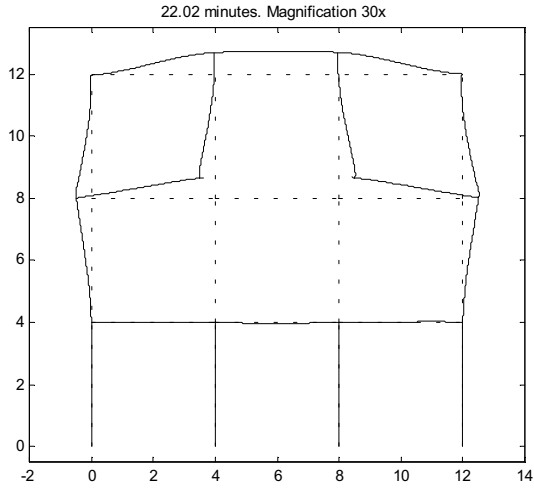
Figure 10-13 Frame deformations before, during and after local collapse.



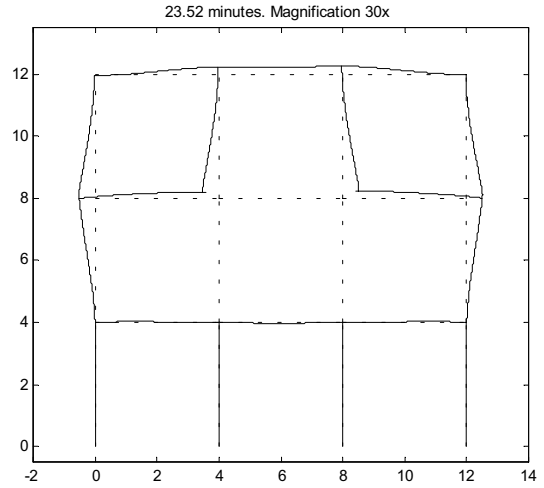
g) 19.02 minutes. Near critical state for outer unexposed columns.



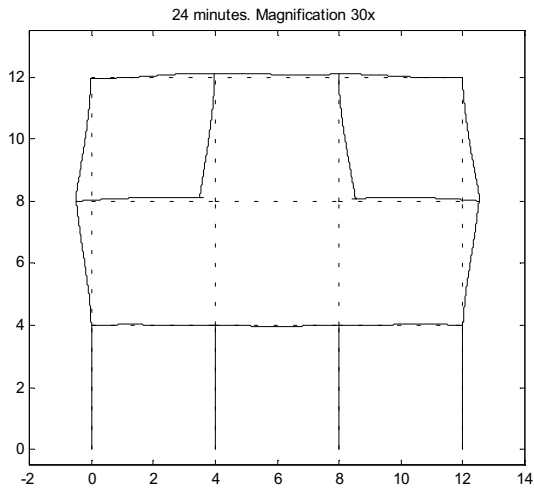
h) 19.5 minutes. Still near critical state for unexposed columns as load redistribution to unexposed members increases.



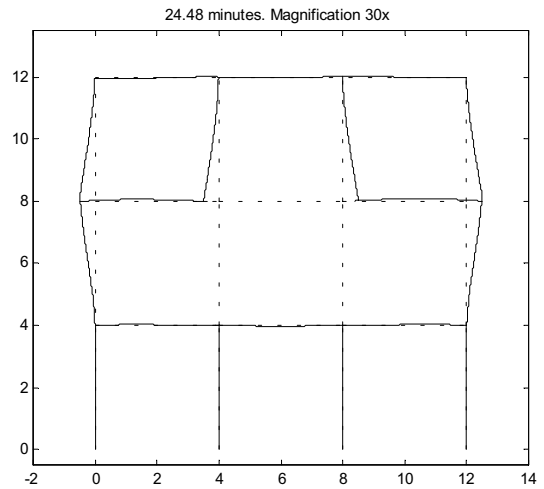
i) 22.02 minutes. Collapse of all exposed members begins.



j) 23.52 minutes. Less deformations of unexposed upper beams with decrease in thermal forces.



i) 24 minutes.



j) 24.48 minutes.

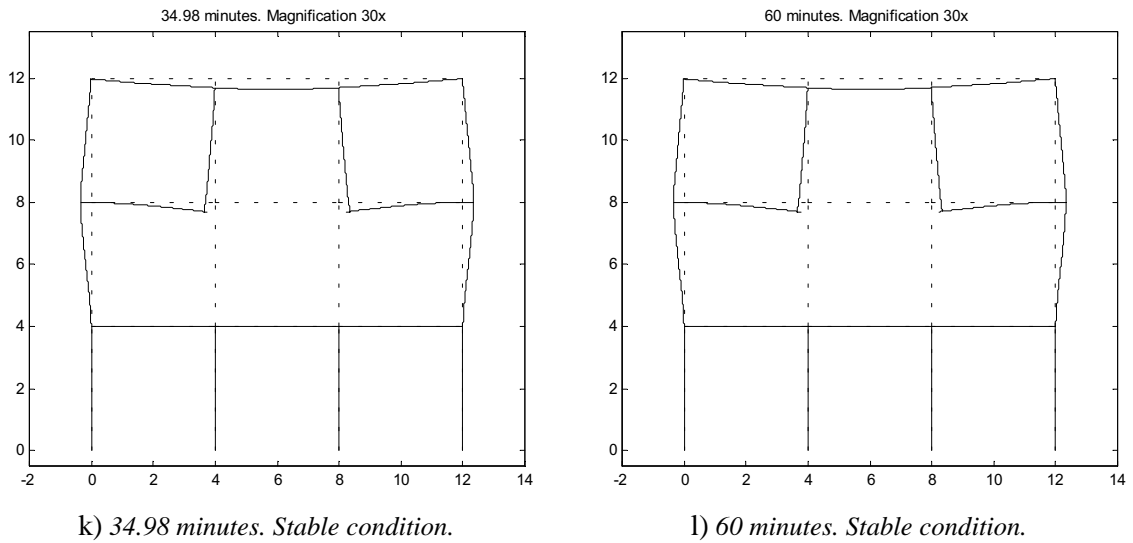


Figure 10-13 Frame deformations before, during and after local collapse.

The vertical deformations over time of Node #121 are presented in figure 10-14. The point is located on the unexposed top of the frame as shown in figure 10-12 (mesh). The thermal strains of the column in the fire exposed compartment have given rise to the large movements. The deformation is dependent on the product of modulus of elasticity and the thermal strain of the exposed steel column. The thermal strain increases almost linearly with temperature. After 700 °C the relative decrease of modulus of elasticity is more abrupt than the thermal strain increase. The generated thermal load per area unit is shown in figure 10-14.

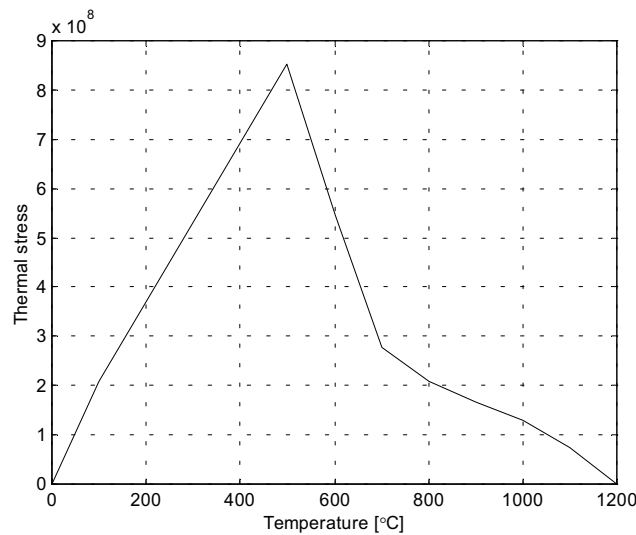


Figure 10-14 Product of initial modulus of elasticity,  $E(\epsilon_{\sigma}=0)$  and thermal strain ( $\epsilon_{th}$ ) for steel with  $E_0(20\text{ }^{\circ}\text{C})=210\text{ GPa}$ .

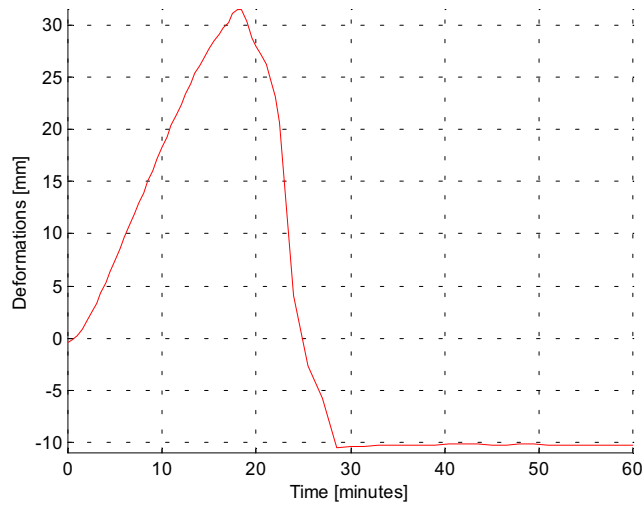


Figure 10-15 Vertical displacement of Node #121 (x~4 y~12).

The deformation caused by the thermal load shown in figure 10-15 is typical for members with perpendicular, adjacent fire exposed steel constructions and worth considering for one reason. Members with less steel area will reach the critical thermal peak before members of larger section area and may potentially hazard the performance of larger structural parts too early.

In the studied frame example, the stress increase is not critical in the unexposed top beams.

In figure 10-16 vertical deformations are shown in exposed beam center span (x~6 y~8, see figure 10-12). Local collapse starts after 17 minutes.

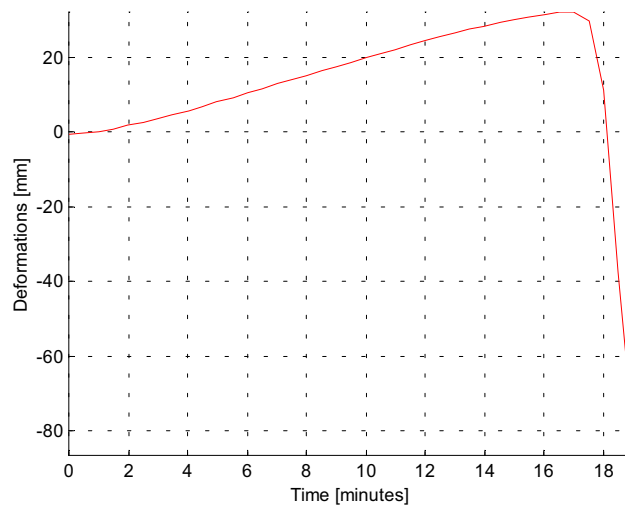


Figure 10-16 Vertical deformations in exposed beam Node 82 (x~6 y~8). Local collapse starts after 17 minutes.

In figure 10-17 horizontal displacements are shown in outer Node 70 ( $x \sim 0$   $y \sim 8$ , see figure 10-12). A deformation peak appears when the column above has lost stiffness with part of cross section reaching yield point. The column below Node 70 never reaches yield point and the peak drops when the thermal load generated by exposed beams decreases at 700 °C.

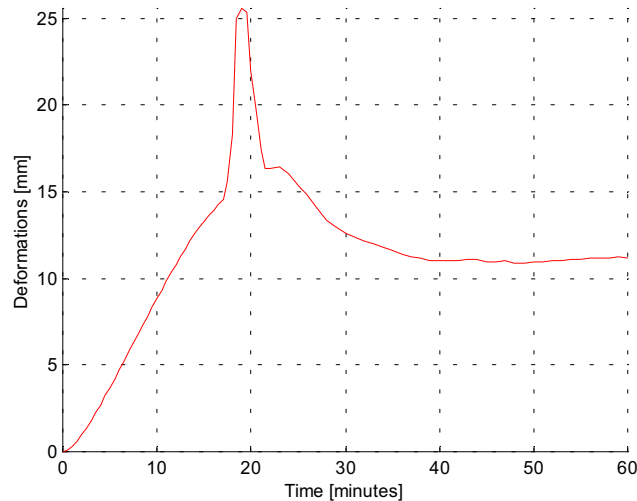


Figure 10-17 *Horizontal displacements in Node 70 ( $x \sim 0$   $y \sim 8$ ). A deformation peak appears when the unexposed column above has lost stiffness with part of cross section reaching yield point.*

In figure 10-18, the normal force is shown in Element 9 ( $x \sim 0$   $y \sim 7.7$ , see figure 10-12). After load redistribution from collapsed fire exposed members, the force of the unexposed column has increased by 90%. A slight drop of load redistribution can be identified at the time of the horizontal deformation peak in Node 70 as described in figure 10-17.

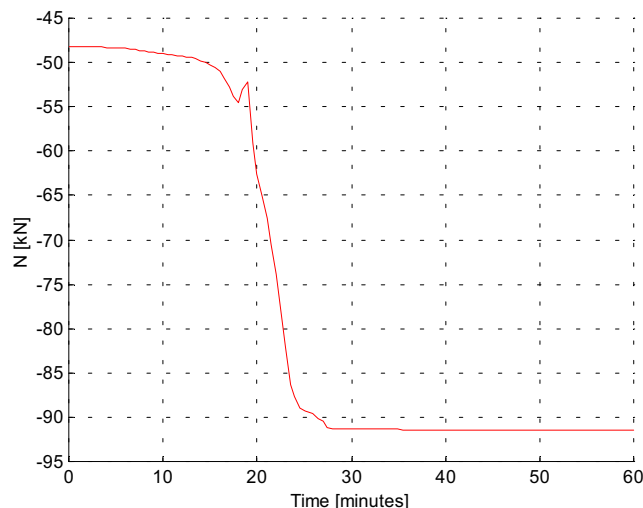


Figure 10-18 *Normal force in Element 9 ( $x \sim 0$   $y \sim 7.7$ ). After load redistribution from collapsed fire exposed members the force of the unexposed column has increased by 90%.*



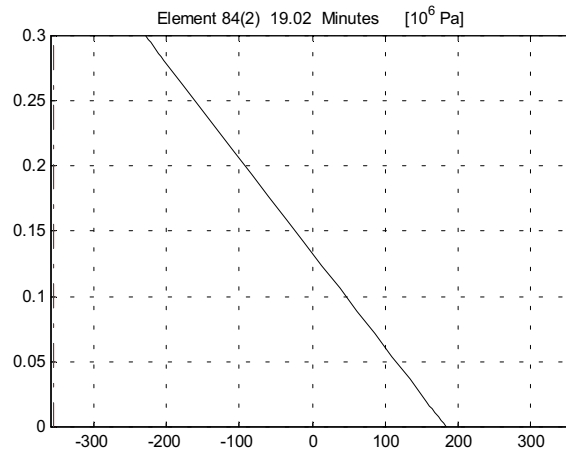


Figure 10-19 *Cross-sectional stress distribution in unexposed column Element 84 (x~4 y~12) after 19.02 minutes. The stress is well below the yield limit throughout the section.*

It was concluded that no global collapse occurred during the scenario due to large load redistribution, although the thermal loads of exposed members generated near-critical stress in outer unexposed members.

The resulting behaviour must be considered unusual in real life. Indirect factors were not taken into account in the theoretical, structural analyses. Lost integrity between compartments due to local collapse would result in exposure in all compartments and global collapse eventually. The purpose of choosing the current load scenario was to be able to evaluate near critical condition as given by the results, as well as a scenario of global collapse and a scenario of no critical conditions due to local collapse of one compartmentation. Slightly higher initial loading degree would have resulted in global collapse during the critical phase, after about 20 minutes of exposure. Less loading might not have initiated the critical behaviour at all.

Provided structural design is done to permit load redistribution, e.g. not too large distance between supports, the overall loading degree may be of major importance to the global performance.

## 11 Conclusions

### 11.1 Columns

In literature no full-scale fire tests on partially exposed columns of slenderness  $\geq 1.0$  (“slender columns”) have been reported. Fire tests on partially exposed columns with slenderness  $< 1.0$  (“short columns”) have been performed but no negative influence on the load-bearing capacity compared with fully exposed columns have been observed. This is mainly due to the fact that the tests involved a wall that the columns reached within a few minutes, after which the direction of horizontal displacement was reversed, but it was also noted that the tested columns have been too short to be seriously influenced by a bowing effect due to the thermal gradient over the cross-section. Computer simulations indicate that there may exist a considerable problem for slender columns partially fire-exposed along its circumference.

Design methods including both plastic capacity and the critical Euler load, e.g. according to Eurocode 3, were found to comply quite well with non-linear simulations and tests in most cases with all 4 sides of the column exposed. For partially exposed slender columns the effect of the thermal moment caused by the cross-sectional gradient was found to be too large to be neglected. Exposure of about 50% of circumference was found to be the worst scenario for columns with a high slenderness ( $>1$ ). It can be concluded that the collapse time will be reduced by 25-75% and the reduction is increased by increase in load utilisation. The best way to avoid the negative influence of partial exposure between 20 and 100% is to avoid this kind of exposure for slender columns. Otherwise the passive fire protection must be designed to resist partial fire exposure.

In practice, most columns are partially restrained in the vertical direction. This will increase thermal stresses for columns and especially for columns with 4-sided exposure. The results from the analyses of partially restrained columns indicate that the disadvantageous effect of increased thermal stress may surpass the advantageous effect of the reduced buckling length. On the other hand, the increased restraint did not increase the degree of load redistribution to the rest of the structural system. A comparison between partially restrained columns subjected to partial fire exposure and partially restrained columns exposed on all four sides have not been covered by this report. Full-scale tests on partially exposed columns of slenderness  $>1.0$  are needed to quantify all the different effects. A generalised design code as Eurocode 3 must be reliable and useful for all combinations of partial fire exposure, restraint and slenderness within given limits of the code.

## 11.2 Beams

The collapse criterion set by design methods considering the bending moment capacity only, allowing the entire cross-section to yield (stress related to 2% strain) and taking advantage of the full corresponding yield stress, were found to comply with results from non-linear analyses and the studied test. This was also the case for partially fire-exposed beams. It is found in this beam study that there is no safety margin between the advanced calculation results and the simple calculations. As only a few comparisons are made examples can probably be found where the simple calculation methods are more advantageous than the complex non-linear FEM-calculations. Thus the assumption of using a design stress based on 2% strain and 100% yielding of the cross-section is on the unsafe side and that is not acceptable. Another stress based on 1.0-1.5% strain might be more relevant to be used in the simplified design method.

The collapse criterion based on a maximum deflection given by beam length divided by 30 as used in the British fire tests more or less coincided with the cross-sectional criterion in the case of the tested and simulated beam. Also fire tests revealed that there was no safety margin to collapse at all for the simplified method.

For statically indeterminate beams the theory of elasticity remains conservative when exposed to fire. The theory of plasticity was found to comply with non-linear analyses. There was indication, although it can not be fully concluded, that load redistributions begin as soon as loss of strength and stiffness starts to develop in any section.

## 11.3 Frames

The frame study in this report supports the experience of the Cardington tests and the computer simulations of these tests. The redistribution of loads, forces and moments from fire-exposed structural members to the "cool" members of the frame structure are of great importance to improve the fire resistance and may also avoid global collapse. The results from the frame analyses also

illustrate that load redistribution does begin before the collapse of single members starts. The overall loading degree is of major importance to the global performance.

One of the purposes of this work was to identify possibly redundant members in complex steel structures, which do not need to be protected. To identify members as redundant, the remaining structure must be designed to take the added loads transferred from collapsed members and loads possibly redistributed from members subjected to capacity loss even before local collapse. An overall low loading degree in combination with a design that permits load redistribution could then possibly compensate for lack of fire protection of single members

## 12 Condensed Literature Review

The literature review is written in a very condensed format where the referenses are divided into 5 group areas as shown below.

- A Experience of structural behaviour and extent of damages in real building fires
- B Fire tests of structures
  - B1 Fire resistance tests
  - B2 Full scale fire tests
- C Basic research on mechanical properties and on behaviour of structural elements
- D FEM-modelling and computer simulation of fire tests
- E Structural fire design methods

Group A literature has three references, which describe two real building fires at Broadgate Phase 8 in London 1990 and at Churchill Plaza Building in Basingstoke 1991.

Group B literature has 8 references and describes fire resistance tests and full scale fire tests. Under B1 different fire tests on external steel columns, unprotected structural steel, connections and composite slabs are presented. Under B2 three references (B5, 6, 7 & 9) describe the Cardington tests, which are the most comprehensive and important ones. Also the BHP William Street Fire Tests, the BHP Collins Street Fire Tests and the fire tests at the Stuttgart-Vaihingen University Germany are shortly presented. Reference (B8) is about fire tests on full scale floor assemblies which have been tested in NRC in Canada.

Group C literature has 6 references dealing with stress-strain relationships at elevated temperatures, modelling steel behaviour, passive fire protection, axial restraint of steel columns and structural behaviour.

Group D literature consists of 10 references on FEM-modelling dominated by simulating the Cardington tests. Temperature calculations, simulation of the thermal and structural behaviour of fire-exposed steel truss, steel beams and columns and steel frames as well as residual deformation after fire are investigated in the different papers.

Group E literature consists of 14 references and the natural fire concept for design is dealt with in most papers. Design methods are put forward especially beams, composite beams, columns, braced frames and more complex structures.

### 12.1 A: Experience of structural behaviour and extent of damages in real building fires

Two real building fires at Broadgate Phase 8 in London 1990 (A1) and at Churchill Plaza Building in Basingstoke 1991 (A2) have provided the opportunity to observe how modern steel framed buildings can perform in fire.

In 1990 a fire developed in a partly completed 14 storey office block on the Broadgate development in London. The fire began inside a large site hut on the first level of the building. The temperatures were estimated to be over 1000 °C. Following the fire structural elements covering an area of

approximately 40x20 m<sup>2</sup> were replaced, but importantly no structural failure occurred and the integrity of the floor slab was maintained during the fire. The direct fire loss was in excess of £ 25M, of which less than £ 2M was attributed to the structural frame and floor damage, the other costs resulted from smoke damage.

At the time of the fire the building was under construction and the passive fire protection to the steelwork was incomplete. The sprinkler system and other active measures were not yet operational.

Following the Broadgate fire it could be seen that some of the elements had lost their load bearing capacity although there were no sign of collapse. It was clear that the composite floor and supporting steel deck had a major influence on the overall stability of the structure, acting as a membrane distributing loads from weakening members.

In 1991 a fire took place in the Mercantile Credit Insurance Building, Churchill Plaza, Basingstoke. The building constructed in 1988 was twelve storeys high. The columns had passive fire protection in the form of boards and composite floor beams had spray applied protection. The underside of the composite floor was not protected and the structure was designed to have 90 minutes fire resistance. The fire started on the eight floor and spread rapidly to the tenth floor as the glazing failed. The fire protection materials performed well and there was no permanent deformation of the steel frame. The fire was believed to be comparatively “cool” due to the failure of the glazing permitting cross wind to increase the ventilation. The estimated cost of repair of the building was over £ 5M, with most of the damage being due to the smoke. No structural repair was required to the protection of steel work.

The Basingstoke fire showed how well a fully protected building might perform but gave no indication of how safe the traditional approach actually is.

## 12.2 B: Fire tests on structures

### B1 Fire resistance tests

4 papers are dealing with different fire resistance tests.

In the paper of Kruppa (B1) in 1981 20 tests were carried out on external steel columns situated outside a fire compartment. The results show that under certain conditions it is not necessary to protect the columns.

D.E.Wainmann and B.R. Kirby, British Steel (B2) have produced two compendiums of UK standard fire test data on unprotected structural steel. The compendiums cover all the fire tests carried out in the UK, according to BS476:Part 8:1972, on hot rolled structural steel sections in which the members were either completely unprotected, or partially protected by materials used only in the fabric of structure, such as concrete, brick and blockwork. The information is presented in the form of a detailed description of the design, preparation and construction for each type of test element and is accompanied in an Appendix, by series of data sheets.

From the fire tests results reported, relationships between heating rate, member size, applied load and fire resistance have been established for several types of load bearing elements based upon analysis carried out.

The paper by Riihimäki (B3) deals with fire resistance of beam-to-column connections and the research is based upon four furnace tests at VTT. The report concludes that connections need passive fire protection in the same extent as the steel members attached. However stresses due to

thermal expansion may sometimes be very important to take into account in the design of connections.

The last reference by Kruppa (B4) is focused upon the fire behaviour and simplified calculation methods of composite beams. The results have also been used for numerical modelling by FEM computer programs.

## **B2 Full scale fire tests**

4 of the 5 reports (B5, 6, 7 & 9) are dealing with the full scale Cardington tests on a BRE 8-storey frame building. The building was designed and constructed to resemble a typical modern city centre office development (Fig ) On plan, the building covered an area of 21 m x 45 m with an overall height of 33 m. The design complied with British Standard BS5950 and the Eurocodes 3 and 4.

The tests on the Cardington frame enabled the differences between the standard fire test and actual behaviour to be studied. This led to the conclusion that the interaction with the cooler structure surrounding the heat affected members within the fire compartment, was extremely beneficial to the heated members. The maximum steel temperature reached during the six fire tests was in excess of 1100 °C. This occurred with no signs of structural collapse.

Three other large scale fire tests, the BHP William Street fire tests, the BHP Collins Street fire tests and the fire tests at the Stuttgart-Vaihingen University Germany are summarily presented.

The forth report (B8) from NRC presents results of 32 standard fire resistance tests conducted on full-scale floor assemblies investigating the effects of subfloor material, gypsum board with different performance and fastenings. Many important results were obtained for different solutions.

## **12.3 C: Basic research on mechanical properties and on behaviour of structural elements**

In the first reference by Bijard, Twilt and Witteveen the axial restraint of steel columns due to thermal expansion is looked upon.

2 of the 6 references viz Y. Anderberg (C2) and L. Twilt (C3) deal with mechanical properties at high temperatures and how to model the steel behaviour. This modelling is useful as input in the FEM-structural programs.

In the TNO-report (C4) thermal properties and thermal response for natural fire curves and the ISO 834 curve of beams and suspended ceilings are investigated. Numerical modelling of mechanical response of beams and columns is also analysed in a limited extent.

At CTICM (C5) thermal and mechanical properties are discussed and the instability of columns with and without passive fire protection are investigated.

In reference C6 the response of structural elements under fire within a highly redundant structure such as a large building is discussed. The behaviour of the element under fire is strongly effected by the surrounding parts which are not subjected to heating. The load redistribution to cooler parts make some elements redundant.

## 12.4 D: FEM-modelling and computer simulation of fire tests

Advanced FEM-modelling of thermal and structural response of fire-exposed steel work is characterising all these 10 reports. Computer programs mentioned in these reports are shown in the Table below:

SAFIR	SISMEF	CEFICOSS	LENAS
VULCAN	DIANA	ANSYS	ABAQUS
INSTAF	GCA (Global Collapse Analysis)	FIROSS	TCD (Tempcalc-Design)
TASEF	SUPER-TEMPCALC		

Table 1 FEM-programs used to predict thermal and/or structural behaviour

In reference D1 the computer program LENAS was used to predict the behaviour of centrally loaded columns fully exposed to fire. The comparisons with tests gave a good agreement as concerns the critical steel temperature.

Reference d2 presents residual deformation of steel beams after fire predicted by a special computer programme devoted to this study. The deformations obtained are largely influenced by the thermal gradient over the cross-section. A method is suggested to calculate the residual deflection of a steel member after a fire. This is based on the assumption that the residual deflection is the same as its deflection at the maximum temperature due to applied load only.

In reference D3 the real behaviour of an external steel truss of the Paris museum “Centre Pompidou” was predicted by use of LENAS-MT. Eurocode 1 was used to obtain the external fire exposure and the maximum temperature was assessed by Eurocode 3. Two furnace tests were also carried out as basis and comparison with computer predictions. Very steep thermal gradients were measured and these play a very important role in the deformation and consequently upon the fire resistance of the steel structure.

Reference D4 illustrates thermal gradients and the load-bearing capacity of fire-exposed steel beams partly embedded in concrete. The study is very comprehensive and cover most steel profiles on the market with and without intumescent paint as passive fire protection. The computer program TCD is used to predict all design diagrams useful for the structural engineer.

In reference D5 an alternative, simplified approach for determining the thermal response of floor-ceiling assemblies comprised of a steel beam and concrete slab is presented. This approach utilises an elementary finite difference model and is intended to be an improvement to the existing lumped heat capacity approach for beams in accordance to the author’s opinion. However modern user-friendly software on the market today is probably to be preferred to this simplified model.

Reference D6 is presenting global collapse analyses of complex fire-exposed steel structures representing offshore platforms in the North Sea. The derrick of two platforms have been designed by the program GCA in an optimised way in order to fulfil the requirements on minimum collapse time and in which direction the tower is allowed to collapse.

Reference D7 is a paper where the computer program SAFIR is used to study the behaviour of a 4 storey frame structure with a fire in one of the bays. The capability of the program to predict temperatures, deflections and axial deformation is demonstrated in a convincing way.



In reference D8 the ABAQUS computer program is used for simulating the Cardington tests as concerns the composite structures under fire. The computations incorporate a simplified treatment of the reinforced slab behaviour to ensure numerical stability. The numerical model was able to follow the behaviour of the structure until the highest temperature of the fire was attained. The simulations showed that relatively good agreement has been achieved between predictions and the test measurements at all times during the fire.

Reference D9 and D10 are the main reports on the Cardington research project. The objective of the research was to gain a better understanding of the natural fire resistance and behaviour of steel framed multi-storey building subjected to fire attack and to correlate existing predictive numerical models.

Six major fire tests were carried out within the eight storey steel framed structure located within the BRE Large Building Test Facility at Cardington, Bedfordshire. It was found that this composite steel framed building possessed a very significant degree of inherent fire resistance even although the steel floor beams remained entirely unprotected against fire.

A very comprehensive numerical modelling has been carried out by several universities and research organisations involved in the project to simulate thermal and structural behaviour observed in all the fire tests. The software used in the project are Ansys, Diana, Lenas, Sismef and Vulcan and the simulations are often in a good agreement with measured behaviour. To simulate large deflections of especially the composite deck have led to necessary and advanced modifications of the original software code. On the whole the numerical modelling has shown that in the future very complicated structural fire behaviour can be predicted instead of relying on full scale fire testing. This work will also establish the basis for a new more rational design methodology for steel framed buildings subject to fire attack.

## **12.5 E: Structural fire design methods**

Reference E1 is the very first manual on fire engineering design of steel structures and was very appreciated at that time. Due to increased knowledge during the last 25 years new methods and manuals are developed.

The second and third reference about Eurocodes present fire design of structural steel and actions due to fire. The two documents have been updated and are now under completion to be EN-standard.

Reference E4 gives guidance and simplified rules for fire design of composite beams. The design methods have partly been introduced in Eurocode 3.

Reference E5 compares the traditional standard fire design with performance-based design and gives examples of performance-based fire design of steel structures in buildings and on offshore platforms. The analytical tools are presented and the savings obtained by using engineering principles.

References E6 and E7 also deal with a comparison between traditional and performance-based fire safety engineering. Many applications are presented with optimised solutions on passive fire protection based on calculations carried out by FEM-programs like TCD (see Table 1). In reference 7 several examples of different design guides for slabs, beams, prestressed concrete units (T-beams, hollow slabs), concrete walls and offshore steel members are developed.

References E8-12 presents an approach to analysis of structural safety in case of fire that takes into account active fire fighting measures and real fire characteristics. The project is called "Natural Fire



Concept” and was sponsored by ECSC. The project is carried out 1994-1998 and is divided into 5 parts namely.

Part 1 Main text

Part 2 Natural Fire Models

Part 3 Equivalent ISO-time methods

Part 4 Fire Characteristics

Part 5 Methodology to deduce from the probability data the “Design Natural Fire Curve”.

The work is very comprehensive and the structural engineer will be able to optimise the design by following the guidelines given.

The ECCS Model Code (E13) on Fire Engineering comprises mechanical and thermal actions (advanced fire modelling), material properties (thermal and mechanical), simple calculations for steel and composite members, connections, global structural behaviour and advanced calculation models.

“Structural Design for Fire Safety” (E14), is the latest manual on this subject and deals with concrete, steel, composite and wooden structures.

## 12.6 References to Condensed Literature Review

### A Experience of structural behaviour and extent of damages in real building fires

1. *SCI – The Steel Construction Institute*

Structural Fire Engineering, Investigation of the Broadgate Phase 8 Fire, 1991

2. *BS, BRE, CTICM, University of Sheffield, TNO, SCI and DETR*

The Behaviour of Multi-Storey Steel Framed Buildings in Fire, A European Joint Research Programme, ISBN 0 900206 50 0, produced by British Steel 1999

### B Fire tests of structures

#### B1 Fire resistance tests

1. *J. Kruppa, CTICM*

Properties and service performance – Fire-resistance of External Steel Columns, Commission of the European Communities – Technical Steel Research 1981.

2. *D.E. Wainmann and B.R. Kirby, British Steel*

Unprotected Structural Steel-1&2 Compendium of UK Standard Fire Test Data, BRE- Fire Research Station and British Steel - 1988.

3. *Juha Riihimäki*

Structural Fire Design of Connections and other Structures in Multi-storey Steel Framed Buildings, Tampere University of Technology, 1991

4. *B. Zhao, J. Kruppa, CTICM*

Fire Resistance of Composite Slabs with Profiled Steel Sheet and of Composite Steel Concrete Beams, 2<sup>nd</sup> part: Concrete Beams, final report CTICM 1995

## **B2 Full scale fire tests**

5. *MRL- Research Melbourne Laboratories*

The Effect of Fire in the Office Building at 140 William Street Melbourne, Australia, BHP, 1991.

6. *D.M. Martin, B.R. Kirby and M.A. O'Connor*

<sup>x</sup>Behaviour of a Multi-storey, Steel Framed Buildings Subjected to Natural Fire Effects, ECSC Sponsored Research Project, Final Report, March 1998

7. *M.A. Sultan, Y.P. Séguin and P. Leroux*

Results of Fire Resistance Tests on Full Scale Floor Assemblies, Institute for Research in Construction, National Research Council Canada, Internal Report No 764, 1998

8. The Real Behaviour of Modern Largely Unprotected Steel Framed Buildings Under Natural Fire Conditions, TNO-report No 98-CVB-R 0457, 1998

9. *BS, BRE, CTICM, University of Sheffield, TNO, SCI and DETR*

The Behaviour of Multi-storey Steel Framed Buildings in Fire, A European Joint Research Programme, ISBN 0 900206 50 0, produced by British Steel 1999

## **C Basic research on mechanical properties and on behaviour of structural elements**

1. *Yngve Anderberg*

Modelling Steel Behaviour. Presented at the International Conference on Design of Structures Against Fire, held at Aston University, Birmingham, UK on 15th and 16th April, 1986. Division of Building Fire Safety and Technology. Lund Institute of Technology, January 1986.

2. *L.Twilt, TNO*

Stress-Strain Relationships of Structural Steel at Elevated Temperatures. Analysis of various options & European proposal.. TNO-report BI-91-015, 1991

3. *L.Twilt and C.Both, TNO*

Technical Notes on the Realistic Behaviour and Design of Fire Exposed Steel and Composite Steel-Concrete Structures, TNO-report BI-91-069, 1991

4. *CTICM*

<sup>x</sup>Increase of the Fire Stability of Steel Structures with Protective Means, CTICM, 1991

5. *J. Bijard, F.S.K., Twilt, L. and Witteveen*

Axial restraint of single steel columns due to rise of temperature , IBBC-TNO report BI-76-53, 1976.

## **D FEM-modelling and computer simulation of fire tests**

1. *D.Talamonia, J.M. Franssen and N.Reicho*

Buckling of centrally loaded columns submitted to fire. Proceedings for "International Conference on Fire Research and Engineering, 10-15 September 1995, Orlando , Florida, USA. pp 533-538

2. *Y.C. Wang*

A theoretical investigation into the residual deformation of steel beams after a fire and its design implications. Proceedings for "International Conference on Fire Research and Engineering, 10-15 September 1995, Orlando, Florida, USA", pp 539-544.

3. *.D.Dhima, J. Kruppa, G. Fouquet and H. Leborgne - CTICM*

Effect of thermal gradient on the fire resistance of a 3 dimensional steel truss. Proceedings for "International Conference on Fire Research and Engineering, 10-15 September 1995, Orlando, Florida, USA", pp 545-556.

4. *K. Lavesson, Sweden*

Load-bearing Capacity of Fire-Exposed Steel Beams Partially Embedded in Concrete - A Theoretical Analysis. Project 95-017, Fire Safety Design, Lund, December 1996.

5. *James A. Milke*

A simplified model for estimating the thermal response of steel beam/concrete slab ceiling assemblies. Proceedings of Second International Conference on Fire research and Engineering, 3-8 August 1997, Gaithersburg, Maryland, USA

6. *L.N Tomlinsson, British Steel, V. Hüller, Studiengesellschaft Stahlanwendung, J.B. Schleich, Profilarbed, J. Kruppa, CTICM, L. Twilt, TNO*

Design and implementation of the computer code fire safety of structural steelwork (Fiross), European commission, technical steel research. EUR 18427, 1998

7. *V.K.R Kodur, D.I. Nwosu, M.A. Sultan and J.M. Franssen*

Application of the SAFIR Computer program for Evaluating Fire Resistance presented at the Third International Conference on Fire Research and Engineering in Chicago 4-8 October 1999.

8. *A.M.Sanad and A.S. Usmani University of Edinburgh and M.A. O'Connor, British Steel*

Finite Element modelling of fire tests on the Cardington Composite Building presented at Interflam' 99, 8 th International Fire Science & Engineering Conference in Edinburgh 29 th June-1 st July 1999.

9. *J.M. Rotter, A:M. Sanad, A:S. Usmani and M.Gillie, University of Edinburgh*

Structural performance of redundant structures under local fires presented at Interflam' 99, 8 th International Fire Science & Engineering Conference in Edinburgh 29 th June-1 st July 1999.

10. *BS, BRE, CTICM, University of Sheffield, TNO, SCI and DETR*

The Behaviour of Multi-storey Steel Framed Buildings in Fire, A European Joint Research Programme, ISBN 0 900206 50 0, produced by British Steel 1999

11. *Yngve Anderberg*

Steel Columns Partially Fire-Exposed- A Theoretical Study. Fire Safety Design, Lund, Sweden, March 1998.

## **E Structural fire design methods**

1. *Pettersson, Magnusson, Thor:*

Fire Engineering Design of Steel Structures, Swedish Institute of Steel Construction, Stockholm 1976.

2. Eurocode 3 Design of steel structures, Part 1.2 Structural Fire Design, Draft prENV 1993-1-2, August 1993.
3. ENV 1991-2-2, Basis of design and actions on structures, Part 2-2 Actions on structures exposed to fire, CEN Brussels 1994.
4. *L.Twilt and C.Both, TNO*  
Technical Notes on the Realistic Behaviour and Design of Fire Exposed Steel and Composite Steel-Concrete Structures, TNO-report BI-91-069, 1991
5. *B. Zhao, J. Kruppa, CTICM*  
Fire Resistance of Composite Slabs with Profiled Steel Sheet and of Composite Steel Concrete Beams, 2<sup>nd</sup> part: Concrete Beams, final report CTICM 1995
6. *Yngve Anderberg*  
European Experiences in Fire Design of Structural Steel. Presented at the ASCE-Structures Congress in Chicago 15-18 April 1996. Fire Safety Design, Lund, Sweden, 1996.
7. *Yngve Anderberg, Sebastian Jeansson, Jens Oredsson*  
Global Analysis of Fire-Exposed Steel Structures. Presented at the Swedish Steel Building Conference of Swedish Institute of Steel Construction in Sundsvall 18 October 1996. Fire Safety Design, Lund, Sweden, 1996.
8. *Yngve Anderberg*  
Performance-based Fire Safety Engineering in Practise - Presented at a seminar held at University of Bandung, Indonesia on November 25, 1997, Fire Safety Design, Lund Sweden.
9. *Yngve Anderberg*  
Fire Engineering Design of Structures based on Design Guides - Presented at the Second International Conference on Performance-Based Codes and Fire Safety Methods, Maui, Hawaii, May 5-9, 1998.
10. *J.B. Schleich and L-. Cajot, ARBED et al*  
Competitive Steel Buildings Through Natural Fire Safety Concept, CEC-Project, Part 1, ( Main text.) ARBED, March 1999
11. *J-M. Franssen and J.F. Codorin, University of Liège, Belgium et al*  
Competitive Steel Buildings Through Natural Fire Safety Concept, CEC-Project, Part 2 (Working group 1 Equivalent ISO-Time Methods and Working group 2: Natural Fire Models) , ARBED, March 1999
12. *L.Twilt and J. Van Oerle, TNO, The Netherlands et al*  
Competitive Steel Buildings Through Natural Fire Safety Concept, CEC-Project, Part 3, (Working group 3: Fire Characteristics for Use in a Natural Fire Design of Building Structures) , ARBED, March 1999
13. *M. Fontana and C. Fetz, ETH, Zürich, Switzerland et al*  
Competitive Steel Buildings Through Natural Fire Safety Concept, CEC-Project, Part 4, (Working group 4: Statistics), ARBED, March 1999

*14. J.B. Schleich and L-. Cajot, ARBED et al*

Competitive Steel Buildings Through Natural Fire Safety Concept, CEC-Project, Part 5, (Working group 5: Methodology to Deduce from the Probability Data the “Design Natural Fire Curve”), ARBED, March 1999

*15. J.Kruppa, Gerry Newman, J.B. Schleich and Leen Twilt*

ECCS Model Code on Fire Engineering, 1999

## 13 References

- /1/ Eurocode 3 Design of steel structures, Part 1.2 Structural Fire Design, Draft prENV 1993-1-2, August 1993.
- /2/ ENV 1991-2-2, Basis of design and actions on structures, Part 2-2 Actions on structures exposed to fire, CEN Brussels 1994.
- /3/ Pettersson, Magnusson, Thor: Fire Engineering Design of Steel Structures, Swedish Institute of Steel Construction, Stockholm 1976.
- /4/ Anderberg, Y.: SUPER-TEMPCALC, A Commercial And User-friendly Computer Program With Automatic FE-Generation For Temperature Analysis Of Structures Exposed To Heat. Fire Safety Design AB, Lund 1991.
- /5/ Zienkiewicz, O. C., Taylor, R. L.: The Finite Element Method, Volume 2, 4<sup>th</sup> Edition, McGraw-Hill International (UK) Ltd, London, 1991.
- /6/ Ottosen, N. S., Petersson, H.: Introduction to the Finite Element Method, Prentice Hall International (UK) Ltd, 1992.
- /7/ Holman, J. P.: Heat Transfer, Seventh edition, Singapore 1990.
- /8/ NAD(S)/SS-ENV 1993-1-2, National Application Document for Eurocode 3 - Design of steel structures Part 1-2:General rules - Structural Design.
- /9/ Wainman D.E., Kirby B.R.: Compendium of UK Standard Fire Test Data. Unprotected Steel 1. British Steel Corporation 1988
- /10/ Anderberg, Y., Pettersson, O.: Brandteknisk dimensionering av betongkonstruktioner (Manual on Fire Engineering Design of Concrete Structures.) Swedish Board for Building Research, 1992. ISBN 91-540-5448-6, T13:1992. In Swedish.
- /11/ Stålbyggnad. Stålbyggnadsinstitutet Publikation 130. Stockholm 1993. ISBN 91 85644 83 8. In Swedish.
- /12/ Johannesson, P., Vretblad, B.: Byggformler och tabeller. Liber Utbildning AB. ISBN 91-634-0501-6. Uppsala, 1993. In Swedish.
- /13/ Jeansson, S.: TCD 5.0 Manual (rev. 4). Fire Safety Design AB, Lund 2001.
- /14/ Thelandersson, S.: Konstruktionsberäkningar med dator. Lund, 1990. In Swedish.
- /15/ BS, BRE, CTICM, University of Sheffield, TNO, SCI and DETR  
The Behaviour of Multi-Storey Steel Framed Buildings in Fire, A European Joint Research Programme, ISBN 0 900206 50 0, produced by British Steel 1999
- /16/ MRL- Research Melbourne Laboratories  
The Effect of Fire in the Office Building at 140 William Street Melbourne, Australia, BHP, 1991.

- /17/ D.M. Martin, B.R. Kirby and M.A. O'Connor: Behaviour of a Multi-storey, Steel Framed Buildings Subjected to Natural Fire Effects, ECSC. Sponsored Research Project, Final Report, March 1998.
- /18/ BS, BRE, CTICM, University of Sheffield, TNO, SCI and DETR  
The Behaviour of Multi-storey Steel Framed Buildings in Fire, A European Joint Research Programme, ISBN 0 900206 50 0, produced by British Steel 1999.
- /19/ The Real Behaviour of Modern Largely Unprotected Steel Framed Buildings Under Natural Fire Conditions, TNO-report No 98-CVB-R 0457, 1998
- /20/ Wiberg, N.E.,: Finita Elementmetoden. ISBN 91-40-03768. Lund 1975.
- /21/ BKR, Boverkets Konstruktionsregler. Karlskrona 1998. In Swedish.